Interim Report 69-3

AD

RCS OSD-1366

Research and Development Technical Report
ECOM 2-68 I-6

THE ENERGY BUDGET AT THE EARTH'S SURFACE: A SIMULATION OF NET PHOTOSYNTHESIS OF FIELD CORN

Contribution by:

D. W. Stewart, E. R. Lemon

MICROCLIMATE INVESTIGATIONS
INTERIM REPORT 69-3

E. R. Lemon — Investigations Leader
U. S. DEPT. OF AGRICULTURE and
CORNELL UNIVERSITY

DECEMBER 1969

ECOM

UNITED STATES ARMY ELECTRONICS COMMAND
ATMOSPHERIC SCIENCES LABORATORY
FORT HUACHUCA, ARIZONA

Cross Service Order 2-68
Microclimate Investigations, U. S. Department of Agriculture
Bradfield Hall, Cornell Univ.: Ithaca, New York 14850

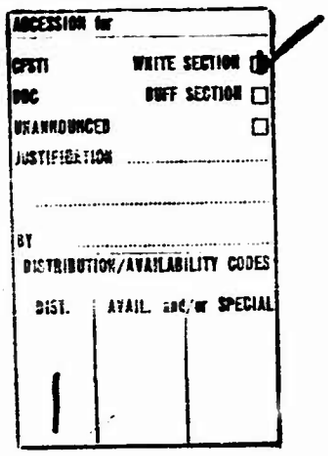

NOTICES

Citation of trade names and names of manufacturers in this report is not to be construed as official Government indorsement or approval of commercial products or services referenced.

The findings of this report are not to be construed as an official Department of Army position unless so designated by other authorized documents.

Destroy this report when it is no longer needed. Do not return it to the originator.

Technical Report ECOM 2-68 I-6
December 1969

Reports Control Symbol
OSD-1366

THE ENERGY BUDGET AT THE EARTH'S SURFACE: A SIMULATION OF NET PHOTOSYNTHESIS OF FIELD CORN

INTERIM REPORT 69-3

Cross Service Order 2-68
Task 1TO-61102-B53A-17

Prepared by

D. W. Stewart, E. R. Lemon

of

Northeast Branch
Soil and Water Conservation Research Division
Agricultural Research Service
U. S. Department of Agriculture
Ithaca, New York

Report No. 407

In Cooperation With

N. Y. State College of Agriculture
Cornell University
Ithaca, New York

Research Report No. 878

For

U. S. Army Electronics Command
Atmospheric Sciences Laboratory
Fort Huachuca, Arizona

Interim Report

62-7 Estimation of Turbulent Exchange Within a Corn Crop Canopy at Ellis Hollow (Ithaca, N.Y.), 1961 -- J. L. Wright and E.R. Lemon

62-8 Studies of Water Relations in a Corn Field in Ellis Hollow (Ithaca, N.Y.) -- J. H. Shinn and E. R. Lemon

62-9 Energy and Water Balance in Plant Communities -- E. R. Lemon

63-1 An Experimental Study of Air Flow in a Corn Plant-Air Layer -- Z. Uchijima and J. L. Wright

64-1 Vertical Fluxes Within the Vegetative Canopy of a Corn Field -- K. W. Brown

65-1 Shortwave Radiation in a Corn Crop -- L. H. Allen and K. W. Brown

66-1 Diffusive Resistances At, and Transpiration Rates from Leaves In Situ Within the Vegetative Canopy of a Corn Crop -- I. I. Impens, D. W. Stewart, L. H. Allen and E. R. Lemon

ECOM Report

2-66I-2 Preliminary Wind Tunnel Studies of the Photosynthesis and Transpiration of Forage Stands -- L. A. Hunt, I. I. Impens and E. R. Lemon

2-67I-1 Comparison of Momentum and Energy Balance Methods of Computing Vertical Transfer Within a Crop -- J. L. Wright and K. W. Brown

2-67I-2 Air Flow and Turbulence Characteristics in a Japanese Larch Plantation -- L. H. Allen

2-67I-3 Estimates of the Diffusion Resistance of Some Large Sunflower Leaves in the Field -- L. A. Hunt, I. I. Impens and E. R. Lemon

2-68I-1 Assession Sources and Sinks of Carbon Dioxide in a Corn Crop Using a Momentum Balance Approach -- E. R. Lemon and J. L. Wright

2-68I-2 Origins of Short-Time CO_2 Fluctuations in a Cornfield -- E. R. Lemon, J. L. Wright and G. M. Drake

2-68I-3 A Study of the Carbon Dioxide Concentration Monitored Over an Agricultural Field Near Ithaca, N.Y. -- L. H. Allen

Interim Report

69-1 Effects of Air Turbulence Upon Gas Exchange from Soil -- B. A. Kimball and E. R. Lemon

69-2 Basic Concepts of Spectral Analysis by Digital Means -- B. A. Kimball

PREFACE

This publication (Interim Report 69-3) represents to a large degree the culmination over ten years of research to understand the integrated soil-plant-atmosphere system. It has been a team effort of technicians, professionals and graduate students. In the beginning, it was necessary to study separately the component part physical and physiological processes under field conditions. This necessitated development of suitable measuring and data-handling techniques. Once there was sufficient knowledge and expertise the team was able to study simultaneously the component parts all together. Finally, Douglas Stewart developed a suitable computer model to simulate a plant community -- both its environment and its interaction -- then tested the model against some of the integrated field measurements. The model is not perfect. It shouldn't be, for we do not understand all the physics and physiology.

Early in 1970 two more Interim Reports will be published. One deals with extensive testing of the model with emphasis on plant water relations. The other report takes up in detail the field instrumentation used in gathering the test data.

There follows a listing of the Interim Reports published to date by the team.

E. R. Lemon

LIST OF INTERIM REPORTS

Interim Report

62-1 Mathematical Study of the First Stage of Drying of a Moist Soil -- W. Covey

62-2 Theoretical Estimate of Photosynthesis under Field Conditions -- C. S. Yocum

62-3 Solar Radiation Balance and Photosynthetic Efficiency -- C. S. Yocum, L. H. Allen and E. R. Lemon

62-4 Radiant Energy Exchanges within a Corn Crop Canopy and Implications in Water Use Efficiency -- L. H. Allen, C. S. Yocum and E. R. Lemon

62-5 Analysis of Micrometeorological Vertical Profiles for the Evaluation of Surface Characteristics and Vertical Fluxes -- W. Covey

62-6 Soil Moisture Analyses, Ellis Hollow (Ithaca, N.Y.), 1960 and 1961 -- J. H. Shinn, K. W. Brown and R. F. West

TABLE OF CONTENTS

LIST OF TABLES

LIST OF ILLUSTRATIONS

INTRODUCTION

In general, the age old question of what constitutes crop yield lies, as yet, unanswered. The plant when it germinates produces a certain amount of leaf area from sources of carbohydrate stored in the seed. It uses this leaf area to intercept radiation which it, in turn, uses to convert CO_2 to carbohydrate. The carbohydrate provides energy and building material for the creation of roots, stem and more leaf area. While simply stated here, the processes of germination, vegetative growth, flowering and fruiting are extremely complex and include many interactions with a constantly changing environment. Because of these complexities, the traditional methods of growth analysis described by Watson (1947, 1952), Williams (1946) and others along with corresponding statistical techniques such as the studies of Black (1955) and Glenday (1956) have not provided an understanding of the mechanisms by which a plant is influenced by and in turn responds to the environment.

An alternative to statistical correlation is the method of mathematically modelling a plant-environment system. That is, the various growth processes are described in mathematical terms and integrated with time. Davidson and Philip (1956) presented one of the first simulation models where they considered only the light environment and its effect on the accumulation of dry matter. Since then computers with their ability to handle detail have been used in not only complex radiation models (de Wit (1965), Duncan, et al. (1967)) but also in growth simulation models (Brower and de Wit, 1968). The latter calculates

the daily accumulation of net photosynthesis and then models the translocation processes where carbohydrates are distributed to the stem and root tissues.

Although models are available which describe the light regime in a plant system in detail, less attention has been applied to the problem of CO_2 exchange and the dissipation of radiation loads on individual leaves through sensible and latent heat exchange. In particular, understanding of the effects of the architecture of the plant system on these exchange processes is lacking.

There are two types of field studies which are essential to the development of a complete model of the plant-environment system. The first is the investigation of net assimilation of CO_2 of individual leaves using leaf chambers. (For example, Gaastra (1959), Hesketh and Musgrave (1962)). In particular, net photosynthesis of individual leaves must be known as functions of light flux density, CO_2 concentration at the leaf surface and leaf temperature (effects of water stress will not be considered directly in this treatment). These functions are used directly in the simulation model described in this study.

The second type of studies necessary for simulation are the in situ investigations made by agrometeorologists. (Lemon (1960), Monteith and Szeicz (1960)). In these studies profiles of air temperature, wind velocity, CO_2 and water vapor concentrations and net radiation are measured above and within a plant community disturbing it as little as possible. Aerodynamic and energy balance methods using these profiles provide estimates of net fluxes of CO_2 and sensible and latent heat (Lemon 1965). Thus these fluxes can be compared to simulated values since the

calculations are independent of the above methods. Also profiles can be generated by the simulation model and compared with measurements. Finally the above measurements made 2-3 meters above the crop and at the soil surface provided needed boundary values for the mathematical solutions.

To construct this simulation model, a rather wide range of information must be assembled. First of all, radiation loads on individual leaves in a plant community must be known. A procedure will be outlined to divide the leaf area of a crop into classes of radiation loads. This is done for visible radiation in conjunction with the calculation of net photosynthesis as well as total radiation loads used in estimating sensible and latent heat. Because of the immense amount of calculations involved, a computer is used. Thus in subsequent theoretical discussions, programming techniques are introduced when they were considered essential to the solution of the equations involved.

Once the distribution of radiation in a crop system is known, the photosynthetic response of individual leaves to radiation can be integrated over the complete crop cover. However, CO_2 supply and leaf temperatures also influence these responses. Thus the exchange processes between the individual leaves and the air stream both above and within the crop have to be introduced in this integration scheme. Since leaf responses and properties of the air stream are interdependent, the equations describing the exchange processes of the air flow and the equations determining the leaf responses are solved simultaneously using successive approximation techniques. Here again a computer was used extensively in these solutions. The development of the various components of the integration scheme along with experimental testing are considered in subsequent chapters.

Chapter I

RADIATION MODELS

As stated in the introduction the radiation regime in the crop is divided into visible, near infrared and thermal regions of the spectrum. Visible radiation supplies the excitation energy to the chlorophyll molecule for photosynthesis. It also determines to a large extent the width of stomatal apertures when the plant is not under water stress. Thus the emphasis here both theoretically and experimentally will be on visible radiation. Theoretical treatments of the near infrared and thermal components are also given.

Review

Visible radiation in crop systems has been extensively studied mainly because of its direct effect on photosynthesis. Anderson's review (1964) provides some indication of the large interest in this area. Therefore, I will not attempt a complete review of this subject but will cover only the studies which are pertinent to the theory developed later in this discussion.

The most widely used equation describing light penetration is the following analogy of Beer's Law;

$$I = I_o e^{-KF} \qquad (1)$$

F is the cumulative leaf area per unit soil area measured from the top of the crop downward;

K is an extinction coefficient;

I is the flux density of visible radiation at F;

and I_o is the corresponding flux density at the surface of the crop. Monsi and Saeki (1953), Takeda and Kumera (1957) and others found that this equation adequately described light penetration in many types of plant communities. Davidson and Philip (1958) used equation (1) (setting K=1) in their growth simulation model.

Since then, Isobe (1962), Anderson (1966) and Chartier (1966a) among others have derived equation (1) by assuming a random distribution of leaf area. K is a property of the mean leaf angle and therefore may or may not be constant with F.

Other equations for light penetration have been developed for different distributions of leaf area. For example, Monteith (1965) used a

positive binomial distribution; Niilisk, et al. (1969) used a negative binomial and a Markov distribution.

A part of the radiation falling on plant leaves is transmitted or reflected. Kasanaga and Monsi (1954) extended the exponential law (Equation 1) to include the effects of leaf transmission. A different approach considers the crop as a homogeneous system characterized by a transmission coefficient (closely related to K) and a reflection coefficient. The Kubelka-Monk theory presented in detail by Allen and Richardson (1968) does this. This theory was compared with measurements by Allen and Brown (1965). In their crop system, the transmission coefficient did not remain constant with F.

There is a considerable advantage to study the light regime in a canopy in terms of the characteristics of individual leaves rather than the crop as a whole. This allows one to take into account differences in leaf properties with depth and eventually, differences in leaf area distributions with depth. There have been at least two attempts (de Wit (1965) and Duncan et al. (1967)) which use leaf angle distributions and leaf transmission and reflection coefficients in describing the light regime in plant communities. These studies are particularly important since the light irradiance levels crossing leaf plants in the crop are calculated. The following theoretical considerations rely heavily on these studies.

Theoretical Considerations

The three regions of the spectral band of radiation considered here, have quite different leaf transmission and reflection coefficients. For visible, they are of the order of 0.1; for near-infrared they vary from 0.4 to 0.5 and for long wave radiation they are approximately zero. These coefficients vary with wavelength to some extent within these regions but this variation is small when compared with the differences between regions. The theory dealing with each region will be considered in turn.

Visible Radiation

De Wit (1965) introduced the following equations relating leaf angle (IL), sun angle (IS), the angle between the sun and the leaf (LS) and the difference between the azimuths of the sun and leaf planes (DA).

$$\mathrm{Sin(LS)} = A + B \sin(DA) \tag{2}$$

$$A = \sin(IS) \cdot \cos(IL) \tag{3}$$

$$B = \cos(IS) \cdot \sin(IL) \tag{4}$$

Sin(LS) is also the projection of the leaf in the direction of the sun's rays. Sin(LS) divided by sin(IS) is the projection of a unit leaf area onto the horizontal and is directly related to the amount of light intercepted by the leaf. To obtain a mean projection (PL), one must integrate equation (2) from -90° to +90°.

That is

$$PL = \frac{\int_{-\pi/2}^{\pi/2} (A + B \sin(DA))\, d(DA)}{\int_{-\pi/2}^{\pi/2} d(DA)} \tag{5}$$

If $IS \geq IL$ $\quad PL = A$

If $IS < IL$ $\quad PL = 2/\pi[B \cos(DAO) - A(DAO)]$ (7)

where $DAO = \arcsin(-A/B)$

Defining

$$\theta_o = (\pi/2 - DAO)$$

equation (7) becomes

$$PL = 2/\pi[\sin\theta_o \cos(IS) \sin(IL)] + (1 - \theta_o/90^\circ) \cos(IL) \sin(IS) \quad (8)$$

Thus PL is identical to F/F' defined in appendix A of Duncan, et al. (1967). For a given increment of leaf area, the effects of the various leaf angles have to be included. Thus the mean projection ($\overline{PL}$) of the leaf area increment becomes

$$\overline{PL} = \sum_{j=1}^{9} PL_j \cdot FR_j$$

where FR_j is the relative amount of leaf area in the leaf angle class j. Nine leaf angle classes are used in this study.

In studying light penetration, a crop can be divided into a number of finite increments with a leaf area of S in each increment. The percent transmission (PT) of light to but not including the n+1 layer is given by de Wit (1965) as;

$$PT = 100 \left(1 - \frac{S \cdot (\overline{PL})}{\sin(IS)}\right)^n \quad (9)$$

Duncan, et al. (1967) derived a different expression using equations by Wilson (1960). The mean probability M of a sun's ray being intercepted by a leaf was defined as

$$M = \frac{S \cdot \overline{PL}}{\sin(IS)} \quad .$$

If leaves are distributed randomly, percent transmission can be expressed as:

$$PT = 100(1 - [\frac{Me^{-M}}{1!} + \frac{M^2e^{-M}}{2!} + \frac{M^3e^{-M}}{3!} + \ldots\ldots]) \quad (10)$$

The terms inside the square brackets are probabilities of 1, 2, 3 etc. leaves being in the path of a sun's ray. Equation (10) reduces to

$$PT = 100(e^{-M})^n \quad (11)$$

Note that equation (8) is a function of S while (11) is not. Figure (1) shows percent transmission of a hypothetical array of leaves as a function of the number of increments into which the leaf area was divided. De Wit suggested that S be used as an empirical parameter to fit measured light profiles with theoretical curves. However for S less than 0.4, small changes occur in PT using de Wit's equation. Note that as n becomes larger equation (8) and (11) give approximately the same answer. Also note that in equation (8) and (11), $\overline{PL}$ appears as a constant. In the actual computer program, $\overline{PL}$ varies with the leaf angle distribution which may vary with F.

Thus far, only penetration of direct radiation from the sun has been considered. Sky radiation can be treated in the same way if we assume the sky is a uniformly bright hemisphere. (de Wit, 1965). The sky is divided into 9 angle classes from the horizon to the zenith. The proportion of light (PD_i) falling on the horizontal from a sky segment from IS_1 to IS_2 is expressed as

$$PD_i = \frac{\int_{IS_1}^{IS_2} 2\pi a \cos(IS) \cdot \sin(IS)\, d(IS)}{\int_{0}^{\pi/2} 2\pi a \cos(IS) \cdot \sin(IS)\, d(IS)} \quad (12)$$

$$= \sin^2(IS_2) - \sin^2(IS_1) \quad .$$

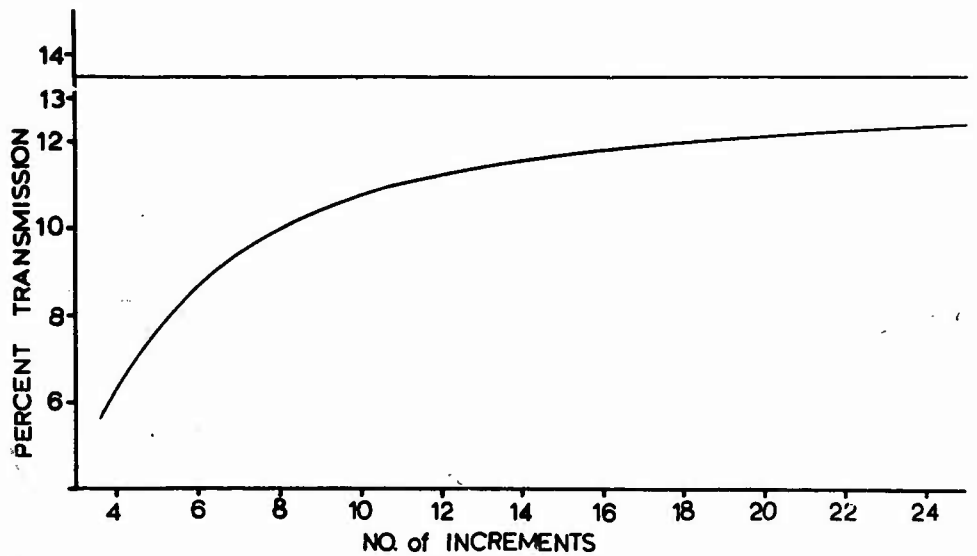

Figure 1. Per cent transmission through a hypothetical array of leaves as a function of the number of increments into which the array is divided. L.A.I. = 4.0 (IS) = 60°, IL = 45°. The straight line represents Equation (11); the asymptotic line represents Equation (9).

'a' is an imaginary radius of the sky hemisphere. PD_i times the total amount of sky radiation is the amount of sky radiation arriving at the angle IS_i where in this case

$$IS_i = (IS_1 + IS_2)/2. \tag{13}$$

Special attention is given to the proportion of sky light which penetrates each increment leaf area of the crop. These values are stored in an array TR_i where i refers to the increment of leaf area. These values are used repeatedly in the program.

The flux density of light striking a given leaf in the canopy is

$$\frac{\sin(LS) \cdot DI}{\sin(IS)}$$

where (DI) is the flux density of direct radiation on a horizontal surface. The amount of light transmitted and reflected are respectively $(\sin(LS) \cdot (DI) \cdot \lambda)/\sin(IS)$ and $(\sin(LS) \cdot (DI) \cdot \mu)/\sin(IS)$, where λ and μ are the leaf transmissivity and reflectivity respectively.

Two simplifying assumptions are: (a) that light is scattered by the leaf diffusely and (b) that only two directions (upward, down) of scattered radiation need be considered. Figure (2) shows an element of leaf dA at angle (IL) to the horizontal. The amount of light reflected (W) from dA is expressed as

$$W = \frac{\sin(LS) \cdot DI}{\sin(IS)} \cdot \mu \tag{14}$$

and

$$W = \int_0^{\pi/2} 2\pi W_o \, r^2 \sin\theta \cos\theta \, d\theta \tag{15}$$

where θ is the angle of elevation from the leaf plane, W_o is the intensity of radiation emitted perpendicular to the plane and r is the radius of

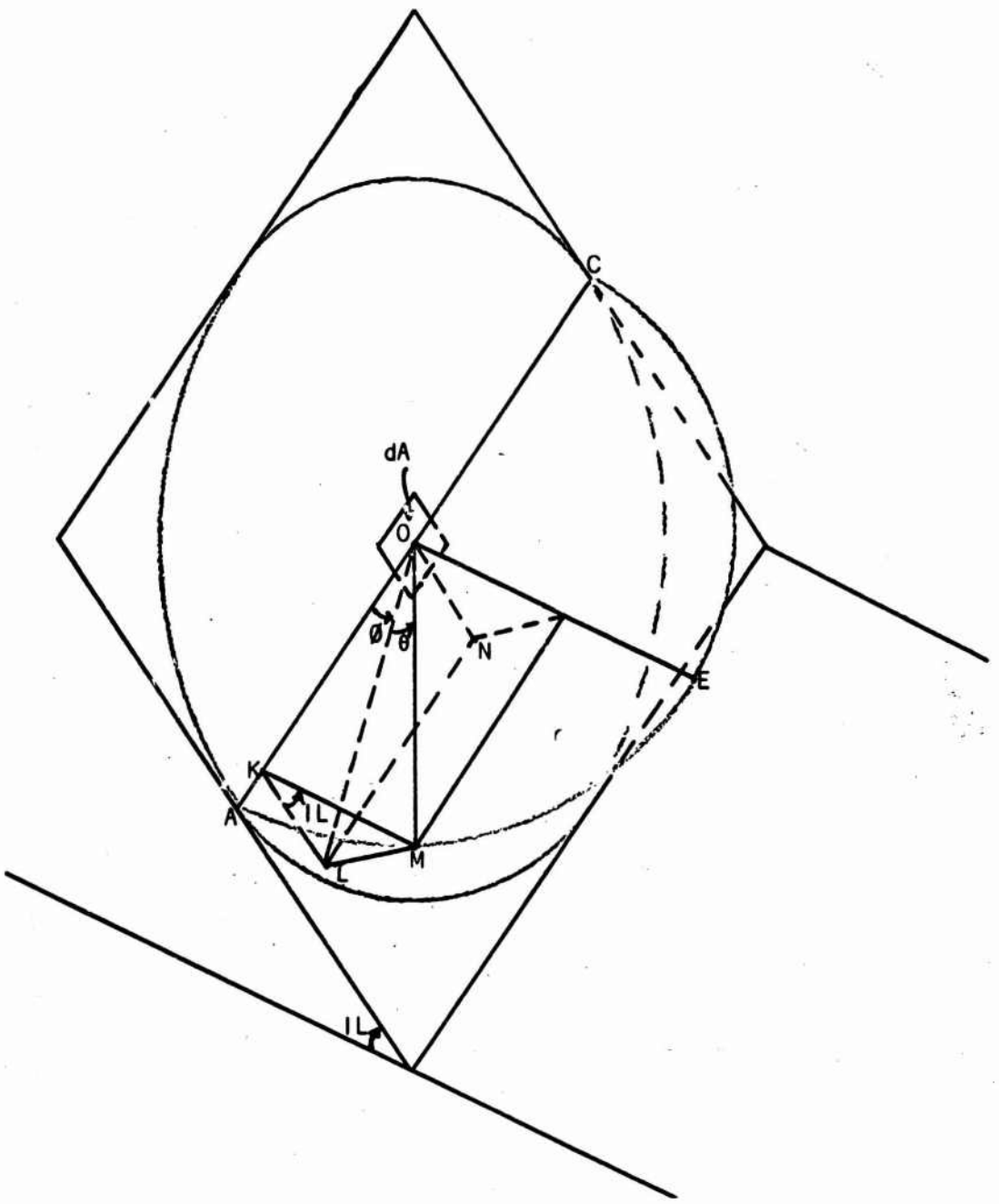

Figure 2. Leaf plane at an angle IL to the horizontal.

an imaginary hemisphere. In figure (2), if ML = z, KL = y, KO = x and OM = r then $\sin\theta_1 = z/r$, $\tan\theta = y/x$ and $\tan(IL) = z/y$. θ is the angle about the normal to the leaf plane at 0; θ_1 is the angle of elevation bounded by the plane A M E C.

Also $$x^2 + y^2 + z^2 = r^2 \qquad (16)$$

Combining the above equations, one obtains

$$\theta_1 = \arcsin \sqrt{\frac{B' \sin^2\theta}{1 + B'\sin^2\theta}} \qquad (17)$$

where $B' = \tan^2 IL$

The amount of radiation W' scattered from dA through the portion of the hemisphere between A M E C and the plane of the leaf is expressed as

$$W' = \int_0^{\pi} \int_0^{\theta_1} W_o r^2 \sin\theta \cos\theta \, d\theta \, d\phi$$

$$= \frac{r^2}{2} W_o \int_0^{\pi} \frac{B' \sin^2 \phi}{1 + B'\sin^2\phi} \, d\phi \qquad (18)$$

The fraction (E) of W' to W is given as

$$E = W'/W = 1/(2\pi) \int_0^{\pi} \frac{B'\sin^2\phi}{1 + B'\sin^2\phi} \, d\phi$$

or

$$E = 1/2 - \frac{1}{\sqrt{4 + 2B'}} \qquad (19)$$

The fraction (E) is both the proportion of radiation reflected downward and the proportion transmitted upwards. (1 - E) is the converse. Therefore the total amount of light scattered upward by the leaf ($Sc\uparrow$) and downward ($Sc\downarrow$) are respectively;

$$Sc\uparrow = \frac{\sin(LS) \cdot DI}{\sin(IS)} \; (\lambda(1 - E) + \mu E) \qquad (20)$$

$$\text{and } Sc\downarrow = \frac{\sin(LS) \cdot DI}{\sin(IS)} \left(\lambda E + \mu(1 - E)\right) \qquad (21)$$

In the program, PL_j replaces sin(LS) where j represents a leaf angle class. PL_j is the light flux density at the leaf surface of angle (j) averaged over various positions around the azimuth. To obtain the total amount of scattered radiation, Sc↑ and Sc↓ are summed over the leaf angle classes for both the direct radiation and the nine classes of sky radiation. A final adjustment is made using equation (11). Percent transmission is a measure of the actual area of leaves reached by direct and sky radiation.

At this stage, direct and sky radiation penetrate into a crop creating sources of scattered radiation. Radiation is assumed to be scattered equally in all directions. Thus, this scattered radiation appears as a uniformly bright infinite plane to other leaves. Assuming this, one can use the procedures already worked out for sky radiation to calculate the penetration both up and down of radiation scattered by the leaves in the crop. These amounts of scattered radiation which penetrate to other levels is simply added to the previous values of Sc↑ and Sc↓. Also the amounts of sky radiation penetrating directly into the canopy are added to Sc↓. Thus one can now define $Sc_i\downarrow$ and $Sc_i\uparrow$ as the total amounts of diffuse radiation in the crop moving up and down respectively at level i.

The soil surface in this study was treated as if it were a layer of leaves with $\lambda = 0.0$ and $\mu = 0.13$.

Of primary interest in a photosynthesis model is the flux densities (Lt_{ij}) of visible radiation on individual leaves in the canopy. The

equation defining the radiation load on a leaf is given as

$$Lt_{ij} = |A + B \sin DA| \cdot \frac{(DI)}{\sin(IS)} + Sc_{i+1}\uparrow + Sc_i\downarrow \qquad (22)$$

for leaves in direct sunlight and

$$Lt_{ij} = Sc_{i+1}\uparrow + Sc_i\downarrow \qquad (23)$$

for leaves shaded from the sun. Leaves in direct sunlight were considered at 18 positions of (DA) between $-\pi/2$ to $+\pi/2$. Also the relative amount of leaf area A_{oi} in direct sunlight for a given increment i was found from

$$A_{oi} = (PT_i - PT_{i+1}) \cdot \frac{\sin(IS)}{(\overline{PL}_i \cdot 100)} \qquad (24)$$

PT_i is the percent transmission of direct radiation to the i^{th} increment (Duncan et al. 1967). Equations 22-24 were used to determine total visible radiation loads at all leaf positions in the crop. These loads were expressed in classes as 0-5%, 5-10%, 10-15% of DI/sin(IS). Leaf areas with radiation loads in the same range were summed. Thus a frequency distribution of leaf area in these classes for each increment was the only information stored from the above calculations.

Another advantage to this procedure is the ability to separate leaf areas with direct radiation loads falling on the dorsal as opposed to the ventril sides of leaves. This happens whenever (A + B sinDA) is negative. Therefore, a separate frequency distribution of these leaf areas could be constructed although in this study this information was not used. Both sides of the leaf were assumed to have equal responses to light.

Near Infrared Radiation

The near infrared radiation can be treated in the same way as the visible radiation with one important difference. Multiple scattering of visible radiation was considered negligible because of the relatively low leaf reflection and transmission coefficients. Niilisk et al. (1969) made this same assumption. However the relatively large values of these coefficients in the near infrared make a consideration of multiple scattering necessary.

Radiation from the sun and sky penetrates to a given leaf area increment and creates first order sources of scattered radiation. Some of this radiation reaches the soil and other leaves and is reflected back to the same increment to create second order sources. This is illustrated in Figure (3). Let $S_i\uparrow$ be the amount of light scattered upward and S_i the amount scattered downward at level i from the first order sources. The amount ($R_i\downarrow$) of $S_i\uparrow$ reflected back is expressed by

$$R_i\downarrow = S_i\uparrow \cdot S \cdot \mu[1 + (TR_{j-1} + S\lambda)^2 + (TR_{j-1} + S\lambda)^2(TR_{j-2} + S\lambda)^2 + \ldots .] \quad (25)$$

Similarly

$$R_i\uparrow = S_i\downarrow \cdot S \cdot \mu[1 + (TR_j + S\lambda)^2 + (TR_j + S\lambda)^2(TR_{j+1} + S\lambda)^2 + \ldots .] \quad (26)$$

In this case j represents the increment of leaf area directly below level i. The assumptions involved in equations (25) and (26) are that the scattered radiation penetrates a given leaf area increment in the same relative amounts as sky radiation. Also, the total amount of radiation reflected and transmitted by a leaf area increment is directly proportional to $S\lambda$ and $S\mu$ respectively where S is the leaf area per increment.

The secondary sources then scatter radiation upwards ($SS_i\uparrow$) and downwards ($SS_i\downarrow$) expressed respectively as

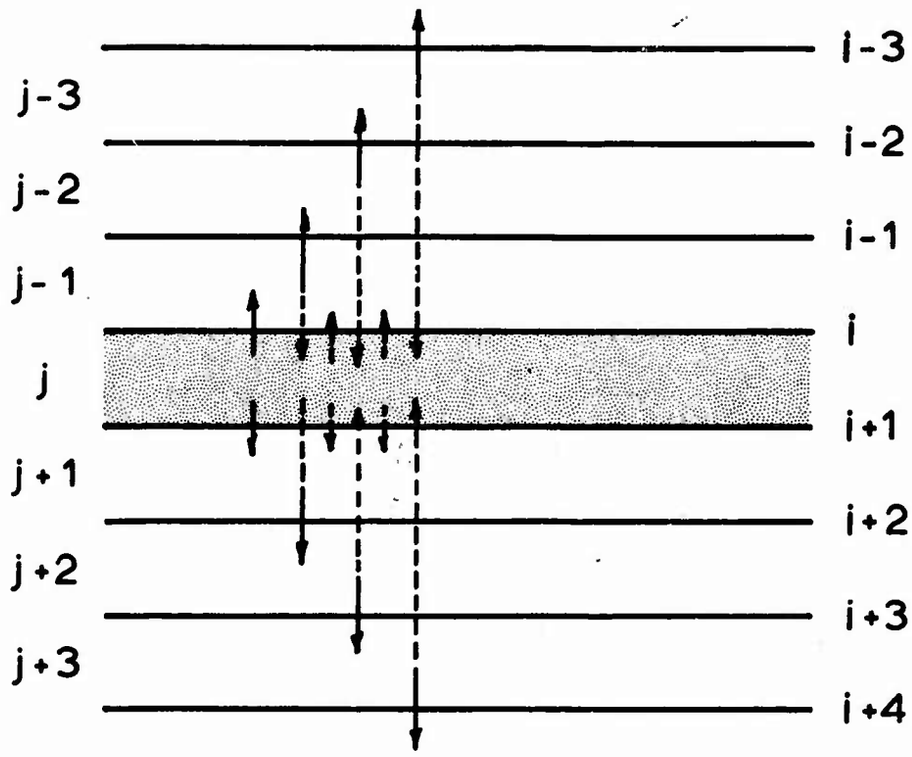

Figure 3. Scattered Radiation. Radiation is scattered from first order sources in increment j. A portion of this scattered radiation is reflected back to create second order sources.

$$SS_i\uparrow = R_i\downarrow \cdot S\mu + R_{i+1}\uparrow \cdot S\lambda \qquad (27)$$

$$SS_i\downarrow = R_i\downarrow \cdot S\lambda + R_{i+1}\uparrow \cdot S\mu \qquad (28)$$

Let $\beta\uparrow = SS_i\uparrow/S_i\uparrow$ and $\beta\downarrow = SS_i\downarrow/S_i\downarrow$. Then the total amounts of radiation scattered upward and downward from increment i are expressed respectively as

$$Sc_i\uparrow = S_i\uparrow(1 + \beta\uparrow + \beta\uparrow^2 + \beta\uparrow^3 + \ldots\ldots) \qquad (29)$$

and $$Sc_i\downarrow = S_i\uparrow(1 + \beta\downarrow + \beta\downarrow^2 + \beta\downarrow^3 + \ldots\ldots) \qquad (30)$$

Note that the soil is considered again as a layer of leaves with zero transmittance and a reflectance of 0.1 for near infrared radiation. These total sources of scattered near infrared radiation can now be treated in the same manner as the first order sources of visible radiation.

Thermal Radiation

Thermal radiation is considered here for completeness. Since thermal radiation varies with leaf temperatures, it is closely related to the energy budget equations which will be considered in subsequent chapters. At this time, I will assume all the leaf temperatures are known.

A leaf in the community 'sees' in an upward direction a fraction of sky and other leaves. 'Looking' downward it 'sees' a fraction of the soil surface and other leaves. (Idso (1968)). The thermal radiation moving downward in the crop TH_i is expressed as;

$$TH_i = (F\ 0\ S\ R_i) \cdot SK + (1 - F\ 0\ S\ R) \cdot \overline{TL}_i \qquad (31)$$

where F 0 S R is the fraction of thermal sky radiation which reaches the level i. Since thermal sky radiation (SK) is regarded as coming from an infinite hemisphere of uniform temperature, this fraction is identical

to the fraction of visible sky radiation penetrating to level i which was calculated above. $\overline{TL}_i$ is an average leaf temperature above the level i. A procedure has been outlined to divide leaf area into classes based on visible radiation loads. A similar procedure can be used to divide the leaf area of each increment into classes of total solar radiation loads. In Chapter IV a procedure is outlined to calculate the leaf temperature of each solar radiation class in each increment. Thus $\overline{TL}$ is weighted according to the leaf area in each radiation class as well as the proximity of the leaf area to the level i. Thus leaf temperatures in increment 1 would be weighted according to the fraction of diffuse radiation which would penetrate from increment 1 to increment i. The stored values of TR are used for this calculation.

A similar procedure can be used to calculate TH↑ or upward directed thermal radiation. The amount of thermal radiation (based on a soil temperature) coming from the soil replaces the sky radiation. A procedure to calculate soil temperature is given in Chapter IV.

All Components

The net radiation can now be calculated for a given level since all components of radiation moving upward or down can be calculated. Thus;

$$R_{n_i} = TH_i\downarrow - TH_i\uparrow + VR\downarrow - VR\uparrow + IR\downarrow - IR\uparrow$$

where VR↑ and VR↓ are the mean values of visible radiation moving upward and downward respectively. Similarly IR↑ and IR↓ are the near infrared components. Thermal radiation and leaf temperatures are discussed in more detail in Chapter IV. Also, comparisons between measured and theoretical profiles of net radiation are given in Chapter IV.

Materials and Methods

A verification of the visible radiation model was attempted by measuring mean radiation flux densities at various levels in stands of corn. These mean values (MV_i) are expressed by

$$MV_i = PT_i \quad (DI'/(\sin(IS) \times 100) + Sc_i\downarrow \qquad (32)$$

$DI/\sin(IS)$ was measured directly. Also measured was $Sc_1\uparrow$, which is the reflected radiation at the crop surface.

Measurements were made over a two-year period (1967, 1968) at the Ellis Hollow, Microclimate Investigations, Experimental Site near Ithaca, New York. A 200 acre field of corn was planted mechanically with a check row planter in an approximation of a hexagonal pattern.

Plants were in 38 cm north-south rows with approximately 46 cm between plant in the rows. A density of about 6 plants/m^2 was initially obtained. In the 1968 study, one-half of the 20 acre field was thinned at emergence to 4.3 plants/m^2. A leaf area index of 5.2 was attained in 1967. In 1968 the LAI's varied depending on thinning and stage of growth from 2.56 to 3.63. In 1968 light was measured at two different stages of growth, one stage just before anthesis and the other two weeks after anthesis.

Light Measurements

The method of measuring visible radiation was essentially that of Federer and Tanner (1966b). A selenium cell was mounted under a cosine correcting head and an 85 c Wratten filter. This combination gives the instrument an approximation to the photon response. That is, the instrument is more sensitive in the red region of the visible band compared to

the blue and compensates for the higher energy of the blue photon. The reasoning used here is that if each photon regardless of its wavelength contributes the same amount of excitation energy to the chlorophyll molecule, then a set number of photons should be the basic unit of radiation rather than an energy unit. A recent action spectra by Bulley, et al. (1969) working with radish leaves showed a variation of ±15% for constant incident quanta.

In this study each photocell was mounted in a threaded plexiglass holder which could be screwed into a cosine correcting head as shown in Figure (4). The head, machined from black plexiglass (Kaufman Glass Co., #2025 Black, Wilmington, Delaware), was similar in shape to the modified Scripps Head used by Kerr, et al. (1967).

Cosine correction depended on the exposed length of the diffusing filter and the distance from the diffusing filter to the top inside edge of the black plexiglass. These distances, were found by trial and error to be 0.130 cm and 0.470 cm respectively. The cosine response was measured by shining a collimated beam of light directly at the diffusing filter. The instrument was mounted vertically on a rotating stand. The response was measured as the instrument was turned through +90° to -90°. Per cent deviation from the cosine law is shown in Figure (5) for three different instruments.

The diffuse filter was made from white acrylic plastic (W = 2447, Kaufman Glass Co., Wilmington, Delaware). It was needed not only for cosine correction but also to reduce the light intensity. To insure a linear response to light intensity to improve stability of the cell, a .883 cm length of filter was used to reduce the incident flux density to

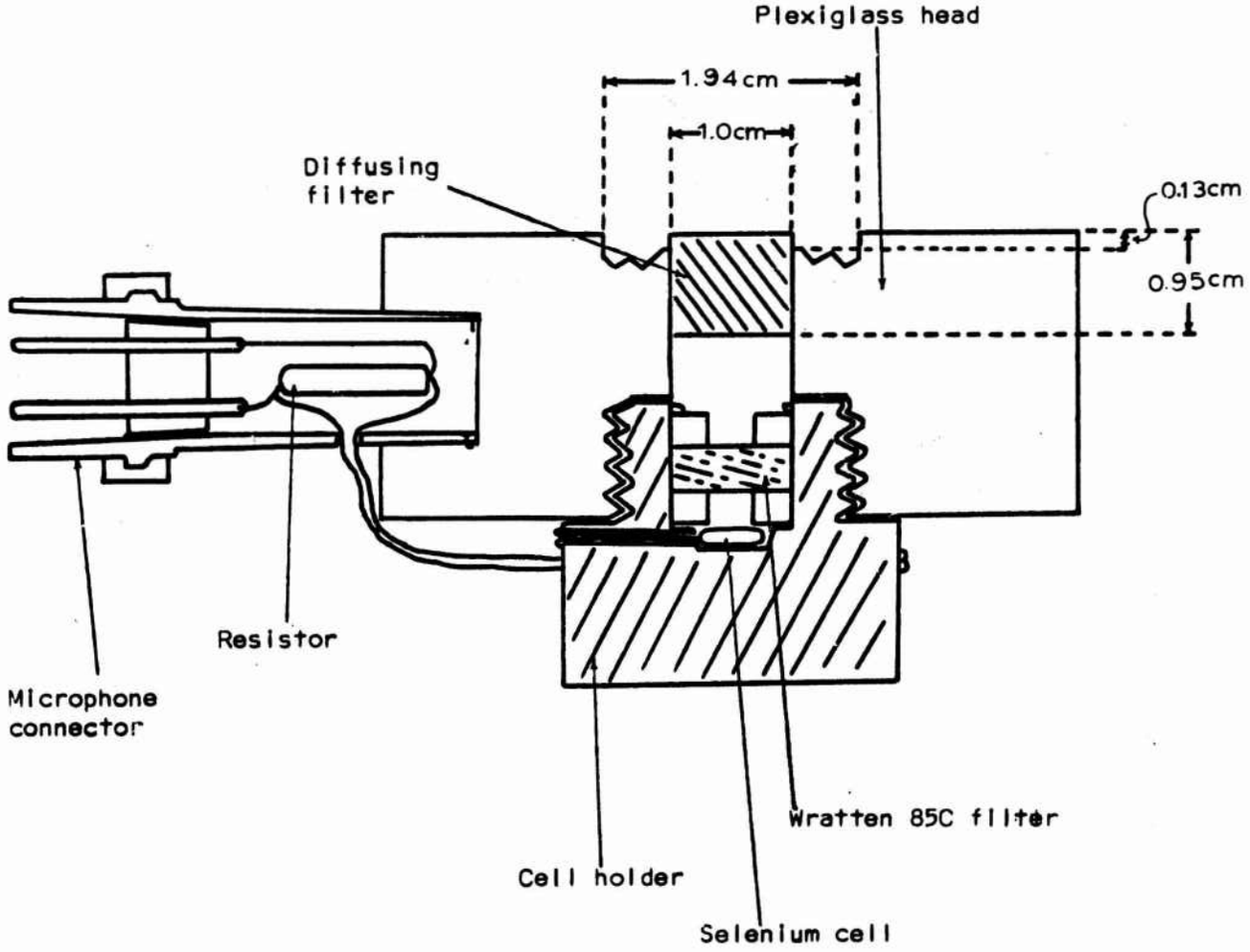

Figure 4. The Custom Mounted Visible Radiation Sensor. A selenium cell is mounted in a threaded plexiglass holder which is screwed into a cosine-correcting head.

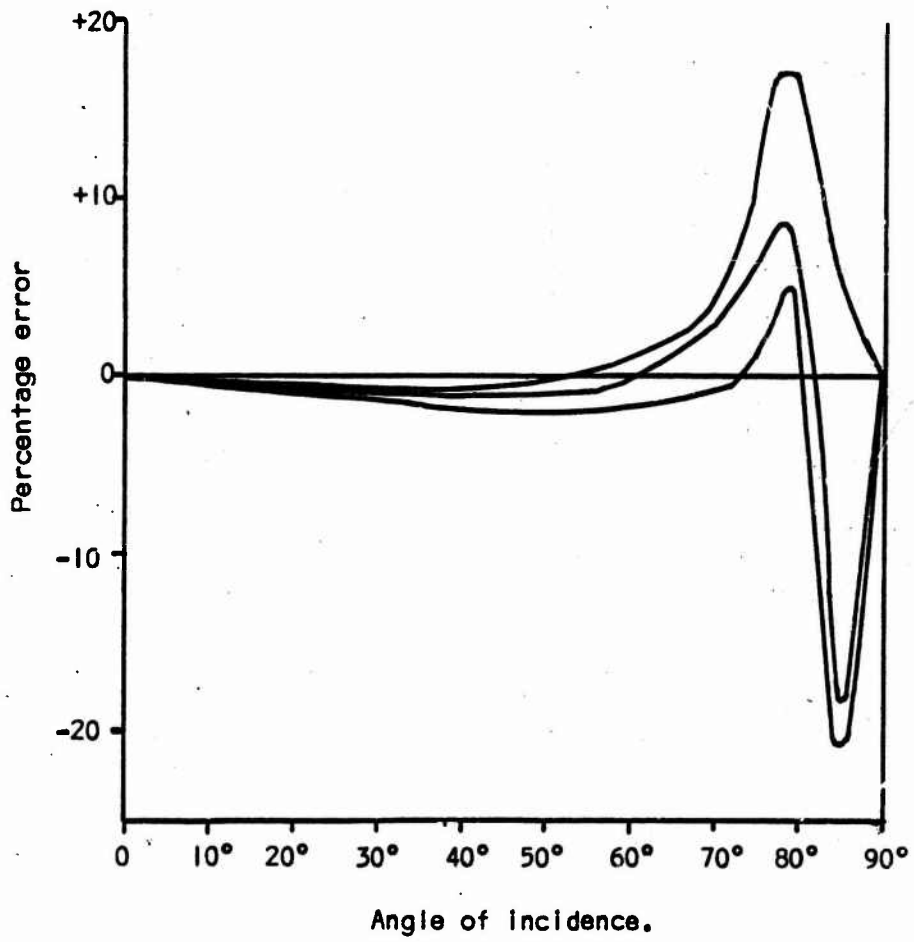

Figure 5. The percentage error from the cosine response for 3 individual cells.

about 8% of the original. The Wratten 85C filter (Eastman Kodak Co., Rochester, New York) was mounted underneath the diffuse filter and also helped to reduce the light flux density on the cell.

A precision carbon film resistor (80.2 ohms) was mounted inside a microphone connector (amphenol 80M C 2M). The cell output was recorded, as a change of potential across the resistor, on a digital recorder (A. D. Data Systems, Rochester, New York) accurate to ±20 microvolts. The response of the instrument in full sunlight was 1-2 millivolts.

There was an advantage to using a carbon film resistor and placing it near the selenium cell. Table (1) shows temperature coefficients with the resistor mounted both in the instrument and outside of it.

TABLE 1

Temperature Coefficients	C^{o-1}
Unit with mounted resistor	.00208
Unit with resistor at room temperature	.00407

The coefficients were measured by inserting a thermocouple junction into the cell holder so that it touched the edge of the cell without blocking any radiation. The instrument was then placed under a heat lamp of constant intensity and its millivolt signal recorded simultaneously with the temperature of the cell. The coefficients were averaged over a change of cell temperature from 15° to 60°C. The resistance of a carbon film

resistor decreases as its temperature increases. This tends to offset the increase with temperature in output from the cells.

In order to obtain an average light irradiance at a given level in the crop an adequate number of measurements have to be made to be representative of that level. During the course of this study, two sampling systems were used. The first system, used in 1967, consisted of aluminum channels (0.0254 x 0.0254 x 5.2 meters) with aluminum sensor holders machined to slide easily in the channels. Each light sensor was attached to an aluminum holder. This holder was pulled from one end of the channel to the other by a pulley system attached to a reversible gear motor (W. W. Grainger, Inc., Syracuse, New York). A tripping mechanism reversed the motor when a holder reached the end of its traverse.

In 1968, the aluminum channels were replaced by wire cable. At a particular level, a selenium cell was placed in a plexiglass holder through which two small outrigger cables were threaded. These outrigger cables were stretched between two welded conduit masts so that they were about 15 cm apart in the horizontal plane. The masts were held in place by guy wires attached to anchor plates. Very high tensions were applied to the outrigger cables and a span of 9 meters was obtained without serious drooping. The same pulley system, reversible gear motor and tripping mechanisms were used to drive the cell back and forth along the span. The cells moved at approximately 1.2 meters per minute. Readings were made every second. Five levels in each stand of corn were sampled.

Four larger versions of the light sensor described above were made using a larger cell (Type A-5, International Rectifier Corp.). They were used to measure incoming total visible, incoming diffuse visible

(sky) and reflected visible from crop surfaces. Diffuse visible was measured by placing a shade ring over a sensor blocking direct radiation from the sun.

All the visible radiation sensors were calibrated against two Epply pyranometers on clear days using the sun and sky as sources of radiation. A standard single domed Epply was used to measure solar radiation. A double hemisphere, high precision Epply pyranometer with a domed Schott RG8 filter as its outer hemisphere was used to measure near infrared radiation. The reading from this latter pyranometer was corrected according to Drummond and Roche (1965). The difference between solar and near infrared radiation was assumed equal to the amount of visible radiation. Values of visible radiation were converted from energy units to μ einsteins/cm^2 sec using the spectral distribution of sun and sky radiation measured by Federer and Tanner (1966a).

Leaf Measurements

As indicated in the theoretical discussion, the leaf area and leaf angle distribution as functions of light are needed in the radiation model. These variables were measured using an improved version of the grid method developed by Loomis et al. (1969). Corn is essentially a two-dimensional plant. Thus, it is possible to place a plant in a natural position against a large grid. In this case, the grid was made up of 1 dm squares. Coordinates were noted whenever leaves crossed vertical lines. The variety of corn (Cornell M-3) used in this study projected its leaves further in the horizontal than the vertical. Thus the intersections with the vertical lines gave a more detail measure of the leaf shape than intersections with the horizontal lines as used by Loomis et al. (1969).

Leaf widths were measured between two sets of coordinates. Figure 6 shows a typical leaf segment against part of the grid. The leaf segment between (x_1,y_1) and $x_2,y_2)$ was approximated by a straight line. The leaf width (W_1) was measured at 0. The area (A) of this segment is expressed in dm^2 as

$$A = W_1 \cdot \sqrt{1 + (y_2 - y_1)^2} \tag{33}$$

The angle (IL) of the leaf segment is found from

$$IL = \arctan (y_2 - y_1) \tag{34}$$

In figure (6), the leaf segment crosses a horizontal line. Since a knowledge of leaf area as a function of height was necessary, A must be divided into A_1(between 1-2 dm) and A_2(between 2-3 dm). These are found from

$$A_1 = W_1 \cdot (x^2 + (2 - y_1)^2)^{1/2} \tag{35}$$

and

$$A_2 = W_1 \cdot ((1 - x)^2 + (y_2 - 2)^2)^{1/2} \tag{36}$$

where x is found from the equation of a straight line,

$$x = x_1 + \frac{x_2 - x_1}{y_2 - y_1} (2 - y_1) \tag{37}$$

A computer program was written to do the above calculations for each leaf segment. All necessary information is supplied if a leaf width is provided with the two sets of coordinates on an I.B.M. card. The program can take the information on cards and calculate the leaf area and leaf angle distributions as functions of height directly. No extensive log for each plant needed to be made. In this study 15-20 plants were measured for each plant density considered.

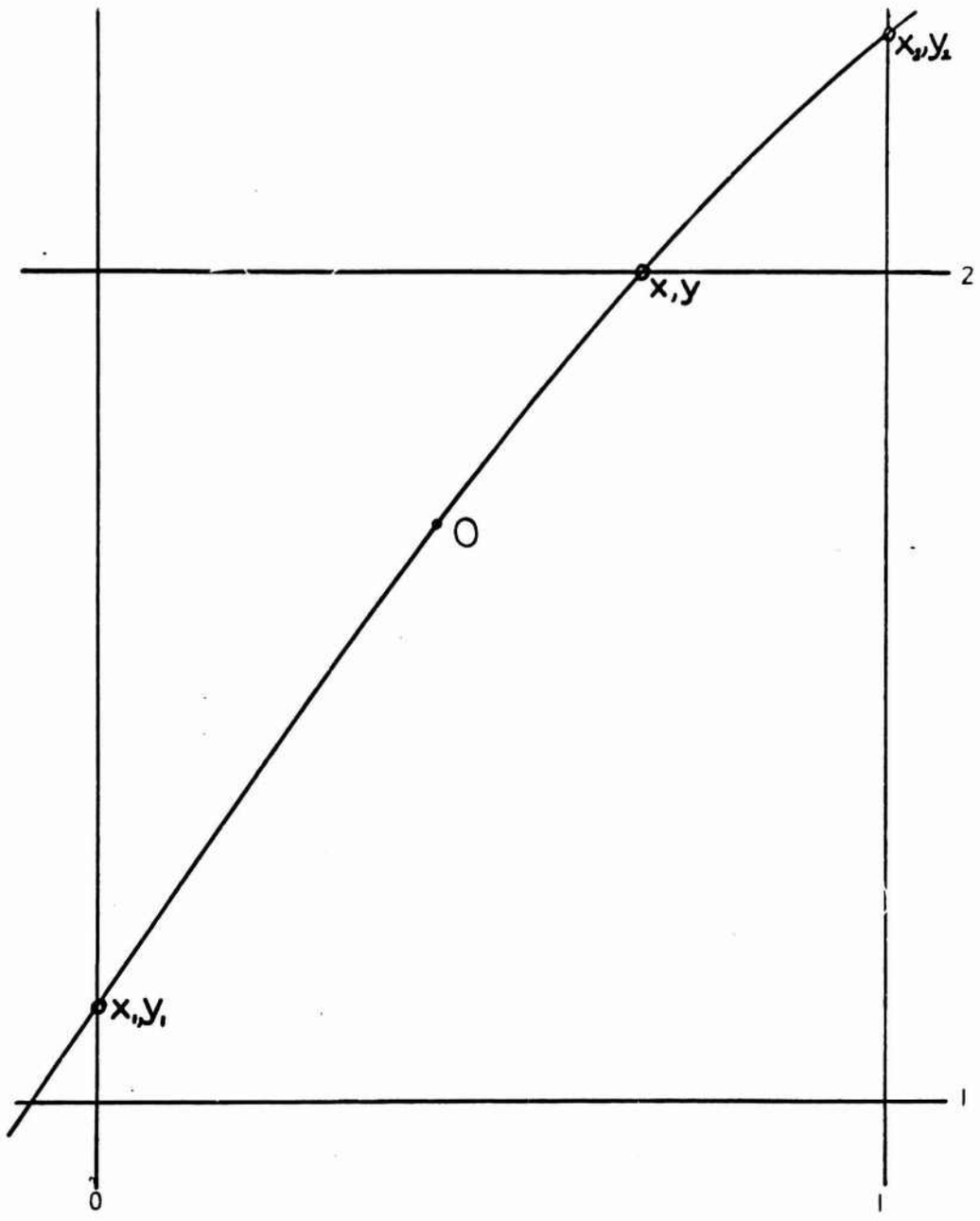

Figure 6. A leaf segment (x_1,y_1), (x_2,y_2) between 1 and 3 dm of height in corn.

Results and Discussion

The purpose of the visible radiation measurements was to obtain an average irradiance at a particular level in the crop to compare with calculations from the model. An average value (AVE) is defined as:

$$AVE = \frac{\int_0^D R_x \, d_x}{\int_0^D d_x} \tag{38}$$

where R_x is the response of the instrument at a particular distance along the sampling track. D_1 is the length of this track. Supposedly the area covered by the width of the sensing head times D_1 is representative of the crop for that particular level. In actual fact the above integration is replaced by spot readings at various positions on the track. Since these readings are at regular small finite intervals one can write;

$$AVE = \frac{\int_0^D R_x \, d_x}{\int_0^{D_1} d_x} \approx \frac{\sum_{i=1}^{N} R_x \cdot \Delta_x}{N\Delta_x} = \frac{\sum_{i=1}^{N} R_x}{N}$$

where N is the total number of observations.

One can calculate a series of running averages for increasing lengths along the track (Figure 7). The fact that the averages approach a constant value as $x \to D$ assures obtaining a representative value for the crop.

Measurements of the plant structure are needed in the model. Figures (8-12) show measurements of leaf area densities, cumulative leaf area indexes and cumulative leaf angle distributions for several densities of

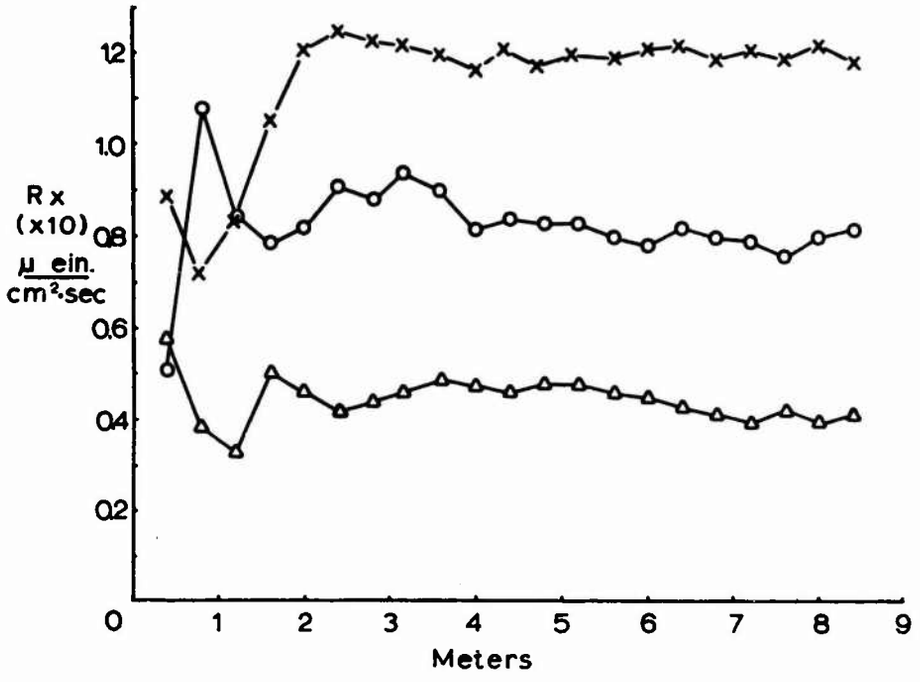

Figure 7. A running average (Rx) as a function of distance along the sampling span for three heights in a stand of corn. L.A.I. = 3.63

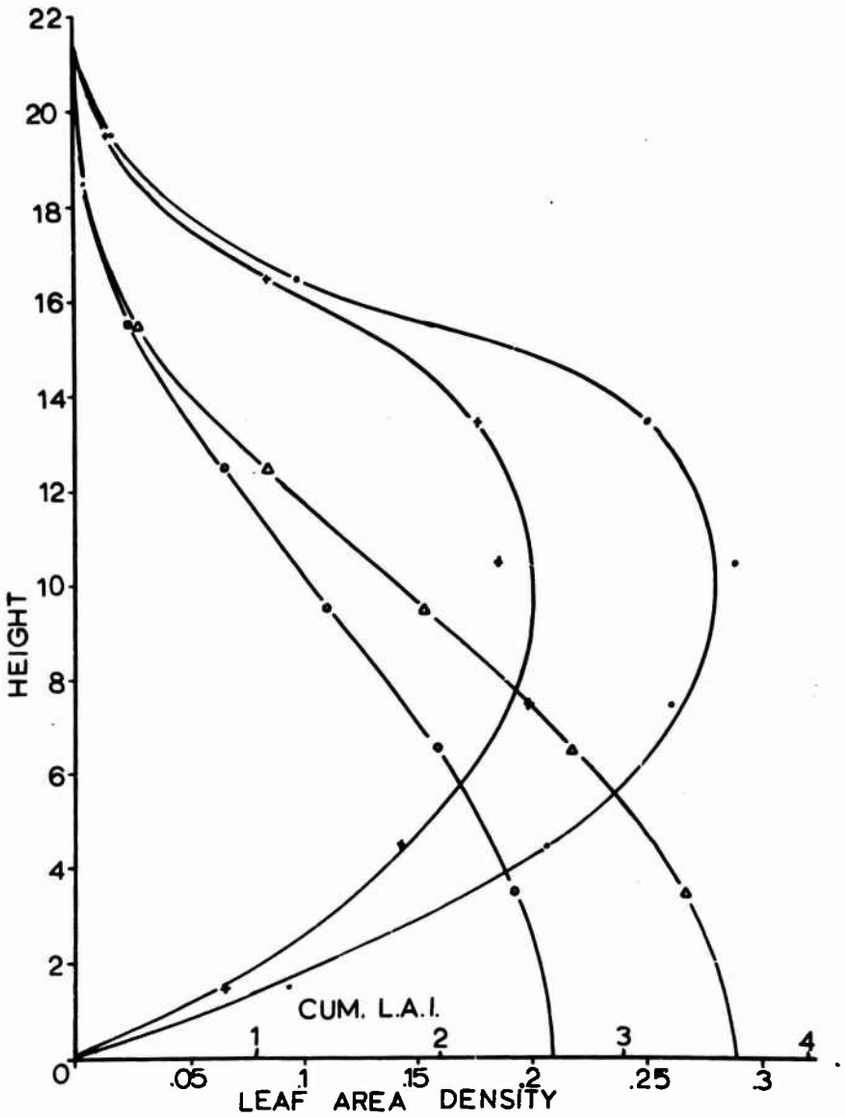

Figure 8. Cum. L.A.I. and leaf area density for two stands of corn as functions of height (1968 study).
(Δ) represents cum. L.A.I. of the stand with total L.A.I. = 3.63.
(o) represents cum. L.A.I. of the stand with total L.A.I. = 2.60.
(•) represents leaf area density $(\frac{dm^2}{dm^3})$ of the stand with total L.A.I. = 3.63.
(+) represents leaf area density $(\frac{dm^2}{dm^3})$ of the stand with total L.A.I. = 2.60.

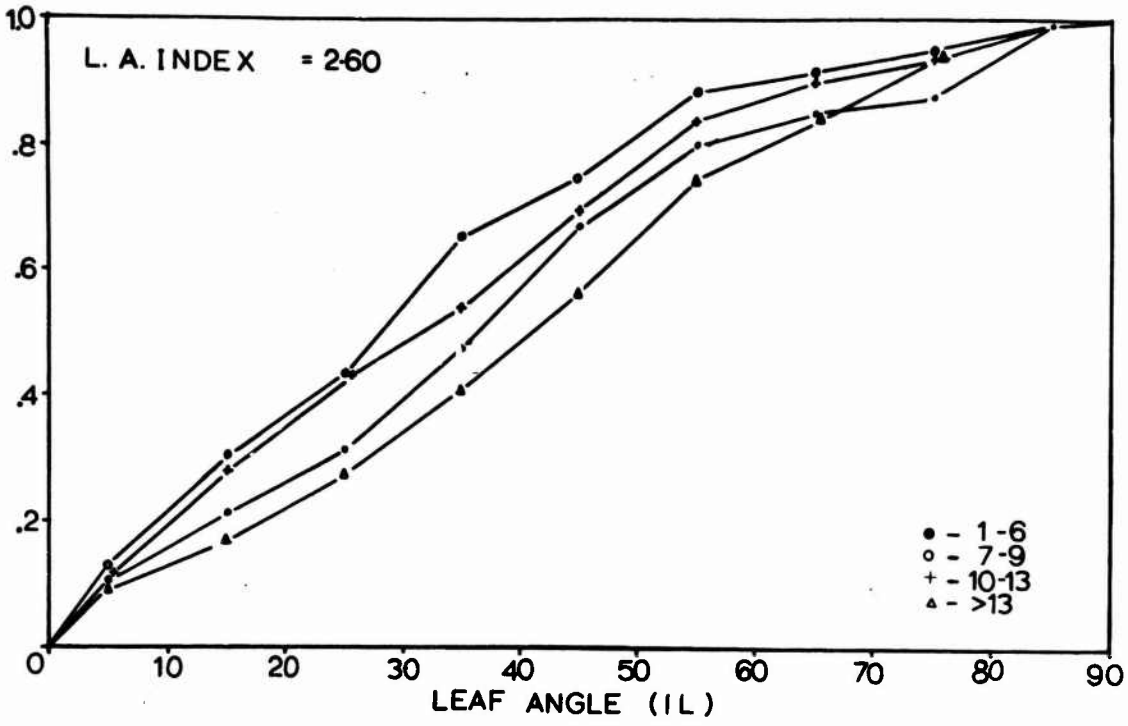

Figure 9. Cumulative leaf angle distribution for the stand of L.A.I. = 2.60. The leaf area is divided into increments of 1-6 dm, 7-9 dm, 10-13 dm and > 13 dm (Study made in 1968).

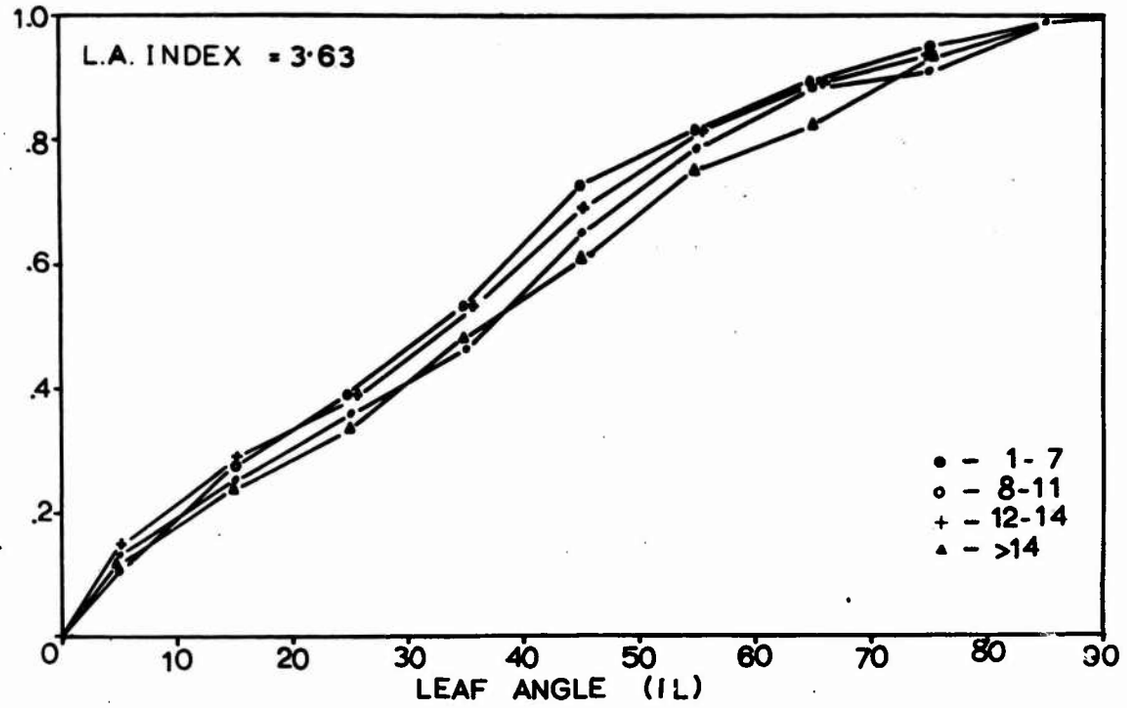

Figure 10. Cumulative leaf angle distribution for the stand of L.A.I. = 3.63. The leaf area is divided into increments of 1-7 dm, 8-11 dm, 12-14 dm and > 14 dm (Study made in 1968).

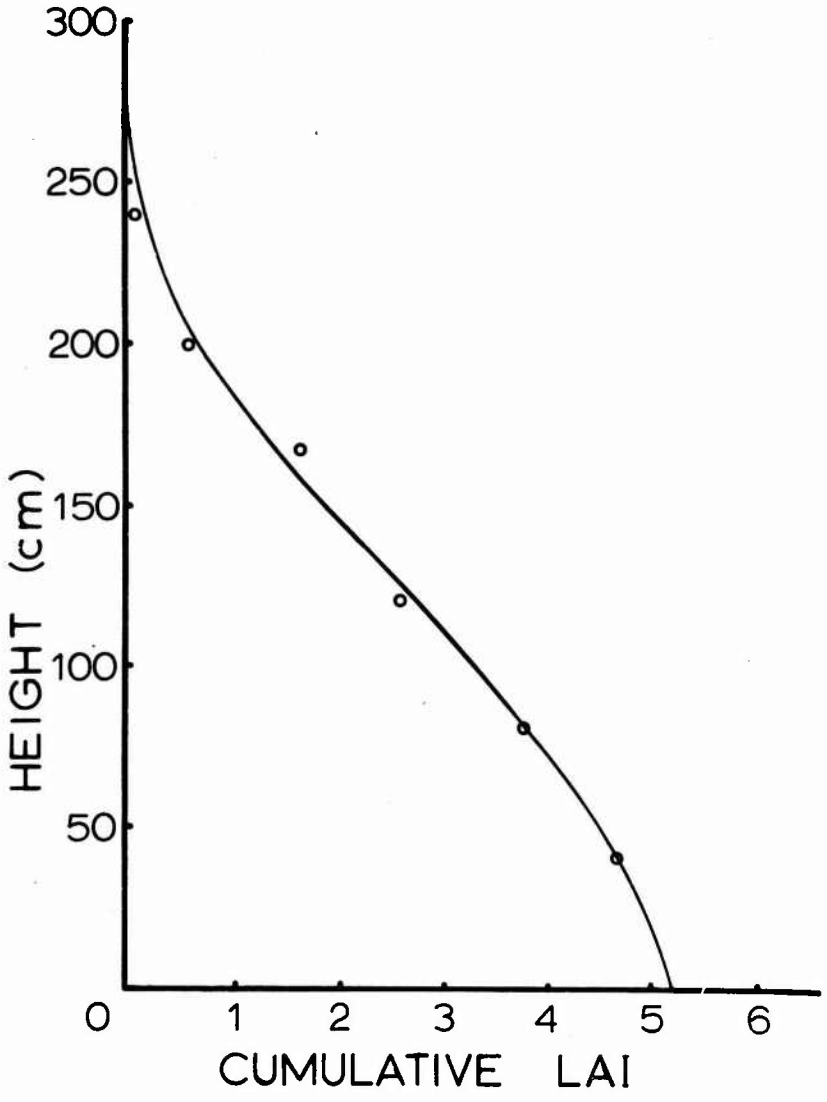

Figure 11. Cumulative leaf area index (CUM. L.A.I.) for the 1967 stand of corn. (L.A.I. = 5.2).

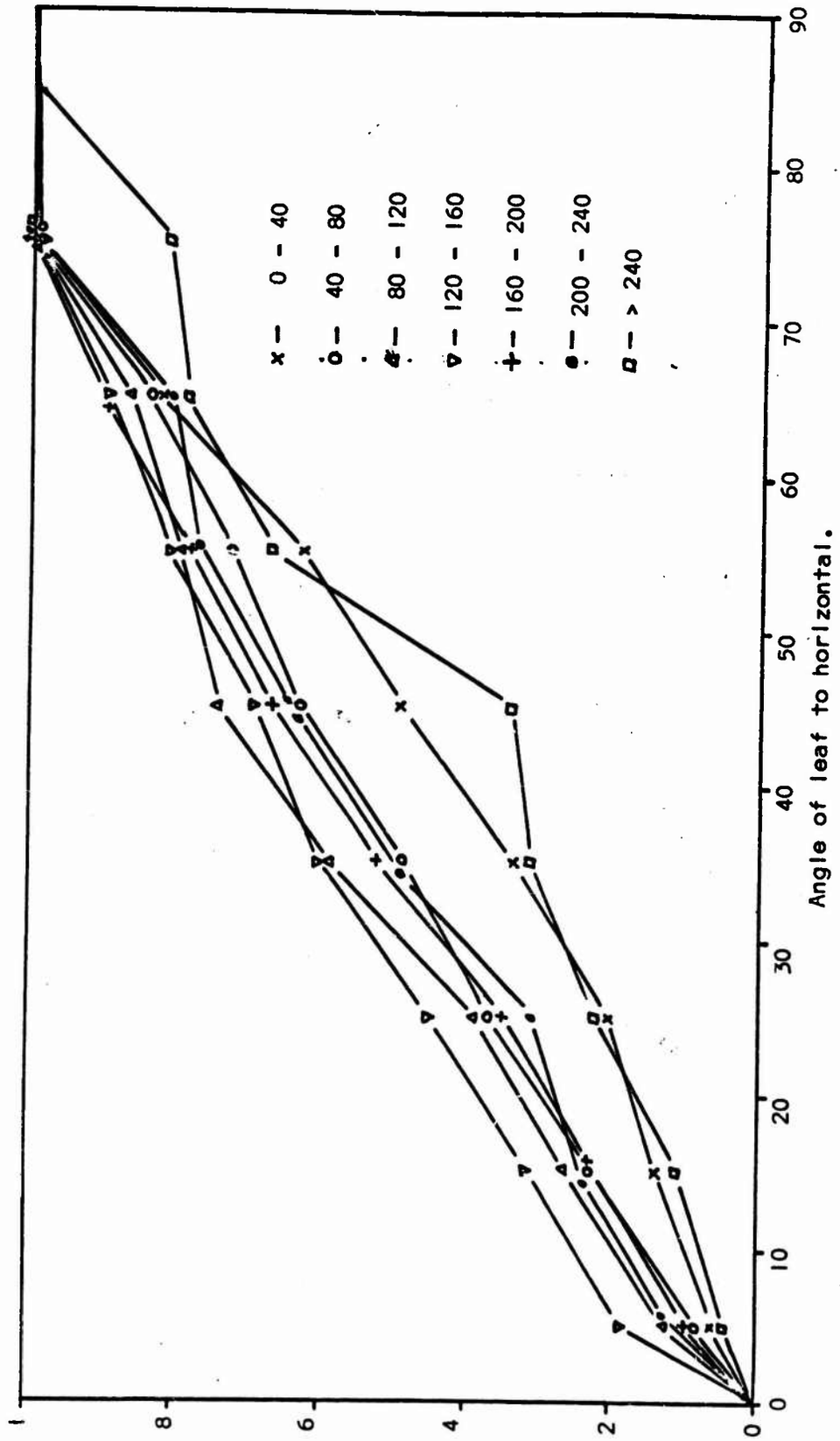

Figure 12. Cumulative leaf angle distribution for the stand of corn with L.A.I. of 5.2 (Study made in 1967).

corn. The leaf angle distributions are of particular interest. Leaf area is distributed approximately equally over the angle classes. The distributions tend to be slightly planophil (more horizontal leaves than erect) especially near the ground. These measurements contrast with the spherical distributions Nichiporovitch (1960) found for corn.

Figure (13) represents calculations using both the de Wit and Duncan models for a leaf area index of 3.63 and a sun angle of 52°. The de Wit and Duncan models give approximately the same answers for small values of S. Reducing S from 0.202 to 0.140 made little difference in the de Wit model. All calculated values agree reasonably well with measurements.

Figures (14-17) represent calculations of the Duncan Model compared with actual measurements in several stands of corn at various sun angles. The measurements differ from one another not only for sun angle but also in the proportion of incoming diffuse or sky radiation. While attempts were made to measure only when the sky was relatively cloud free, especially near the sun, perfectly clear skies are rather rare at the location of the field site.

The 1967, data were taken in a stand of corn which had a higher L.A.I. and in general was more uniform than the 1968 stands of corn. Thus, Figure (14) shows slightly better agreement with the model than the 1968 studies (Figures 15, 16).

In the 1968 measurements, certain trends are noticeable. Measurements below a L.A.I. of 2. tend to be higher than the calculations. These deviations tend to increase with lower sun angles. The lowest angle reported shows a wide deviation from the model but these low irradiance levels are much more difficult to measure exactly.

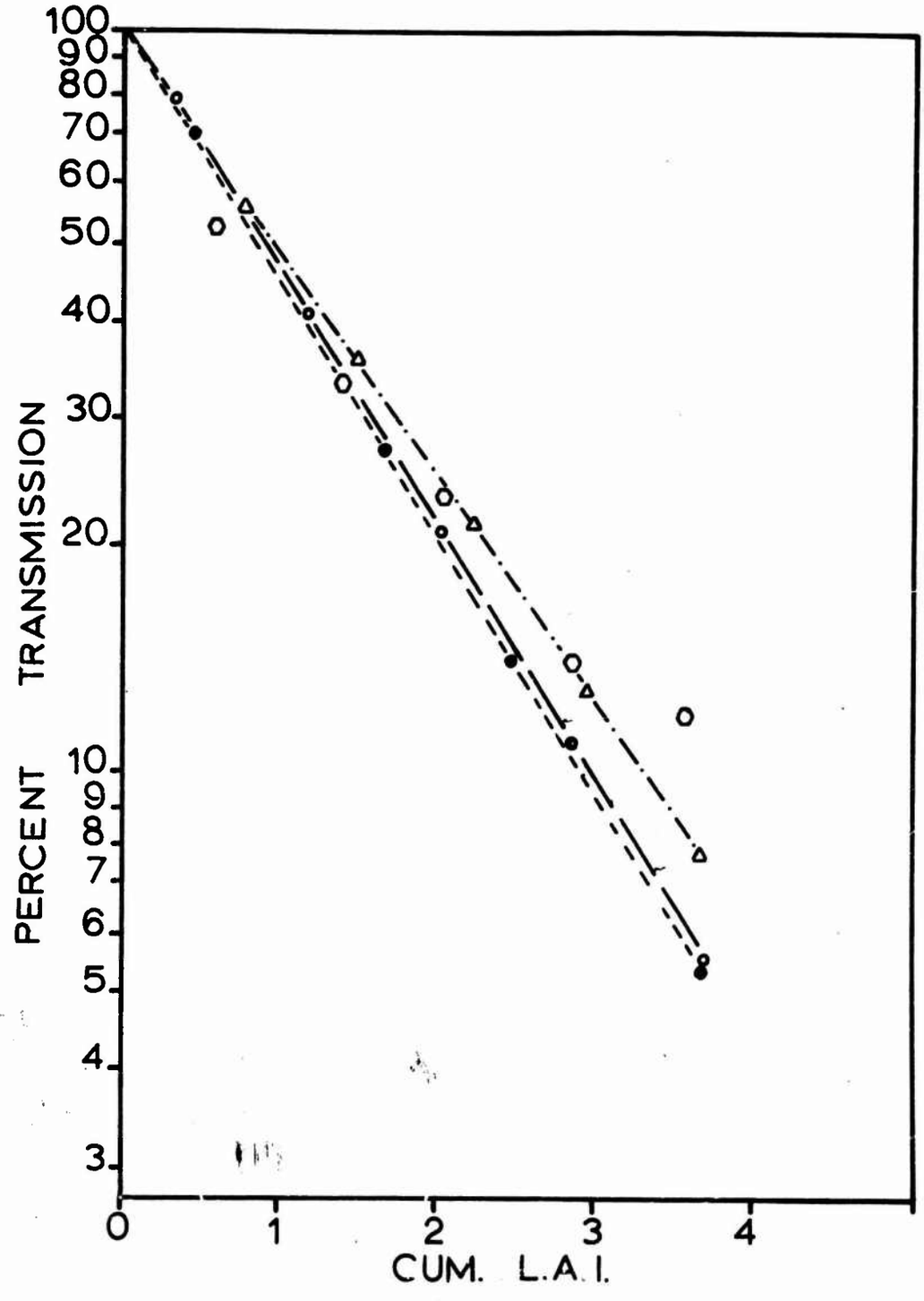

Figure 13. Per cent transmission as a function of cum L.A.I.
(o) represents the de Wit model with S = .202.
(•) represents the de Wit model with S = .140.
(Δ) represents the Duncan model with S = .726.
(O) represents actual measurements.

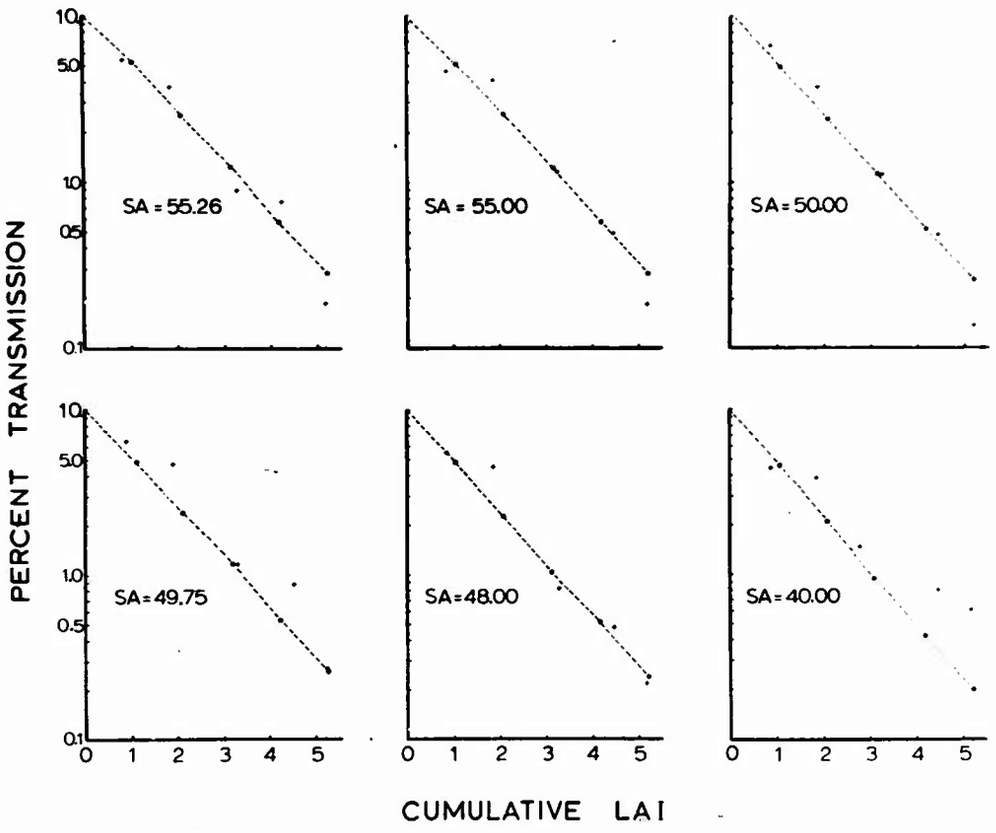

Figure 14. Per cent transmission as a function of cumulative leaf area index (1967 studies).
--●-- Theory
\+ Measurements

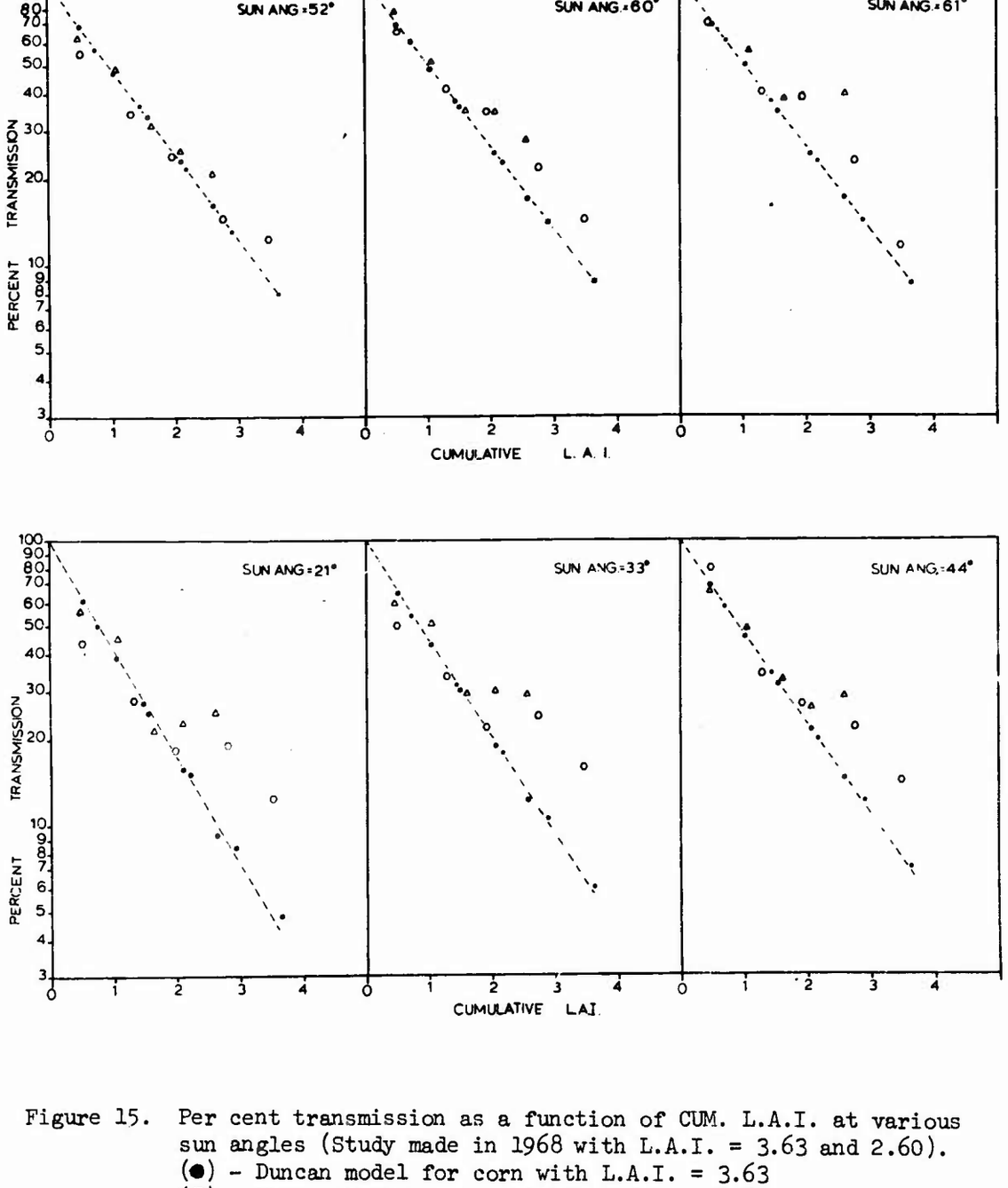

Figure 15. Per cent transmission as a function of CUM. L.A.I. at various sun angles (Study made in 1968 with L.A.I. = 3.63 and 2.60).
(●) - Duncan model for corn with L.A.I. = 3.63
(O) - Measurements for corn with L.A.I. = 3.63
(o) - Duncan model for corn with L.A.I. = 2.60
(Δ) - Measurements for corn with L.A.I. = 2.60

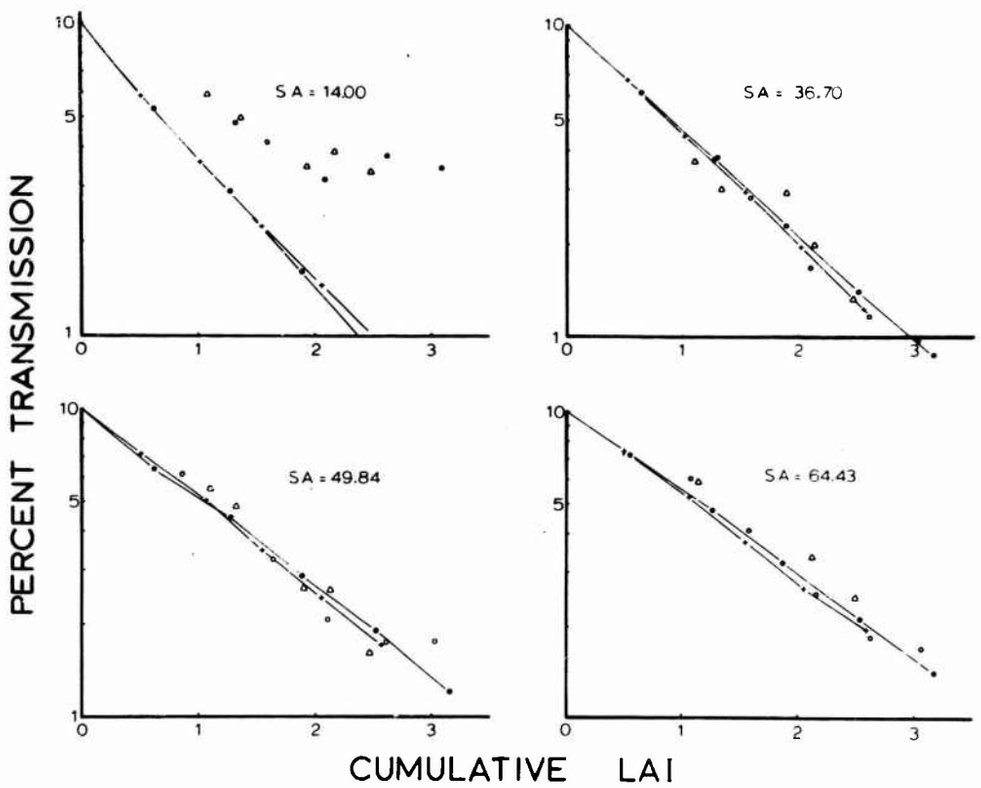

Figure 16. Per cent transmission as a function of CUM. L.A.I. at various sun angles (Study made in 1968 with L.A.I. = 3.13 and 2.38).
(●) Duncan model for corn with L.A.I. = 3.13
(o) Measurements for corn with L.A.I. = 3.13
(+) Duncan model for corn with L.A.I. = 2.38
(Δ) Measurements for corn with L.A.I. = 2.38

The Duncan model assumes random distribution of leaf area. Corn planted in a 15" hexagonal pattern with plants oriented randomly about their stems should give a good approximation to this random distribution. Any point in the canopy could have leaves from four to five plants in its vicinity. Another assumption is independence between leaf increments. If a plant is missing from the above pattern which invariably happens in large plots of machine planted corn, a certain amount of dependence between levels is introduced. This would allow more light into the lower levels than the model would predict and would give a larger error for corn with a lower L.A.I.

Figure (17) is particularly interesting as it represents measurements from a completely overcast sky. The agreement of measurements with the model is particularly encouraging for this rather extreme type of cloud cover. However, the effects of reflection from cloud banks for partially overcast skies have not been studied here and could lead to serious errors for partially cloudy days.

The scattering theory is tested in figure (18). Where the proportion of reflected radiation is plotted as a function of sun angle for both calculated and measured values. There is reasonably good agreement between the model and calculations at sun angles from 55° to 65°. There is a tendency for the model to overestimate at the highest sun angles (60-65°). As sun angle decrease below 50°, the model underestimates the measured values in increasing amounts. This deviation is probably due to specular reflection from the leaf surfaces. In the model we assume all light is reflected diffusely. Because the amounts of radiation involved are quite small, these discrepencies shouldn't influence a

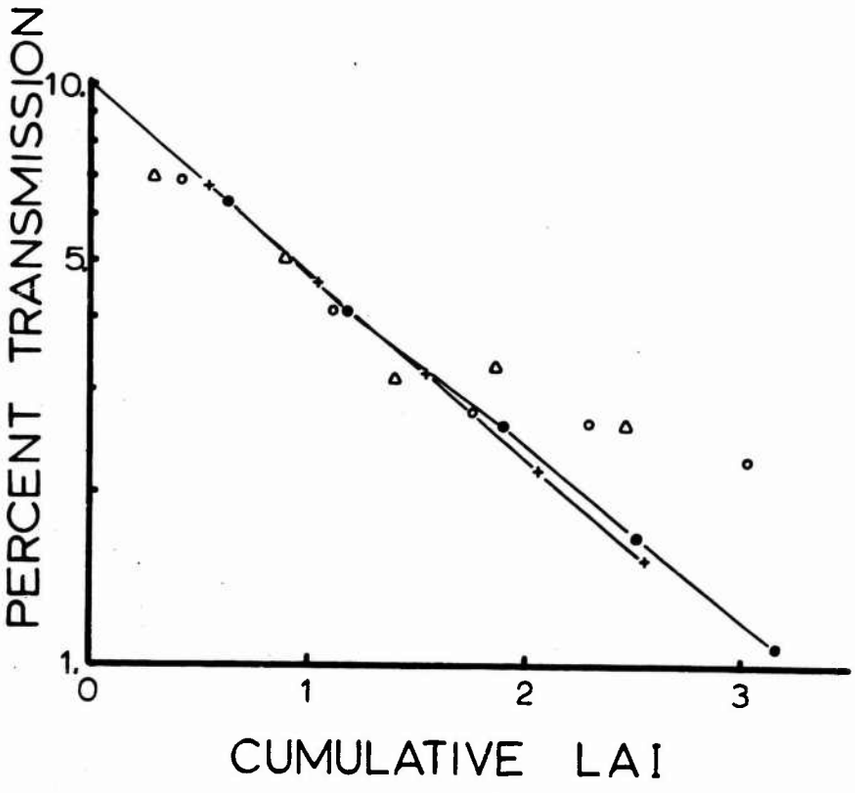

Figure 17. Per cent transmission as a function of cumulative leaf area index when the sky was completely overcast.

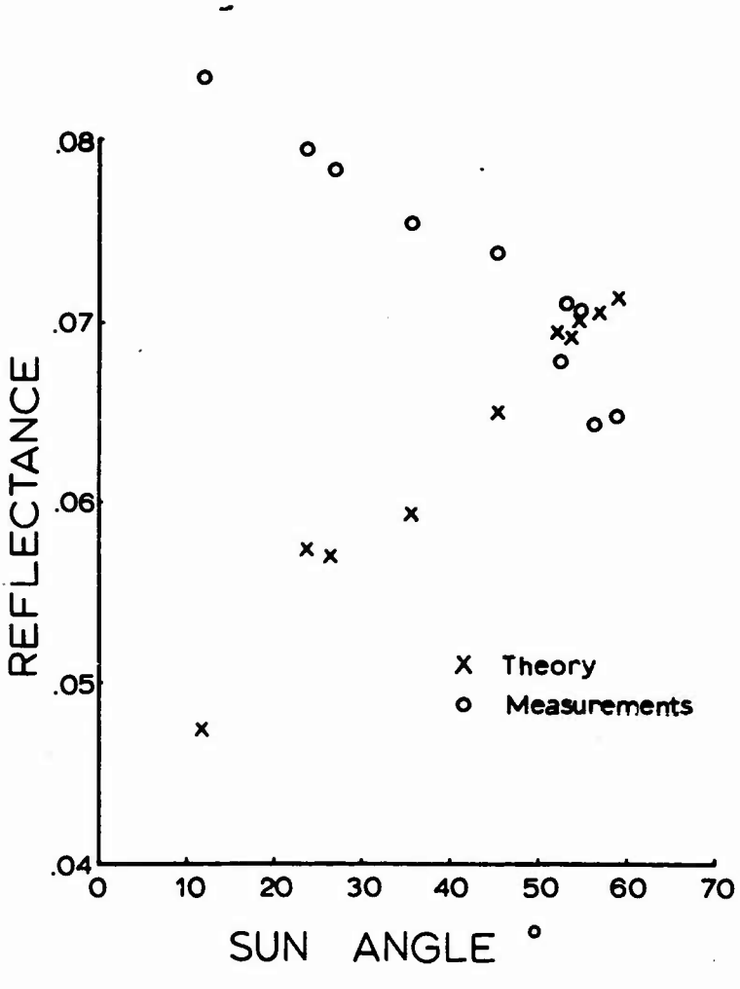

Figure 18. Reflectance of visible radiation from the crop as a function of sun angle.

photosynthesis model. However the scattering theory introduced in this study is not good enough when the measure of reflected radiation is the prime concern such as in remote sensing situations.

Conclusions

The radiation model based on a random distribution of leaf area successfully predicts the penetration of visible radiation into corn. There is a tendency to overestimate amounts of radiation at the bottom of the stands at the lower leaf area indexes. However, this was not considered a serious error. In fact, one could argue that if the leaf area surrounding gaps in the planting pattern is small compared with the total leaf area, the model will describe the light regime better than the measurements as far as calculations for photosynthesis are concerned.

The basic equations relating percent transmission to cum. leaf area index from both the de Wit and Duncan models were tested in this study. They gave essentially the same answers when S, the amount of leaf area per increment, less than 0.2 was used. The Duncan equation was favored because it was independent of S and thus less empirical. Also final answers could be obtained with fewer calculations as the leaf area could be divided into larger increments.

In general, the agreement between equations and measurements was sufficiently good that a general photosynthesis model was constructed based on the development outlined above. Various parts of this model will be considered in subsequent chapters.

Chapter II

A LEAF PHOTOSYNTHESIS MODEL

In many instances, one can best treat a crop in terms of an array of leaves. Thus, it is particularly useful to first mathematically model the responses of individual leaves. This process incorporates a large amount of information into the concise form of mathematical equations. The information is then readily accessible when one integrates over the total leaf area in a crop response model.

In this study a mathematical treatment is developed to describe net photosynthesis of leaves as a function of temperature, CO_2 concentration at the leaf surface and light flux density. At this stage, the model is highly specific to corn and other tropical grasses. The model is tested against experimental leaf chamber measurements. The measurements were made on attached leaf blades of field grown corn.

Theoretical Considerations

Representing gaseous exchange characteristics of a leaf by a network of resistances is becoming increasingly common. (For example, Moss (1966), Lake (1967) and Waggoner (1969)). The representation by Lake is the most detailed, and with some modification, is presented in Figure (19). In this figure, r_s is the stomatal resistance, r_i is the resistance of the cell walls, r_m, r_{w1}, and r_{w2} are internal cell resistances and r_c is a carboxylation resistance to be defined below.

A corn leaf under a visible radiation load releases very little or no CO_2 into a CO_2 free environment even when the stomates are open (Moss (1966)). It is generally agreed that r_s, r_i and r_m are of the same order of magnitude, (Waggoner (1969)). Therefore for corn, r_{w2} is much greater than r_{w1} and Figure (19) can be simplified to Figure (20).

Following Chartier (1966b), (1969) and using Figure (20), net photosynthesis (N) and gross photosynthesis (P) can be expressed as

$$N = \frac{C - C_1}{r_s + r_m} \tag{39}$$

and

$$P = \frac{C - C_1}{r_s + r_m} + R \tag{40}$$

where R is respiration and C_1 is the concentration of CO_2 at the chloroplasts. Rabinowitch (1951) derived an expression relating C_1, light irradiance(I) and P by assuming the following equations;

$$P = k_1[A]\, C_1 \tag{41}$$

$$P = k_2[ACO_2]\, [H] \tag{42}$$

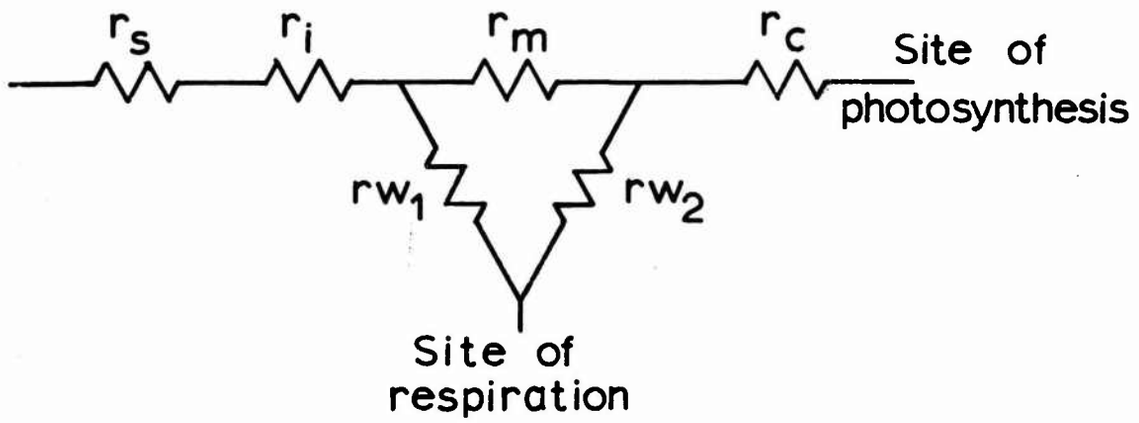

Figure 19. The resistance network for a leaf: a modification of the network by Lake (1967).
r_s - stomatal resistance
r_i - cell wall resistance
r_m, r_{w1}, r_{w2} - internal cell resistances
r_c - carboxylation resistances.

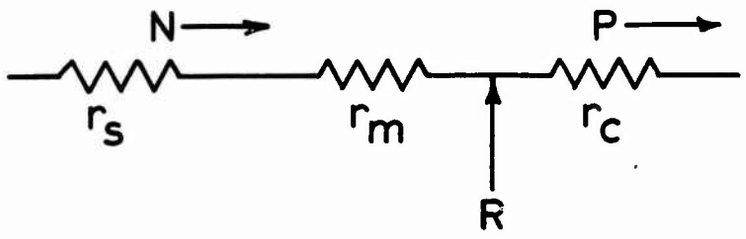

Figure 20. A simplified resistance network for a leaf
N - net photosynthesis
P - gross photosynthesis
R - respiration

and $$[H] = k_3 I \quad . \tag{43}$$

[A], [ACO_2] and [H] are concentrations of ribulose diphosphate, phosphoglyceric acid and triphosphopyridine nucleotide respectively. k_1, k_2 and k_3 are proportionality constants. Combining equations (41-43) one obtains;

$$P = \frac{\alpha I}{1 + \frac{\alpha r_c}{C_1} I} \tag{44}$$

where $$\alpha = k_2 k_3 A_o \tag{45}$$

and $$r_c = \frac{1}{A_o k_1} \quad . \tag{46}$$

When C_1 is eliminated from equation (40) using (44), the following quadratic is obtained:

$$(r_s + r_m)P^2 - P[\alpha I(r_s + r_m + r_c) + C + R(r_s + r_m)] + C\alpha I + R\alpha I(r_s + r_m) = 0 \tag{47}$$

The stomatal resistance under conditions of no water stress often appears as a hyperbolic function of I of the form;

$$r_s = \gamma + \frac{\beta}{I + I'} \tag{48}$$

where γ, β and I' are constants (Kuiper (1961)). Its incorporation here is an improvement on Chartier's (1966b) treatment where he assumed r_s was a constant. In equation (48) the differential of P with respect to I at P and I equal to zero is found as

$$\left.\frac{\partial P}{\partial I}\right|_{\substack{P = 0 \\ I = 0}} = \alpha \tag{49}$$

When I is large, $P \rightarrow P_M$ and $r_s \rightarrow \gamma$

Equation (47) reduces to

$$P_M = \frac{C + R(\gamma + r_m)}{\gamma + r_m + r_c} \tag{50}$$

Let $N_M = P_M - R$ (51)

Then $$N_M = \frac{C + R(\gamma + r_m) - R(\gamma + r_m + r_c)}{\gamma + r_m + r_c} \tag{52}$$

or $$N_M = \frac{C}{\gamma + r_m + r_c} - \frac{R\, r_c}{\gamma + r_m + r_c} \tag{53}$$

The second term on the right in (53) is small and a good approximation of N_M is given by;

$$N_M = \frac{C}{\gamma + r_m + r_c} \tag{54}$$

Finally by adding r_c to both sides of equation (47) one obtains

$$r_c = (r_s + r_m + r_c) - \frac{\alpha I(r_s + r_m + r_c) + C + R(r_s + r_m)}{P} + \frac{CI\alpha + R\alpha I(r_s + r_m)}{P^2} \tag{55}$$

Thus r_c, and $\gamma + r_m + r_c$ can be found experimentally from a series of measurements of net photosynthesis at various light flux densities at a known concentration of CO_2. The procedure will be considered in more detail below.

In this treatment, photosynthesis (P) is assumed independent of temperature. However, temperature effects on N are introduced via the

respiration term (R). Following Waggoner (1969), the respiration rate can be expressed as

$$R = R_x \, EXP[9000 \ln(Q) \, (\frac{1}{303} - \frac{1}{T})] \tag{56}$$

where R_x is the respiration rate at 303°K. The temperature T is in °K. Q is the rate of increase of R for each 10° rise in temperature and is assumed equal to 2. Note that "photorespiration" has been ignored here which again limits this development to corn and other efficient tropical grasses (Moss (1966)).

In summary, net photosynthesis (N) can now be expressed as the following function of light irradiance (I), CO_2 concentration at the leaf surface (C) and temperature (T);

$$N = \frac{-B_x - \sqrt{B_x^2 - 4A_xC_x}}{2A_x} - R \tag{57}$$

where $R = R_x \, EXP[9000 \ln Q \, (\frac{1}{303} - \frac{1}{T})$ (58)

$$A_x = r_s + r_m \tag{59}$$

$$B_x = -(\alpha I(r_s + r_m + r_c) + C + R(r_s + r_m)) \tag{60}$$

and $$C_x = C\alpha I + R\alpha I(r_s + r_m) \tag{61}$$

Materials and Methods

Leaf chamber measurements were made by Dr. R. B. Musgrave of the Cornell University Agronomy Department. The leaf chamber has been described in detail by Heikel (1968). In brief, the chamber is of the semi-open type. That is, air enters an inlet port to the leaf chamber and out via an outlet port as in an open system. While in the leaf chamber, air is rapidly recirculated through the chamber and a set of cooling coils. This recirculation keeps the air at a high turbulence level and provides control of the leaf temperature. Also the air inside the chamber, because of the rapid mixing, is at a uniform concentration of CO_2. Net photosynthesis is calculated from measurements of the flow rate at the inlet and/or outlet port and the CO_2 concentration difference between the inlet and outlet ports. The CO_2 concentration inside the chamber can be varied by adjusting the flowrate into the chamber. Input air is drawn from a large mixing tank to avoid the usual fluctuations of CO_2 concentration in the ambient air under field conditions. The leaf chamber is large enough to enclose one whole leaf-blade. It is also quite mobile so that attached leaves of field corn can easily be measured. Leaf temperature is controlled to a maximum variation of $\pm 2^{\circ}C$(Heikel and Musgrave (1969)). In this study, the radiation load was supplied by a bank of incadescent lamps (Sylvania, #300PAR56/2NSP). These particular lamps transmit 60 percent of the infrared radiation through the back of the lamp. This considerably reduces the heat load on the leaf. Light irradiance levels on the leaf were changed by placing layers of cheese-cloth between the lamps and the leaf chamber. The irradiance in the chamber under various numbers of cheesecloth layers was measured by an

uncorrected Weston sun-light meter. The readings were converted to μ einsteins/cm^2sec using conversion factors of Gaastra (1959).

Measurements were made at the Microclimate Investigations Experimental Site in Ellis Hollow near Ithaca, New York during July and August, 1968. The variety measured was Cornell M-3. The measurements were made in the same field as, and in cooperation with, studies of natural exchanges of CO_2, heat and water vapor between a corn crop and the environment conducted by Dr. E. R. Lemon and associates. Individual leaf measurements of net photosynthesis at full sunlight intensity were made on various leaves of several plants. More important to this study were measurements of net photosynthesis as a function of light intensity at a constant concentration of CO_2 on two separate leaves. Net photosynthesis as a function of CO_2 concentration at a constant light flux density (0.230 μ einsteins/cm^2sec) was measured on one leaf. Respiration rates at 30°C were also measured in the leaf chamber.

Field measurements of stomatal resistance as a function of light flux density were rade independently of the leaf chamber measurements by R. W. Shawcroft[1]. A Van Bavel porometer (Van Bavel et al. (1965)) was used to measure stomatal resistance to water vapor diffusion of leaves in their natural positions in the field. The resistance to diffusion of CO_2 was obtained by multiplying the resistances to water vapor by the ratio of the diffusion coefficients for water vapor and for CO_2 in air. Measurements were made at various times on a clear day on both shaded and unshaded leaves to obtain stomatal resistances at a large range of light flux densities. Resistances of the upper and lower surface of the leaf were added in parallel to give the total resistance of the leaf.

---

[1]Unpublished data to be submitted in partial fulfillment of the Ph.D. requirements at Cornell University.

Immediately after making a stomatal resistance measurement the light sensor described in Chapter I was placed parallel and close to the leaf plane to obtain the light flux density at the leaf surface. A similar procedure was used by Turner (1969). The data were fitted by regression to the hyperbola described by equation (48) to obtain values of γ, β and I'. The measurements were made when soil moisture was not limiting. This theory is extended in Chapter IV to conditions of water stress by increasing the value of γ.

Results and Discussions

In equations (57-61), unknown leaf parameters are R_x, r_s, r_m, r_c and α. R_x is the leaf respiration at 303°K. From measurements in a dark leaf chamber, R_x was found to be 5.0 mg/dm^2 hr. The stomatal resistance (r_s) was related to the light flux density by equation (48)

$$r_s = \gamma + \frac{\beta}{I + I'}$$

From the field measurements by R. W. Shawcroft, γ, β and I' were found to be 1.46 sec/cm, 0.036 sec^{2}cm/μ einstein and 0.0015 μ einsteins/cm^2 sec respectively for the corn variety, Cornell M-3, used in this study.

Photosynthesis as a function of light irradiance is used to determine r_m and r_c. Figure (21) shows measurements of N at various light irradiances. A curve is drawn by hand through the points. From this curve estimates of α and N_M are determined graphically.

Let $r = r_s + r_m + r_c$ (62)

From (48), (54) and (62)

$$r = \frac{C}{N_M} + \frac{\beta}{I + I'} \quad (63)$$

Knowing N_M from Figure (21), r is determined as a function of I. Combining (62) and (59), one obtains

$$r_c = r - \frac{\alpha I r + C + R(r_s + r_m)}{P} + \frac{CI\alpha + R\alpha I(r_s + r_m)}{P^2} \quad (64)$$

Thus r_c can be evaluated for a given r_m using values from the curve of

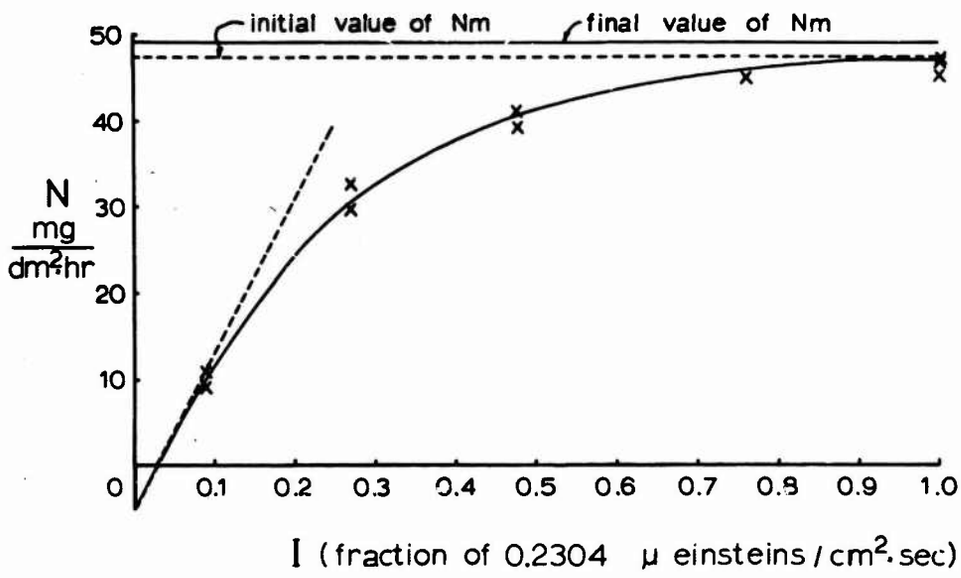

Figure 21. Net photosynthesis (N) as a function of light flux density (I) at a CO_2 concentration of 260 ppm.

Figure (21). Finally r_m is evaluated us g

$$r_m = r - r_s - r_c \tag{65}$$

Equations (64) and (65) are solved simultaneously for r_m and r_c. In practice r_c and r_m are not constants with I. This represents a discrepency between theory and measurements since both r_c and r_m are defined as constants. Ten values of r_c and r_m are evaluated at light irradiances of 0.1, 0.2, 0.3 . . . of 0.230 μ einsteins/cm^2sec. (0.230 μ einsteins/cm^2sec corresponds to 10,000 ft. candles). These values are averaged and used in equations (57-61) to generate theoretical light and CO_2 curves. By using a value of N_M of 47.4 mg/dm^2 hr which is a reasonable estimate from Figure (21), and average values of r_m and r_c the theory tends to overestimate N at intermediate light flux densities (a maximum of 16%) and underestimate N at high flux densities (a maximum of 4%). These differences were reduced to 8% and 1% respectively by adjusting N_M from 47.4 to 49.4 mg/dm^2 hr. Corresponding values of $\bar{r}_c$ and $\bar{r}_m$ for N_M equal to 49.4 mg/dm^2 hr are 0.20 and 1.65 sec/cm respectively. This adjustment also improved agreement between the theoretical and measured CO_2 curve. These theoretical curves with measurements are shown in Figures (22) and (23).

It should be pointed out that measurements in Figure (23) were made at a light irradiance of 0.230 μ einsteins/cm^2sec. The leaf used in Figure (23) had a higher net photosynthesis rate (N = 56.5 mg/dm^2 hr) at 260 ppm CO_2 than the two leaves used in Figure (22) (N = 46.5 mg/dm^2 hr). The theoretical values in Figure (23) were obtained by multiplying equation (57) by P_r where P_r = 56.5/47.0. When this leaf model is used -

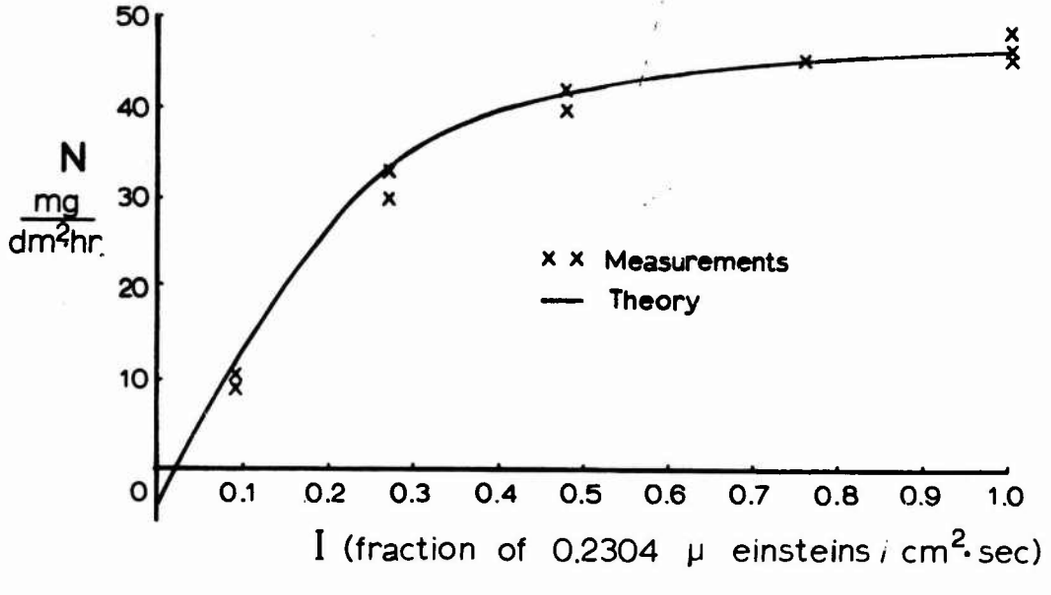

Figure 22. Net photosynthesis (N) as a function of light flux density (I) at a CO_2 concentration of 260 ppm.

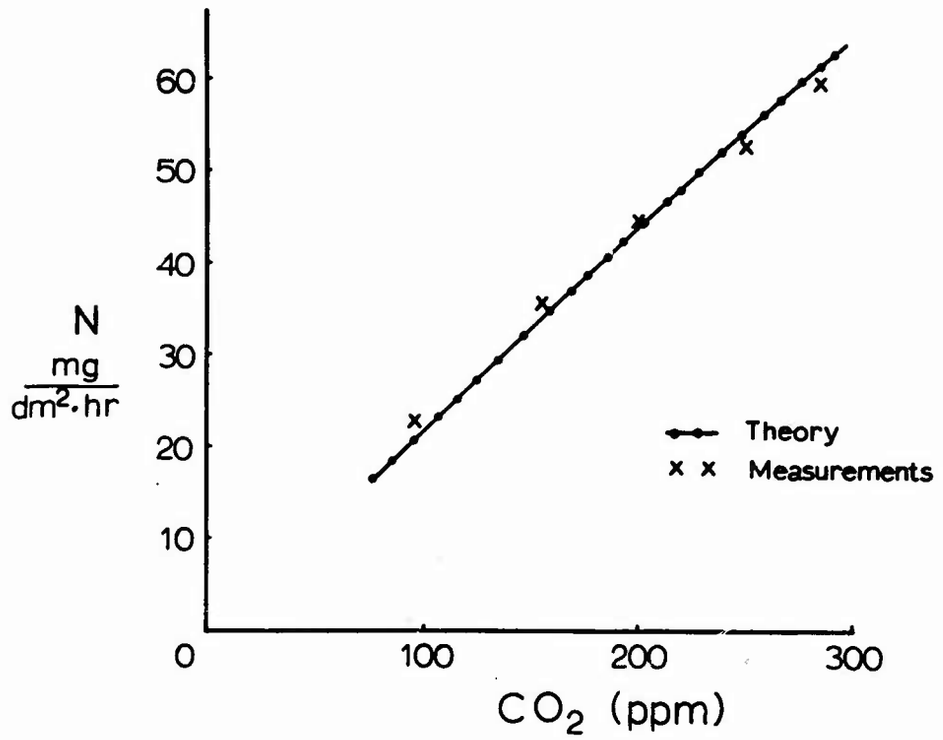

Figure 23. Net photosynthesis (N) as a function of CO_2 concentration at a light flux density of 0.230 μ einsteins/cm^2/sec.

in the simulation of the crop response P_r is defined as

$$P_r = \frac{\bar{N}_{260}}{46.5} \quad .$$

$\bar{N}_{260}$ is the value of net photosynthesis measured at 260 ppm CO_2 at 0.230 μ einsteins/cm^2sec averaged over a representative number of leaves in the crop. Note that if $\bar{N}_{260}$ is measured as a function of depth into the crop, this function can easily be incorporated into the crop model. The measurements made in this study showed no significant variation of N with depth. $\bar{P}_{260}$ was found to be 47.2 mg/dm^2hr for the field corn under consideration in this study.

Conclusions

A mathematical model of net photosynthesis of an individual corn leaf has been developed in this study. The model is tested using experimental leaf chamber measurements of net photosynthesis as functions of CO_2 concentrations and light flux densities. By forcing r_c, the carboxylation resistance, and r_m, the mesophyll resistance, to be constants, the theory tended to slightly overestimate photosynthesis rates at intermediate light flux densities. However the agreement between theory and measurements was considered satisfactory (a maximum discrepency of 8%) considering the rather simple assumptions used in the theoretical model.

Chapter III

THE BOUNDARY LAYER RESISTANCE OF PLANT LEAVES

The concept of a boundary layer was first conceived by Prandtl who divided flow around a body into two parts; a thin layer near the surface of the body where friction or shear plays an important role and the remaining part of the flow where friction may be neglected. Boundary layer theory which was developed around this concept has proved extremely useful in engineering applications. It is not surprising therefore that these ideas have been applied to flow of air over leaves. A leaf in its natural environment exchanges heat, CO_2, O_2 and water vapor with what is normally a highly turbulent air stream. The resistance to diffusion encountered in the leaf boundary layer is relatively large compared to eddy diffusion in the turbulent air stream. For this reason it is an important consideration in the study of the energy balance of single leaves, net photosynthesis and the water use of plants.

The concept of diffusion of mass and heat across boundary layers is expressed in terms of a resistance to diffusion, r_a. Resistances to the diffusion of heat (ra_h), water vapor (ra_w), and CO_2 (ra_c) are defined as

$$ra_h = \rho C_p \frac{(T_L - T_a)}{H} \tag{66}$$

$$ra_w = \frac{\rho C_p}{\gamma'} \frac{(e_L - e_a)}{LE} \tag{67}$$

and

$$ra_c = \frac{(C_L - C_a)}{N} \tag{68}$$

H, LE and N are respectively fluxes of sensible heat, latent heat and net photosynthesis per unit area. e_L, T_L and C_L are vapor pressure, temperature and CO_2 concentration at the leaf surface; e_a, T_a and C_a are the corresponding values of the air stream; ρ, C_P and γ' are the density of air, the specific heat of air and psychrometric constant respectively. This concept of resistance lends itself to the understanding of exchange processes from a leaf. For example, ra_c can be added to the left of r_s in the series of resistances of Figure (20) in Chapter II. The leaf itself has two surfaces, and ra for a given surface should be added in series with the stomatal resistance for that surface. However, measurements by Shawcroft described in Chapter II indicated that the stomatal resistance for the upper and lower leaf surfaces were approximately equal. Thus, only a small error is introduced by adding the total leaf stomatal resistance and the total leaf boundary layer resistance in series. In a leaf chamber ra_c is considered zero because of the highly turbulent flow in the chamber. In the natural environment this is not necessarily true.

In order to extrapolate leaf chamber measurements to the natural field environment, the size of the leaf boundary layer resistance under natural conditions must be approximated. From dimensional analysis, the boundary layer resistance is a function of a length parameter (in this case the width of the leaf), the velocity of the free air stream in the vicinity of the leaf and in the case where free convection is important, to the temperature difference between the leaf and the air stream. To obtain these functions experimentally one is confronted with two alternatives. The experimenter can work in a wind tunnel, usually with artificial leaves, and determine precise relationships (For example Thom 1968,

Parkhurst et al. (1968)). However, since the level of free stream turbulence is very low in wind tunnels, the experimenter has difficulty relating his measurements to field conditions. On the other hand, working in the field on intact leaves also presents problems. Here the measurements are necessarily less precise since working conditions are far from ideal. Also unsteady state conditions in the field make it difficult to relate measurements to the wind velocity and leaf to air temperature gradients.

Two studies which were made on attached leaves in the field are Hunt et al. (1968), and Kanemasu et al. (1969). An energy balance method was used in both studies. (Hunt et al. (1968), also used a transient method which will be discussed in detail below). Under steady state conditions the energy balance equation of a leaf is

$$R_n = \frac{\rho C_p}{\gamma'} \frac{E(T_L) - E_a}{ra_w + r_s} + \rho C_p \frac{T_L - T_a}{ra_h} \qquad (69)$$

where R_n is the net radiation load on the leaf, r_s is the stomatal resistance to water vapor flow and $E(T_L)$ is the saturated vapor pressure as a function of leaf temperature. If one assumes $ra_w = ra_h$ and measures all other components [R_n is measured with a net radiometer positioned above and below the leaf; r_s is measured with a leaf porometer (eg. Van Bavel et al., 1965)], equation (69) can be solved for ra. However, a large number of components have to be measured before ra can be calculated. This necessarily reduces the accuracy of the method. Kanemasu et al. (1969) reduced the number of variables by measuring the latent heat term directly. All but the leaf under study were stripped from a

bean plant growing in a pot. The pot was weighed at intervals to determine the latent heat.

Most of the wind tunnel work to date has been with artificial leaves. For example, Parkhurst et al. (1968) made artificial leaves out of two layers of thin copper sheeting with heating wire between the copper sheeting. By passing a constant known current through the heating wire and measuring T_L and T_a with thermocouples, equation (66) was used to determine ra_h. Thom (1968) used a similar technique to measure ra_h. In addition he glued blotting paper to his metal leaves and soaked them with various liquids. By attaching the metal leaf to an arm of a weighing balance, evaporation from the leaf was estimated. Thus Thom was able to measure ra_w as well as ra_h.

There are some properties of leaves such as leaf hairs, curvature and flexibility which are difficult to simulate with artificial models. Pearman (1965) used a transient method to measure ra_h on real leaves under controlled conditions. A leaf was heated above the ambient air temperature with microwaves. Transient times were recorded from the time the microwave source was shut off until leaf temperature equilibrium was re-established. Natural and forced convection was studied.

In general then, there are few data on boundary layer resistances of real leaves. Because of this and a need for specific data on corn (Zea mays) leaves, a transient method was developed to measure ra_h on excised leaves placed in a wind tunnel. To understand this transient method some theoretical considerations are needed.

Theoretical Considerations

Consider a leaf under a radiation load with a high shortwave component. If the radiation load changes, the leaf temperature will adjust to a new level. The final equilibrium state can be described by;

$$R_{n_s} - 2\varepsilon\sigma\, T_f^4 - \frac{\rho C_P}{ra_h}(T_f - T_a) - \frac{\rho C_P}{\gamma'}\,\frac{e(T_f) - e_a}{ra_w + r_s} = 0.0 \qquad (70)$$

where R_{n_s} is the total incoming radiation, T_f is the final leaf temperature, ε is the thermal emissivity of the leaf (taken to be 1.0 in this study) and σ is the Boltzman constant. The unsteady state can be described by

$$R_{n_s} - 2\varepsilon\sigma\, T_L^4 - \frac{\rho C_P}{ra_h}(T_L - T_a) - \frac{\rho C_P}{\gamma'}\,\frac{(e(T_L) - e_a)}{ra_w + r_s} = \frac{M}{A}\, s\, \frac{dT_L}{dt} \qquad (71)$$

T_L is the leaf temperature, M/A is the mass per unit area of the leaf, s is the specific heat of the leaf (taken to be 0.9)and t is time. Combining equations (70) and (71) one obtains:

$$\frac{\rho C_P}{ra_h}(T_L - T_f) + \frac{\rho C_P}{\gamma'}\,\frac{e(T_L) - e(T_f)}{(ra_w + r_s)} + 2\varepsilon\sigma(T_L^4 - T_f^4) = \frac{M}{A}\, s\, \frac{dT_L}{dt} \qquad (72)$$

at this point, two simplifying assumptions are made.

First; $e(T) = bT + d$ (73)

where b and d are constants. This is a reasonable assumption between 20° and 35°C. In this range, b is equal to 2.08 mb/°C; d is not used in the calculations. Also one assumes;

$$T_L^4 - T_f^4 = 4\bar{T}^3 (T_L - T_f) \qquad (74)$$

where $\bar{T}$ is the average of T_o and T_f where T_o is the initial temperature.

The percentage error of this assumption can be expressed as;

$$\text{Percentage Error} = \frac{\int_0^\infty 4\varepsilon\sigma\bar{T}^3(T_L - T_f)\,dt}{\int_0^\infty \varepsilon\sigma(T_L^4 - T_f^4)\,dt} \times 100. \qquad (75)$$

Equation (75) can be evaluated by assuming an exponential increase of decrease of leaf temperature with time. The percentage error has a maximum value of 4% for the temperature differences considered in this study.

Using the above simplifications, equation (72) becomes;

$$(T_L - T_f)\left(2\varepsilon\sigma\bar{T}^3 + \frac{\rho C_p b}{\gamma'(ra_w + r_s)} + \frac{\rho C_p}{ra_h}\right) = -\frac{M}{A} s \frac{d(T_L - T_f)}{dt} \qquad (76)$$

By integrating equation (76) and solving for ra_h, one obtains;

$$ra_h = \rho C_p / \left[\frac{M}{A} s \frac{\ln(2)}{t_{1/2}} - \left(8\varepsilon\sigma\bar{T}^3 + \frac{\rho C_p}{\gamma'} \frac{b}{(ra_w + r_s)}\right)\right] \qquad (77)$$

where $t_{1/2}$ is the time required for the leaf to reach the midway point between the initial and final leaf temperatures. By assuming ra_w is equal to ra_h, equation (77) can easily be solved by iteration for ra_h.

Materials and Methods

A corn leaf was cut from a plant under water, placed in a beaker so that the cut end was under water and inserted into the working section of the wind tunnel through a hole cut in the floor. The rim of the beaker was flush with the floor of the wind tunnel. A leaf was arranged to protrude at an angle from the floor in a more or less natural manner or was placed in a leaf holder so that a large portion of the leaf was held at zero angle of attack to the wind velocity across the width of the wind tunnel. A third treatment consisted of placing two leaves upwind of the leaf in the natural position. This was done to study the effect of free stream turbulence generated by the two upwind leaves on the boundary layer resistance of the third leaf. Turbulent intensities were measured by a heated thermocouple annemometer. (Hastings, Model Am-62X).

A bank of incadescent lamps immersed in a plexiglass water bath was placed on the ceiling of the working section. The ceiling and sides of the working section were made from clear plexiglass as well. Thus a shortwave radiation load equivalent to full sunlight intensity could be placed on the leaf. One could change the radiation intensity by changing the setting of a large rheostat which was connected in series with the lights.

Very fine copper-constantan thermocouples (.005 inches in diameter) were used to measure the leaf to air temperature difference. Larger copper-constantan thermocouples referenced to an ice bath were used to measure the air temperature at each end of the working section of the windtunnel. All temperatures were continuously recorded on strip chart recorders. By changing the radiation load on the leaf and recording the

leaf to air temperature difference continuously, $t_{1/2}$ could be evaluated. The air temperature remained reasonably constant for small changes in the radiation loads. This procedure was repeated six to ten times at various radiation loads for each wind speed. Each treatment was repeated for three to four leaves.

Equation (77) has a stomatal resistance term, r_s, which has not been discussed as yet. Leaves were placed in the wind tunnel prior to sunset and left in the dark for several hours. This was done to close the stomates prior to the start of the experiment. The experiment was conducted at night since stomates of corn and many other agricultural crops once closed do not open readily at night under a radiation load. Preliminary measurements made with a porometer indicated that r_s values were of the order of 14.0 sec/cm for the conditions of this experiment. Values of r_s of 14.0 sec/cm or greater make the latent heat term of equation (77) negligible.

Results and Discussions

The following equation can be derived (Gebhart (1961)) from the Polhausen similarity solution for the two-dimensional boundary layer of a flat plate.

$$ra_h = 1.92\ (L'/u)^{1/2}\ P_r^{2/3} \qquad (78)$$

L' is the width of the plate, u is wind velocity and P_r is the Prandtl number. The Prandtl number is the kinematic viscosity of the fluid (in this case, air) divided by its thermal diffusivity. Figure (24) shows measurements of ra_h plotted against $(L'/u)^{1/2}(P_r)^{2/3}$ for a horizontal leaf. Six to ten measurements at different radiation loads were made at a given wind velocity for a particular leaf. No significant correlation was found between the leaf to air temperature differences and r_a at even the lowest wind velocity (41 cm/sec). Because of the difficulty in maintaining a constant air temperature at the lowest wind velocities, the method was not precise enough to study natural or mixed convection. Thus, means and standard deviations were calculated from the six to ten measurements at each wind velocity for a particular leaf. A least squares method was used to find the best linear fit to the data using all the measurements. The line was forced through the origin. The sum of squares of the deviations from this line was used to calculate a sample standard deviation of the slope which was in turn used with the 't' distribution (Snedecor (1956)) to establish a confidence interval for the slope at the 95% level. The slope and confidence interval for the data in Figure (24) is $1.51 \pm 0.032\ \text{sec}^{1/2}/\text{cm}$. This is significantly lower than the slope of the theoretical line. Since a leaf has leaf hairs,

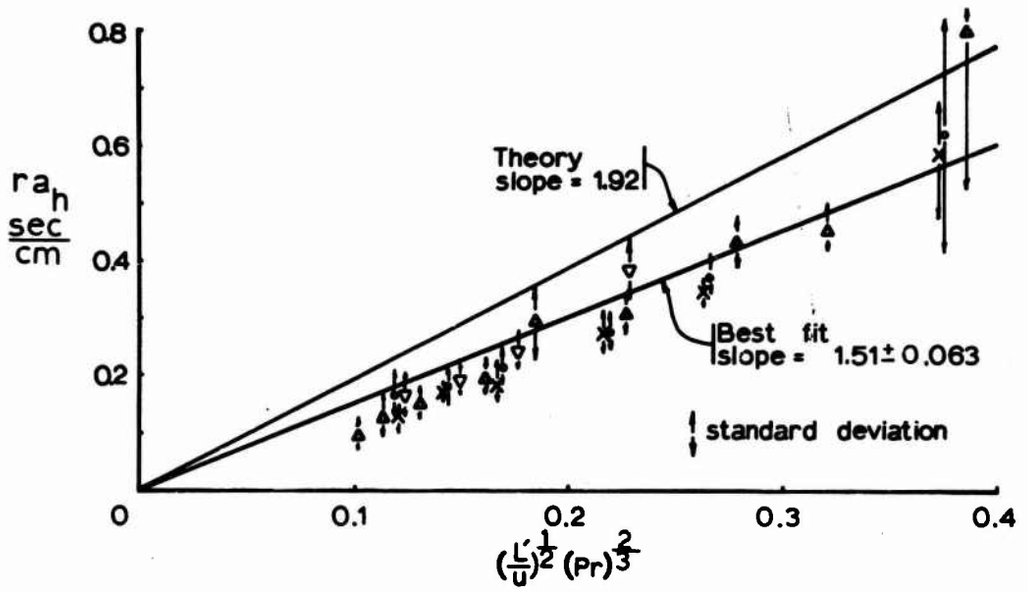

Figure 24. Boundary layer resistance for heat ra_h as a function of $(L'/u)^{1/2}(Pr)$ for a leaf in the horizontal position. L' (cm) is the leaf width, u (cm/sec) is the wind velocity and Pr is the Prandtl number.

ridges undulations etc., it is not surprising that a leaf has a boundary layer resistance lower than that of a flat plate.

Figure (25) shows similar measurements for the leaf in a natural or more upright position. This slope with 95% confidence interval is 1.72 ± 0.040 $sec^{1/2}/cm$. These values are significantly higher (the confidence intervals do not overlap) than corresponding values for the leaf in the horizontal position. The leaf in the upright position acts as a bluff body in the air stream. Separation occurs as the air moves around the leaf. The movement of air is retarded close to the underside of the leaf. Thus heat transfer from the underside is less than that for the side facing the air stream. This effect of separation on heat transfer per unit area has been verified experimentally with cylinders (Gebhart (1961)). This effect would be especially noticeable for corn leaves in this upright position because the edges of the leaf tend to fold around the mid rib creating a half cylinder effect. This folding could lead to appreciably less heat transfer per unit area than a leaf at zero angle of attack.

The effect of free stream turbulence on the boundary layer resistance is shown in Figure (26). With no leaves in the wind tunnel the heated thermocouple annemometer detected less than 1.0% turbulent intensity. When two leaves were placed upwind of the annemometer turbulent intensities ranged from a maximum of 15.5% at 86 cm/sec to a minimum of 5.4% at 330 cm/sec. The slope of the best linear fit to the measurements in Figure (26) with its 95% confidence interval is 1.47 ± 0.043 $sec^{1/2}/cm$. Thus, the turbulence generated by two leaves upwind caused a 15% decrease in boundary layer resistance. This result is

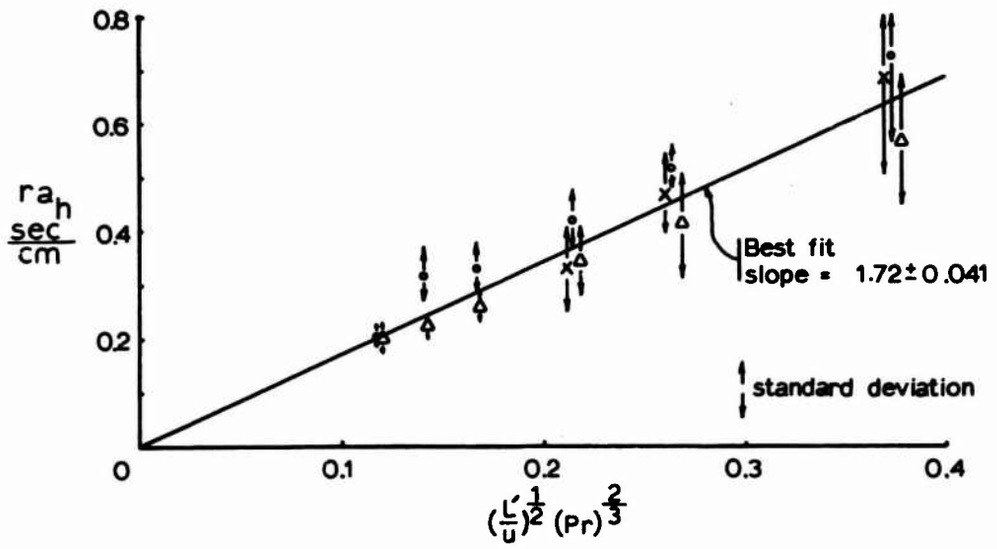

Figure 25. Boundary layer resistance for heat (ra_h) as a function of $(L'/u)^{1/2}(Pr)$ for a leaf in an upright position. L' (cm) is the leaf width, u(cm/sec) is the wind velocity and Pr is the Prandtl number.

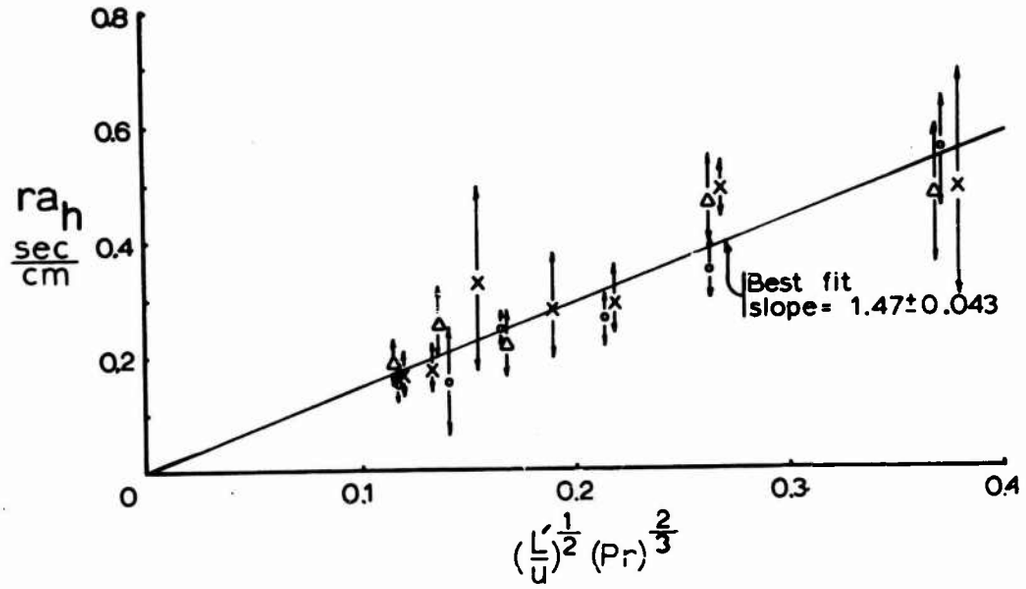

Figure 26. Boundary layer resistance for heat (ra_h) as a function of $(L'/u)^{1/2}(Pr)$ for a leaf in an upright position with two leaves upwind. L' (cm) is the leaf width, u (cm/sec) is the wind velocity and Pr is the Prandtl number.

comparable to those of Maisel and Sherwood (1950). Working with spheres at Reynolds numbers similar to this study (5,000 to 20,000) they found a 25% decrease in boundary layer resistance when turbulent intensities were increased from 4% to 25%.

The difficulty remains as to how to extrapolate wind tunnel measurements to the field. Obviously, the structure of turbulence in the field is quite different than the free stream turbulence generated by leaves in the wind tunnel. However, this wind tunnel study serves as a useful comparison with field measurements. Data from Kanemasu et al. (1969) obtained from measurements made under field conditions on attached bean leaves are shown in Figure (27). The measurements are plotted against $(L/u)^{1/2}$. The increase of turbulent exchange from the leaf surface in the field should lead to a suppression of the Prandtl number effect. Thus functions of $(L/u)^{1/2}$ rather than $(L'/u)^{1/2}(P_r)^{2/3}$ will serve for field conditions. This also means that ra_h, ra_w and ra_c are assumed equal. The slope with its 95% confidence limit of the least squares fit to the data of Kanemasu et al. is 0.60 ± 0.31 $sec^{1/2}/cm$ for a 5 cm leaf width and 0.43 ± 0.19 $sec^{1/2}/cm$ for a 10 cm leaf width. The data in Figure (27) are plotted using the 5 cm width. Also shown in Figure (27) are the best fit to the wind tunnel data with and without leaves upwind. The slope is reduced by approximately 15% by turbulence generated by two leaves in a wind tunnel. The field measurements represent a further reduction of about 56%.

Because of lack of knowledge of the nature of turbulence immediately above and within a plant community, one can only speculate as to causes of the relatively low boundary layer resistances in the field. However, very high turbulent intensities have been reported under field conditions.

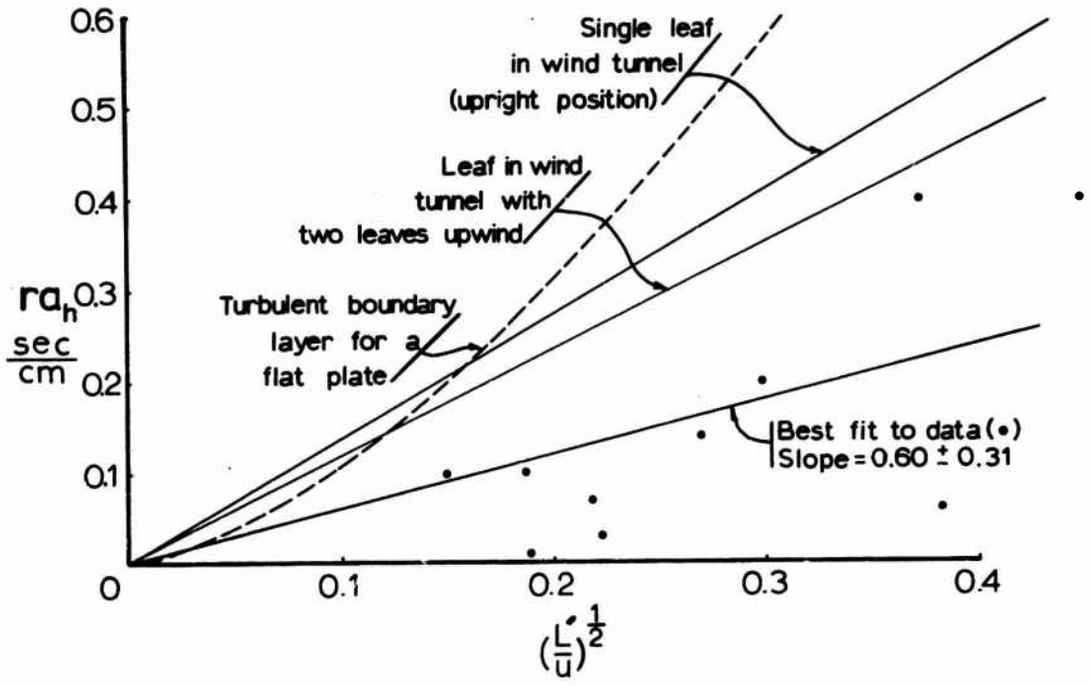

Figure 27. Boundary layer resistance for heat (ra_h) as a function of $(L'/u)^{1/2}$ where L' (cm) is the leaf wind and u (cm/sec) is the wind velocity.

(Allen (1968)). Also movement of leaves and unsteady wind conditions would result in transient boundary layers and disrupted flow around the leaf. Also, speculations have been made (Hunt et al. 1966) on the existence of turbulent boundary layers on leaves in the field. However, turbulent boundary layers in the classical fluid mechanics used of this word exist at Reynolds numbers much higher than those encountered in this study. Figure (27) shows the theoretical curve for a turbulent boundary layer for a flat plate (Gebhart (1961)). The turbulent r_a values become abnormally large as $(L'/u)^{1/2}$ increases because the theory does not apply at low wind speeds. A review article by Kestin (1966) makes clear that experimental measurements verify the theory at high Reynolds numbers. An extrapolation of this theoretical and measured curve to lower Reynolds numbers intersects the curve describing the laminar boundary layer at a Reynolds number of about 50,000. (The highest Reynolds number used in this study was approximately 20,000.) However, it is clear that free stream turbulence does enhance heat transfer at relatively low Reynolds numbers. Considering the high turbulent intensities and unsteady state conditions encountered in the field, measurements of Kanemasu et al. (1969) represent a reasonable extrapolation of the wind tunnel measurements reported in this study.

Conclusions

Measurements of the boundary layer resistance for heat (ra_h) made in a wind tunnel can be described by the following equation;

$$ra_h = 1.72\ (L'/u)^{1/2}(P_r)^{2/3} \qquad (79)$$

Free stream turbulence generated by two leaves upwind of a third leaf caused a reduction of ra_h on the third leaf of approximately 15%. Thus, ra_h under these conditions can be described by

$$ra_h = 1.51\ (L'/u)^{1/2}(P_r)^{2/3} \qquad (80)$$

Turbulent intensities measured downwind from the two leaves ranged from 15.5% at 86 cm/sec to 5.4% at 330 cm/sec. Under field conditions, measurements by Kanemasu et al. (1969) suggest the following function,

$$ra = 0.60\ (L'/u)^{1/2} \quad . \qquad (81)$$

This equation represents a further reduction in ra values of 56%. Unsteady state and highly turbulent conditions in the field suggest that the function derived from the measurements of Kanemasu et al. represents a reasonable extrapolation of the wind tunnel measurements reported here.

Chapter IV

SIMULATING THE CROP RESPONSE

The net photosynthesis rate of an individual leaf was expressed in Chapter II as a function of the visible radiation load, the leaf temperature and the CO_2 concentration at the leaf surface. Presumably, if these variables can be estimated for all the leaves in a plant community, the individual leaf photosynthesis rates can be integrated over the total leaf area to obtain the photosynthesis rate of the crop. A method of calculating the distribution of visible radiation was described in Chapter I. Discounting the effects of movement of leaves, this distribution of visible radiation is independent of the air stream above and within the canopy of plants. The leaf temperature and CO_2 concentration at the leaf surface are dependent on the air stream. The problem becomes one of describing in mathematical terms the turbulent transport of heat, momentum and mass from some reference height above the crop surface to the individual leaf surfaces. The problem actually has two boundaries since conditions both at this reference height and at the soil surface must be known. This system of equations which describe the turbulent transport between the leaf and the environment must of necessity include source and sink terms caused by the amount of CO_2, sensible and latent heat given off or taken up by the leaves themselves. That is, the leaf temperatures and CO_2 concentrations are dependent both on the exchange properties of the air stream and the leaf characteristics themselves. This interaction can be studied with such a system of

equations. The method of formulating turbulent transport and the solution of this system of equations which include the calculations of the rates of net photosynthesis as well as sensible and latent heat exchange will now be considered in detail.

Theoretical Consideration

Above the Vegetation

Many of the theoretical treatments to date have placed the upper boundary at or near the top of the crop (Philip (1964), Waggoner and Riefsnider (1965), Cowen (1968)). However, the top of the crop is difficult to define in terms of height. Also the variation of wind velocity, air temperature, etc. with height is at a maximum in this region. Thus a better boundary to the problem is at an arbitrary height say two to four meters above the crop, yet still within the crop boundary layer, where the variables such as air temperature and CO_2 concentration are approximately constant and where the shearing stress and fluxes from the crop are constant with height. In this study, four meters above the crop was chosen as the reference height.

The exchange processes for mass, heat and momentum are described by one-dimensional continuity equations both above and within the plant community. For momentum

$$\frac{\partial \tau}{\partial z} = 0 \qquad (80)$$

where

$$\tau = \rho K_M \frac{\partial u}{\partial z} \qquad (81)$$

τ is the shearing stress, ρ is the air density, K_M is the eddy diffusivity for momentum, u is the wind velocity and z is the distance in the vertical direction. From considerations of the Reynolds stresses and the Prandlt mixing length concept (Sutton (1955)), the neutral wind profile can be derived as;

$$u = \frac{u^*}{k} \ln\left(\frac{z - D}{z_o}\right) \tag{83}$$

where u^* is the friction velocity and is expressed as;

$$u^* = \sqrt{\tau/\rho} \quad .$$

Other undefined variables are k, the von Karmen's constant (taken to be 0.4 in this treatment), D the zero plane displacement and z_o the roughness length. A crop forces the reference plane upwards from the ground surface to D. z_o is the distance above D where the wind profile extrapolates to zero. In this treatment, z_o and D are treated as crop constants and are estimated from measurements of z_o and D in corn as functions of the crop height which were presented in Lemon (1965).

For diabatic conditions, the theory developed by Swinbank (1964) and the Keyps formulation (Ellison (1957), Panofsky (1961), Sellers (1962)) are most commonly used. In differential form the Swinbank and Keyps equations which relate wind velocity to height are given respectively as

$$\frac{\partial u}{\partial z} = \frac{u^*}{kz} \{1 - \exp(- \frac{(z - D)}{L})\}^{-1} \tag{84}$$

and

$$S_k^4 + \chi' \frac{K_H}{K_M} (\frac{z - D}{L}) S_K^3 = 1 \tag{85}$$

where

$$S_k = \frac{k(z - D)}{u^*} \frac{\partial u}{\partial z} \tag{86}$$

and

$$L = - \frac{u^{*3} T \rho C_P}{k g H} \tag{87}$$

H is the sensible heat flux from the crop surface and is considered positive in the upward direction. (This sign convention is also used for

net photosynthesis and latent heat flux). L is the Monin-Obukhov length, χ' is a constant and K_H is the eddy diffusivity for heat and is defined as

$$K_H = H/\rho C_p \frac{\partial T}{\partial z}) \tag{88}$$

where T is the air temperature. Both of the above theories have been modified to describe the exchange of heat and mass across the crop boundary layer. For the purposes of this study, both were in general agreement. The Swinbank approach is incorporated into this model because it is basically simpler and involves much less numerical computation. Thus, only this approach will be described here.

By integrating (84) one obtains

$$u = \frac{u^*}{k} \ln \left\{ \frac{\exp(\frac{z - D}{L}) - 1}{(\exp\frac{(z_o)}{L} - 1)} \right\} \tag{89}$$

Combining (81) with (84) one obtains

$$K_M = u^* k L \{1 - \exp(-z/L)\} \tag{90}$$

Swinbank (1968) presented evidence that the eddy diffusivity for heat K_H and momentum (K_M) are related by

$$\frac{K_H}{K_M} = 2.7(z/L)^{0.24} \tag{91}$$

for unstable conditions. There are two difficulties with this expression. It obscures the fact that the ratio K_H/K_M approaches a constant value as (z/L) increases (That is as the free convection region is approached (Ellison (1957)). Also at low values of $|z/L|$ (near neutral conditions)

this ratio falls as low as 1.2 or lower. Data presented by Panofsky (1965), (Figure (28)) indicates that this ratio is much higher at near neutral conditions. Therefore K_H/K_M was defined as;

$$K_H/K_M = -1.4 \exp(1.5(z/L)) + 3.0 \tag{92}$$

Using equation (92), K_H/K_M approaches 3.0 as $|z/L|$ approaches infinity and at neutral conditions (z/L) becomes 1.6. Figure (28) shows both equations (91) and (92) along with data plotted by Panofsky (1965). These data were taken from studies by Swinbank (1964).

Combining equations (88) and (90) and (92) one obtains

$$\frac{\partial T}{\partial z} = \frac{H}{\rho C_p u^{*2}(-1.4 \exp(1.5(z/L)) + 3)\ (1 - \exp(-z/L))} \frac{\partial u}{\partial z} \tag{93}$$

Integrating, one obtains

$$T_{ch} = T_h - \frac{H}{\rho C_p u^* L} \int_{y_{ch}}^{y_h} \frac{dy}{(-1.4 \exp(-1.5y) + 3)\ (1 - \exp(y))} \tag{94}$$

$$= T_h - \frac{H}{\rho C_p u^* L} (FY) \tag{95}$$

where $y = (-z/L)$,

T_{ch} is the air temperature at a height (ch) immediately above the crop and T_h is the air temperature at the reference height (h) four meters above the crop. FY is the integral in equation (94). Similar expressions for water vapor pressure (e) and CO_2 concentration (c) are respectively,

$$e_{ch} = e_h - \frac{\gamma' LE}{\rho C_p u^* k L} (FY) \tag{96}$$

and

$$C_{ch} = C_h - \frac{N_t}{u^* k L} (FY) \tag{97}$$

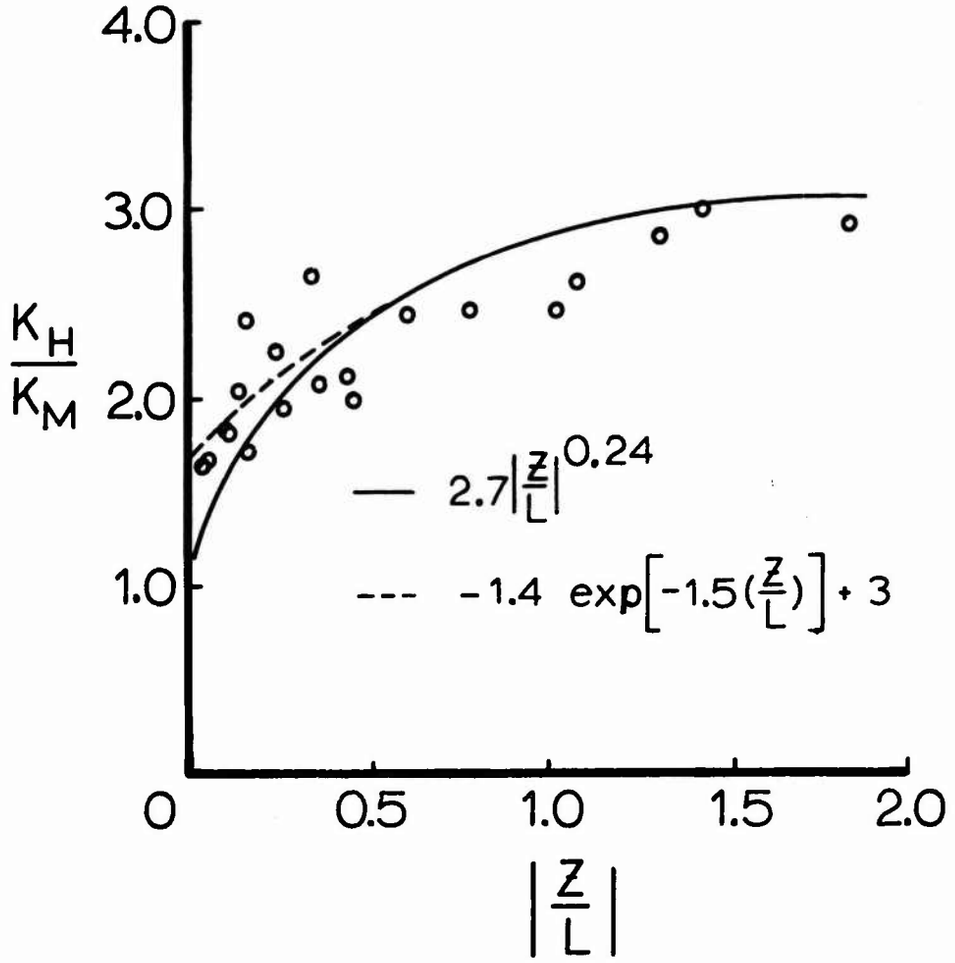

Figure 28. The ratio of the eddy diffusivity of heat (K_H) and momentum (K_M) as a function of the instability parameter z/L after Panofsky (1965). Measurements (o) by Swinbank (1964).

LE and N_t are the latent heat flux and the total net photosynthesis of the crop. Equations (96) and (97) are derived by assuming the eddy diffusivities for heat and mass transfer are identical. Wind velocity, the eddy diffusivity for momentum and the eddy diffusivity for sensible heat at the top of the crop are expressed respectively as,

$$u_{ch} = u_h - \frac{u^*}{k} \ln \left\{ \frac{\exp(\frac{h - D}{L}) - 1}{\exp(\frac{ch - D}{L}) - 1} \right\} \tag{98}$$

$$K_{Mc} = u^* k L \{1 - \exp(\frac{ch - D}{L})\} \tag{99}$$

and

$$K_{Hc} = K_{Mc}(-1.4 \exp(1.5(ch - D)/L) + 3) \tag{100}$$

Equations (94) - (100) assume that u* and L are known. They can be determined if z_o, D and H are known. The two equations with u* and L as unknowns are,

$$u^* = k U_h / \ln \left\{ \frac{\exp\frac{(h - D)}{L} - 1}{\exp\frac{(z_o)}{L} - 1} \right\} \tag{101}$$

and

$$L = \frac{u^{*3} T_h \rho C_p}{k g H} \tag{102}$$

They can be solved numerically by the method of variable position described in Conte (1965). Therefore, the above theory allows us to estimate the needed variables at or near the top of the crop from measurements at some reference height above the crop. Note that the crop parameters D and z_o and the values of H, N_t and LE must be known. This interrelationship between the changes in the air properties and the sources and sinks will be explained in detail below.

Exchange within the Crop

In the crop, the equations of continuity for momentum and mass and sensible heat transfer are;

$$\frac{\partial \tau}{\partial z} = \frac{1}{2} \rho u^2 C_d f \tag{103}$$

and

$$\frac{\partial Q}{\partial z} = Q'' f \tag{104}$$

Where Q represents the vertical flux of mass or sensible heat and Q" represents the flux of the same quantities from a unit area of leaf surface. C_d is a drag coefficient and f is the leaf area density. Following Sutton (1955), the shearing stress can be expressed as

$$\tau = \rho \overline{u'v'} \tag{105}$$

where u' and v' are deviations from the mean horizontal and vertical wind components. Assuming u' is equal to v' and that

$$u' = \ell \frac{du}{dz} \tag{106}$$

τ can be expressed as;

$$\tau = \ell^2 \frac{du}{dz} \tag{107}$$

Therefore, equation (103) can be expanded to

$$\frac{\partial}{\partial z} (\rho K_M \frac{\partial u}{\partial z}) = 1/2 \rho C_d u^2 f \tag{108}$$

or

$$\frac{\partial}{\partial z} (\rho \ell^2 (\frac{\partial u}{\partial z})^2) = 1/2 \rho C_d u^2 f \tag{109}$$

Equations (108) or (109) are usually solved by assuming ℓ or K_M and f

are constants or linear functions with height (Cionco (1965), Lemon et al. (1963)). Assumptions about f can be avoided by changing the independent variable from z to F, the cumulative leaf area index measured from the top of the crop downward. (Perrier and Hallaire (1968)). The transformation is given by,

$$\frac{\partial F}{\partial z} = -f \tag{110}$$

Equation (103) can be solved by assuming the turbulent intensity (B) is constant with L or z. The turbulent intensity is expressed as

$$B = \frac{\sqrt{u'v'}}{u} \tag{111}$$

Combining (103), (105) and (111) results in

$$B^2 \frac{\partial u^2}{\partial z} = 1/2\ C_d u^2\ f \tag{112}$$

Then $$u = U_{ch} \exp\left(- \frac{C_d}{2B^2} F\right)$$

or $$u = U_{ch} \exp(-\gamma_o F) \tag{113}$$

where γ_o is a constant. The difficulty with this equation is that the region near the top of the crop has very little leaf area but is where the wind velocity decreases a relatively large amount. To apply equation (113) to this region would produce unreasonably large values of γ_o. In this same region, the exponential wind equation (89) predicts the wind profile reasonably well. Thus a height (h_1) with a cumulative leaf area index of F_1 below the top of the crop but above $D + z_o$, was chosen where the wind profile begins to deviate from the exponential law. Then

$$u = U_{h1} \exp(-\gamma_o(F - F_1)) \tag{114}$$

was used to predict the wind profile further into the crop where

$$U_{h1} = U_h - \frac{u^*}{k} \ln \left\{ \frac{\exp(\frac{h - D}{L}) - 1}{\exp \frac{h_1 - D}{L} - 1} \right\} \quad . \tag{115}$$

The constants γ_o and h_1 were determined empirically from wind profile data.

The eddy diffusivity in the crop was assumed to be proportional to the wind velocity. Cowan (1968) made this same assumption. The proportionality factor (δ) was determined by

$$\delta = \frac{K_{Mc}}{u_{ch}} \tag{116}$$

The ratio of the eddy diffusivities for heat and momentum in the crop was assumed constant. Wright and Brown (1967) have shown that this is a reasonably good assumption. Thus in the crop

$$K_M = \delta u \tag{117}$$

and

$$K_H = (\frac{K_{Hc}}{K_{Mc}}) \quad K_M$$

or

$$K_H = (\frac{K_{Hc}}{K_{Mc}}) \quad \delta u \quad . \tag{118}$$

Again the eddy diffusivities for mass transfer are assumed equal to K_H.

Sensible Heat and Mass Exchange

The transfer of sensible heat and mass transfer within the crop is described by equation (104). For sensible heat, equation (104) can be expressed as;

$$- \frac{\partial H}{\partial L} = \rho C_p (\frac{T_L - T}{r_a}) \tag{119}$$

where T_L is the leaf temperature and T is the air temperature of the bulk air stream surrounding the leaf. In actual fact, at a given level in the crop, leaves will be at a range of temperatures governed mainly by their respective radiation loads. In Chapter I a method was presented which divided the leaf area of a given leaf area increment, into classes of visible radiation loads. This same procedure can be used to divide the same leaf area into classes of solar radiation loads. This procedure will be discussed in more detail below. Since twenty classes were used, equation (119) can be written as

$$-\frac{\partial H_i}{\partial L} = \rho C_P \frac{\sum_{j=1}^{20} (T_{L_{ij}} - T_i)}{r_{a_i}} FR_{ij} \qquad (120)$$

FR_{ij} represents the frequency distribution of the leaf area classes at the leaf area increment i. Since

$$H = +f \rho C_P \frac{\partial T}{\partial L} \qquad (121)$$

equation (120) can be expressed as;

$$-\frac{\partial}{\partial L}\left(fK \frac{\partial T_i}{\partial L}\right) = \frac{\Sigma(T_{L_{ij}} - T_i)\ FR_{ij}}{r_{a_i}} \qquad (122)$$

Replacing the differentials with finite differences, one can write

$$-f_i K_i \frac{(T_{i-1} - T_i)}{S} + f_{i+1} K_{i+1} \frac{(T_i - T_{i+1})}{S} = S \frac{\Sigma(T_{L_{ij}} - T_i)}{r_{a_i}} FR_{ij} \qquad (123)$$

where S is the leaf area per increment. Figure (29) represents a crop divided into n increments. Note that T_i is the air temperature at the

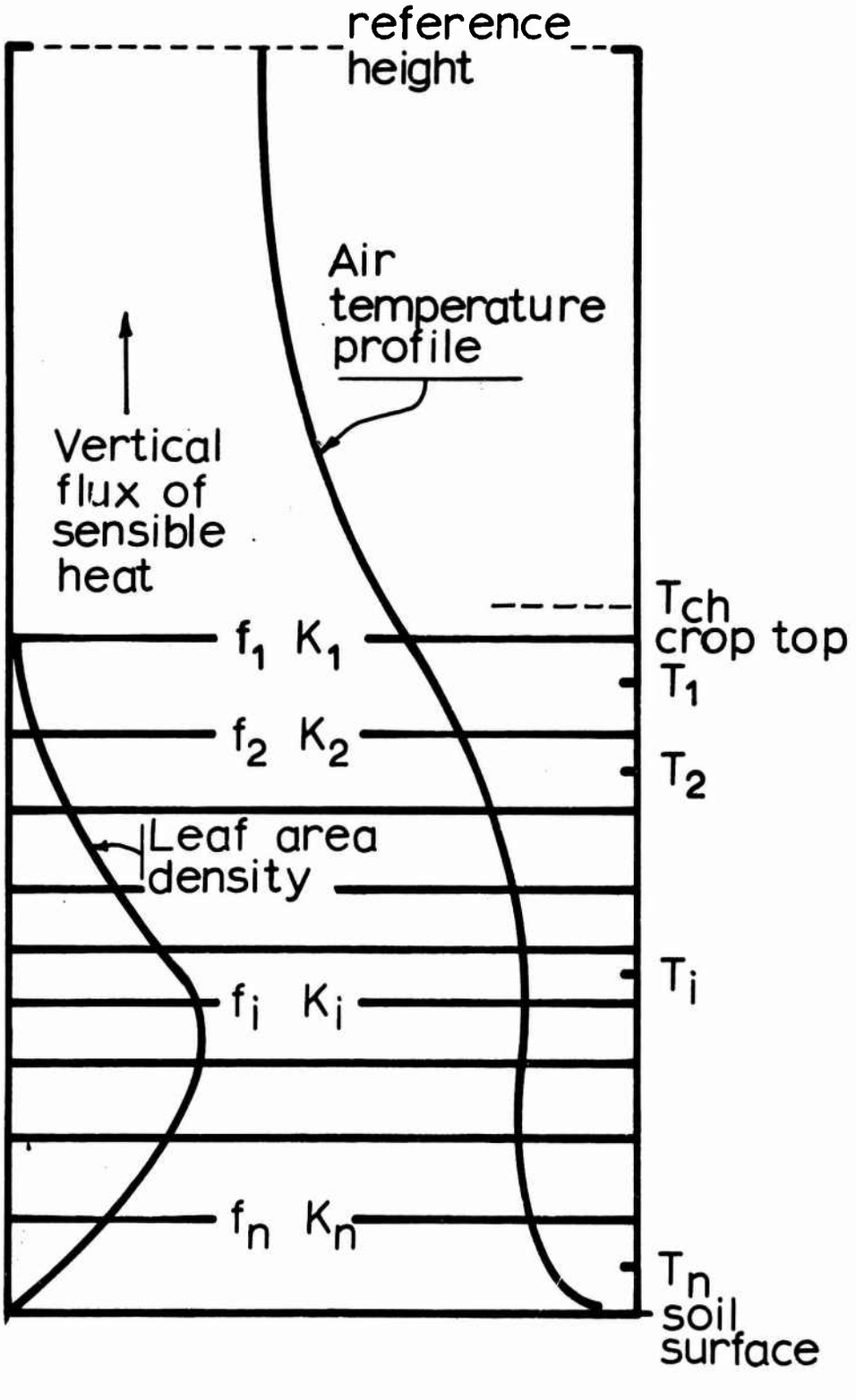

Figure 29. A representation of the crop divided into n leaf area increments. Air temperature and leaf area density are shown as functions of height (z).

center of increment i. On the other hand, f_i and K_i are estimated at the dividing line between increment i-1 and increment i.

The subscripted K's refer to the eddy diffusivity for mass and heat transfer and can be evaluated from equation (118). The values of r_a can be evaluated from (114) and the relation

$$r_a = 0.6\ (L'/u)^{1/2} \tag{124}$$

determined from measurements of Kanemasu (1968) which were presented in Chapter III. L' is the leaf width. Equation (123) can also be written as;

$$-(f_iK_i)T_{i-1} + (f_iK_i + f_{i+1}K_{i+1} + \frac{S^2}{r_a})T_i - (f_{i+1}K_{i+1})T_{i+1} =$$

$$\frac{S^2}{r_{a_i}} \Sigma\ T_{L_{ij}}\ FR_{ij} \tag{125}$$

The corresponding equation at the first increment just below the top of the crop is;

$$-K_{ch}\left(\frac{T_{ch} - T_1}{\Delta z}\right) + K_1f_1\left(\frac{T_1 - T_2}{S}\right) = S\ \frac{\Sigma(T_{L_{ij}} - T_1)}{r_{a_i}}\ FR_{ij} \tag{126}$$

Δz is chosen so that T_1 is the air temperature at the middle of the first leaf area increment. That is, Δz is twice the distance from the middle of the first increment to the top of the crop. Fortunately the change of temperature with height is quite linear in this region. Thus, relatively large values of z do not introduce appreciable error. At the increment of leaf area next to the soil surface, equation (123) becomes

$$-f_nK_n\ \frac{(T_{n-1} - T_n)}{S} - FHS = \frac{S^2}{r_{a_n}} \Sigma\ T_{L_{nj}}\ FR_{nj} \tag{127}$$

where FHS represents the flux of sensible heat from the soil. Thus,

assuming leaf temperatures, FHS and T_{ch} are known, equations (125) (126) and (127) represent a system of n linear equations in n unknowns.

This system of equations can best be treated in matrix notation expressed as

$$(AM + BM)\,(T) = (FH) \qquad (127)$$

$$\text{or} \qquad (T) = (FH)\,(AM + BM)^{-1}$$

where

$$AM = \begin{pmatrix} \frac{K_{ch}S}{z} + K_1f_1 & -K_1f_1 & 0 & . & 0 & 0 \\ 0 & +K_1f_1 + K_2f_2 & -K_2f_2 & . & 0 & 0 \\ 0 & -K_2f_2 & +K_2f_2 + K_3f_3 & . & . & . \\ 0 & 0 & -K_3f_3 & . & . & . \\ . & . & . & . & . & . \\ . & . & . & . & . & . \\ 0 & 0 & 0 & . & -f_nK_n & +f_nK_n \end{pmatrix}$$

$$BM = \begin{pmatrix} S^2/r_{a_i} & 0 & 0 & . & . & . \\ 0 & S^2/r_{a_2} & 0 & . & . & . \\ 0 & 0 & S^2/r_{a_3} & . & . & . \\ . & . & . & . & . & . \\ . & . & . & . & . & . \\ . & . & . & . & . & . \end{pmatrix}$$

$$FH = \begin{pmatrix} \Sigma T_{L_{1j}} \cdot FR_{1j} \cdot S^2/r_{a_1} + K_{ch} \cdot T_{ch} \cdot S/z \\ \Sigma T_{L_{2j}} \cdot FR_{2j} \cdot S^2/r_{a_2} \\ \cdot \\ \cdot \\ \cdot \\ \Sigma T_{L_{nj}} \cdot FR_{nj} \cdot S^3/r_{a_n} + FHS \end{pmatrix}$$

and

$$T = \begin{pmatrix} T_1 \\ T_2 \\ \cdot \\ \cdot \\ \cdot \\ T_n \end{pmatrix}$$

A similar equation for water vapor is E

$$E = (FLE)\ (AM + EM)^{-1} \tag{128}$$

$$EM = \begin{pmatrix} S^2\ \Sigma FR_{ij}/(r_{a_1} + rs_{1j}) & 0 & 0 & \cdot & \cdot & \cdot \\ 0 & S^2\ \Sigma FR_{2j}/(ra_2 + rs_{2j}) & \cdot & \cdot & \cdot & \cdot \\ 0 & \cdot & \cdot & \cdot & \cdot & \cdot \\ 0 & \cdot & \cdot & \cdot & \cdot & \cdot \\ 0 & \cdot & \cdot & \cdot & \cdot & \cdot \\ \cdot & \cdot & \cdot & \cdot & \cdot & \cdot \end{pmatrix}$$

$$\text{FLE} = \begin{pmatrix} S^2 \Sigma e(T_{L_{1j}})/(r_{a1} + rs_{1j}) + K_{ch} e_{ch} S/\Delta z \\ S^2 \Sigma e(T_{L_{2j}})/(r_{a2} + rs_{2j}) \\ \vdots \\ S^2 \Sigma e(T_{L_{nj}})/(r_{an} + rs_{nj}) + \text{FLHS} \end{pmatrix}$$

where FLHS is the flux of latent heat from the soil

$$\text{and } E = \begin{pmatrix} e_1 \\ e_2 \\ \vdots \\ e_n \end{pmatrix}$$

where ei is the water vapor pressure of the air stream at the i^{th} increment. The values of the resistance rs_{ij} are derived from equation (48) expressed in subscripted form as;

$$rs_{ij} = \gamma + \frac{\beta}{I_{ij} + I'} \qquad (129)$$

I_{ij} is the light flux density at class j of increment i. Since the leaf area classes for visible radiation loads were calculated simultaneously with the leaf area classes for solar radiation loads, it was not difficult to assign a leaf resistance value to each class of solar radiation loads.

The equation describing CO_2 exchange is solved in a less direct manner. Net photosynthesis (N) per unit leaf area is related to CL, the CO_2 concentration at the leaf surface by equation (57). (This equation

will be written here simply as N = fn(CL)). The continuity equation for CO_2 exchange can be written as

$$-\frac{\partial N_t}{\partial F} = fn(CL) \tag{131}$$

where N_t is the vertical flux of CO_2. Once again there is a range of N's and CL's in a given leaf area increment which depend on the distribution of visible radiation loads and are represented by N_{ij} and CL_{ij}. The leaf surface concentrations of CO_2 can be expressed as

$$CL_{ij} = C_i - ra_i N_{ij} \tag{132}$$

Thus equation (131) can now be written as

$$-\frac{\partial N_{ti}}{\partial F} = \Sigma fn(C_i - ra_i N_{ij})\, FR_{ij} \tag{133}$$

In matric notation this reduces to

$$(AM)(C) = FC \tag{134}$$

where

$$FC = \begin{pmatrix} S^2\, \Sigma fn(C_i - ra_1 N_{1j}) FR_{1j} + K_{ch} C_{ch}\, S/\Delta z \\ \vdots \\ S^2\, \Sigma fn(C_n - r_{a_n} N_{nj}) FR_{nj} + FS \end{pmatrix}$$

and

$$(C) = \begin{pmatrix} C_1 \\ C_2 \\ \vdots \\ C_n \end{pmatrix}$$

FS and C_{ch} are the flux of CO_2 from the soil and the CO_2 concentration at height ch respectively. In this situation it was impossible to separate the air CO_2 concentrations into a separate vector. Thus equation (134) was solved iteratively for (C). For the initial guess, all C's were set equal to the concentration of CO_2 at the reference height.

Using matrix theory and in the case of CO_2 an additional iteration sequence, the vectors (T), (E), and (C) are evaluated. Once they are known the sources and sinks of sensible (SO_H) and latent (SO_E) heat and CO (SO_c) are calculated for each leaf area increment from;

$$SO_{Hi} = \rho C_P \Sigma(T_{L_{ij}} - T_i)\ FR_{ij}\ \ S/rai$$

$$SO_{Ei} = \rho C_P \Sigma(e(T_{Lij}) - e_i)\ FR_{ij}\ S/(ra_i + rs_{ij})$$

and $$SO_{ci} = \Sigma fn(C_i - ra_i N_{ij})\ FR_{ij}\ S$$

The vertical flux of sensible heat from the crop surface is obtained by summing the sources and sinks over all the leaf area increments and adding the flux from the soil surface. A similar procedure is used for latent heat and CO_2.

Leaf Temperatures

The leaf temperatures are obtained by solving the energy balance equation for individual leaves. This is expressed as

$$R_{n_{ij}} = H_{ij} + LF_{ij} \qquad (135)$$

where

$$R_{n_{ij}} = TH_i\downarrow + TH_{i+1}\uparrow - 2\sigma T_{L_{ij}}{}^4 + A_j \cdot DS \cdot 0.3/\sin(IS).$$

$$H_{ij} = \rho C_P\ (TL_{ij} - T_i)/ra_i$$

and $$LE_{ij} = \frac{\rho C_P}{\gamma} \left(\frac{e(T_{L_{ij}}) - e_i}{rs_{ij} + ra_i}\right) \qquad (136)$$

A_j is a fraction of twenty minus 0.025. That is, A_j is one of 0.05 - 0.025, 0.10 - 0.025, 0.15 - 0.025, . . . 1.0 - 0.025. The number 0.025 is subtracted to put the radiation flux density in the middle of its respective class. These flux densities are expressed as fractions of DS · 0.7/sin(IS) which represents approximately the largest solar radiation load. DS is the amount of direct solar radiation measured on the horizontal plane above the crop. $TH_i\uparrow$ and $TH_{i+1}\downarrow$ are the amounts of thermal radiation moving up and down in the crop as discussed in Chapter I. An anomaly arises here because the leaf temperatures must be known before the thermal radiation values can be calculated. This difficulty is discussed below in connection with successive approximations. Equation (135) represents 20 non-linear equations, for each increment i. To save computation, only every sixth equation was solved for $T_{L_{ij}}$ using once again the method of variable position. The leaf temperatures for in-between classes were found by linear interpolation. Also the following equation was used to adjust the leaf temperatures.

$$\frac{\partial R_n}{\partial F} = \frac{\partial H}{\partial F} + \frac{\partial LE}{\partial F}$$

or $$\frac{\partial R_n}{\partial F} = \rho C_P \frac{\Sigma(\psi T_{L_{ij}} - T_i)FR_{ij}}{ra_i} + \frac{\rho C_P}{\gamma'} \frac{(e(\psi T_{L_{ij}}) - e_i)FR_{ij}}{ra_i + rs_{ij}}$$

Since net radiation as a function of F is calculated in the model the above equation can be solved iteratively for ψ. Then ψ was used to adjust the leaf temperatures so that the $\partial R_n/\partial L$ was equal to the sources of sensible and latent heat for a given increment.

The Soil Surface

The soil surface represents the second boundary of this two boundary mathematical problem. In this treatment, the soil surface is defined in terms of a heat flux into the soil (SHF) and a soil moisture tension (SM). The first term is measured directly using soil heat flux plates near the surface. The second is estimated from soil moisture tension measurements made at various depths in the soil. Mass and heat exchange between the soil surface and the air stream above the soil is described using the theory of Owen and Thompson (1963). This approach has been used extensively by Chamberlain (1968) who studied the movement of gases to and from a variety of rough surfaces.

The resistance to diffusion from the surface to the air stream is defined for sensible and latent heat respectively as;

$$rzH = \rho C_p \, u^* \frac{(e_s - e_{zh})}{H_s} \tag{137}$$

and

$$rzE = \frac{\rho C_p}{\gamma'} \, u^* \frac{(TS - T_{zh})}{LE_s} \tag{138}$$

where H_s and LE_s are fluxes of sensible and latent heat per unit area of soil respectively. TS is the soil temperature, e_s is the vapor pressure at the soil surface, e_{zh} and T_{zh} is the air water vapor pressure and air temperature at a reference height (zh) above the soil surface. This was arbitrarily taken as the middle of the n^{th} leaf area increment. In these equations, the friation velocity u* is defined as

$$u^* = \frac{u_{zh} \, k}{\ln(z/z_o)} \tag{139}$$

where u_{zh} is the velocity of the air stream at the reference height and z_o is a roughness length which is a characteristic of the soil surface. The resistances were determined from the following equation by Owen and Thompson (1963),

$$rzH = \frac{u_{zh}}{u^*} + 0.52\left(\frac{u^* zh}{\nu}\right)^{0.54} (Pr)^{0.8} \qquad (140)$$

where ν is the kinematic viscosity of air and zh is the reference height. For rzE, the Prandtl number (Pr) is replaced by the Schmidt number. The various numerical constants in equation (143) were determined by measurements of Chamberlain (1966).

The energy balance for the soil surface can now be expressed as

$$R_{ns} = \frac{\rho C_P}{\gamma'} u^* \left(\frac{es - e_{zh}}{rzE}\right) + \rho C_P u^* \left(\frac{T_s - T_{zh}}{raH}\right) + SHF \qquad (141)$$

The vapor pressure at the soil surface is derived from

$$es = e(T_s) \exp\left(\frac{S_M}{R_v T_s}\right) \qquad (142)$$

where $e(T_s)$ is the saturated vapor pressure at temperature T_s and R_v is the gas constant for water vapor. R_{n_s} is defined as;

$$R_{ns} = VIS(1 - ALB_1) + NIR(1 - ALB_2) + TH\downarrow(n) - (TS)^4 \qquad (143)$$

where VIS and NIR are the total amounts of visible and near infrared radiation respectively which penetrates to the bottom of the canopy; ALB_1 and ALB_2 are the soil albedos for visible and near infrared radiation and $TH\downarrow(n)$ is the thermal radiation moving downward from the n^{th} increment of leaf area. Once again, a non-linear equation must be solved.

Again we solve equation (145) for T_s using the method of variable position. Once T_s is known, the fluxes of sensible and latent heat from the soil surface can be calculated using equations (137) and (138) respectively. The flux of CO_2 from the soil was simply estimated using measurements of Moss (1959) as a guide.

Successive Approximations

It is obvious by now that the solution to each system of equations presented in the preceding sections of this chapter has depended on the solution of some other part of the model. This interdependency makes necessary the use of successive approximations to solve all the equations simultaneously. At the beginning of this routine, the soil, air and leaf temperatures were set equal to the reference temperature at the reference height above the crop. The air water vapor pressures were also set equal to the value at the reference height. Then the thermal radiation components were calculated. Knowing the thermal radiation and the air temperatures and air water vapor pressures the leaf and soil temperatures were calculated. Then the sources of latent and sensible heat were calculated which were used in turn to calculate profiles of air temperature and water vapor pressure. Note that by integrating the sources the total sensible and latent heat was calculated for the crop. The procedure was repeated until the values of the sources from individual leaf area increments converged to a constant value.

A similar procedure was used to calculate net photosynthesis once the leaf temperatures were known. The initial values of the CO_2 concentrations of the air stream were set equal to the CO_2 concentration at the reference height. Knowing the air CO_2 concentrations sources and

sinks of net photosynthesis were calculated which were in turn used to calculate a CO_2 profile.

Thus the complete solution resulted in not only the source and sink distribution of net photosynthesis but similar distributions of sensible and latent heat as well. Also profiles of air temperatures, air water vapor pressures and CO_2 concentrations are also calculated. These prove extremely useful in verifying the model by comparing theory with experimental results.

Materials and Methods

The experimental verification of a mathematical model is an extremely important part of its development. In this case, field measurements of profiles of air temperature, CO_2 and water vapor concentrations along with vertical fluxes of CO_2, sensible and latent heat were compared to the calculations of the model. Such measurements along with many of the necessary plant properties (such as leaf area, leaf angle distribution, mesophyll and carboxylation resistances, etc.) were provided in a comprehensive study of momentum and energy exchange above and within stands of corn. The complete study was made at the Microclimate Experimental Site in Ellis Hollow near Ithaca, New York. The visible radiation and leaf area measurements described in Chapter I were part of this larger study. The leaf chamber measurements made by Dr. R. B. Musgrave and described in Chapter II were made in cooperation with this study. The complete study represented contributions from a team of individuals. The author was the team member directly responsible for the radiation and leaf area measurements.

The field measurements were made in a 20 acre field of corn which was planted at a density of 6.0 plants/m^2. The corn (variety - Cornell M-3) was planted in 38 cm wide, north-south rows with approximately 46 cm between plants in the rows. A check row planter was used to place the seeds in a hexagonal pattern. Early in the season of 1968, one-half the field was thinned to 4.4 plants/m^2. During August of 1968, this same portion of the field was twice more thinned, first to 2.4 and then to 1.4 plants/m^2. Measurements in each half of the field were made before

and after each thinning in August. Measurements in the thinned and unthinned portions of the field were made simultaneously.

A major facet of the field study consisted in applying the energy balance to estimate vertical fluxes of CO_2, sensible and latent heat. The energy balance equation can be written as;

$$R_n(z) = LE(z) + H(z) + \frac{1}{\lambda} N_t(z) + SHF \qquad (144)$$

Net radiation (R_n), and the vertical fluxes of sensible heat (H), latent heat (LE) and CO_2(N_t) are expressed as functions of height (z). The constant, λ, is a factor which converts gms of CO_2 into energy units. It is based on the amount of energy required to convert a mole of CO_2 into a mole of carbohydrate (Lemon (1962)). The above fluxes can be expressed as;

$$LE(z) = -\frac{\rho C_P}{\gamma'} K_H(z) \frac{\partial e(z)}{\partial z} \qquad (145)$$

$$H(z) = -\rho C_P K_H(z) \frac{\partial T(z)}{\partial z} \qquad (146)$$

and

$$N_t(z) = -\lambda K_H(z) \frac{\partial C(z)}{\partial z} \qquad (147)$$

The sign convention adopted here considers upward fluxes as positive. Thus combining equations (145) - (147) with (144) and rearranging, results in,

$$K_H(z) = \frac{R_n(z) - SHF}{-\frac{\partial C(z)}{\partial z} - \rho C_P \frac{T(z)}{\partial z} - \frac{\rho C_P}{\gamma'} \frac{\partial e(z)}{\partial z}} \qquad (148)$$

Note that once again the assumption is made that the eddy diffusivities for mass and heat transfer are identical. Therefore by measuring net

radiation, and the gradients of air temperature, water vapor and CO_2 concentrations above and within vegetation, the eddy diffusivity as a function of height can be calculated. Then by substituting the K_H values along with the above gradients in equations (145) - (147) the vertical fluxes of CO_2, sensible and latent heat can be calculated.

Net radiation was measured in the stands of corn with the same sampling system described in Chapter I. The Fritchen net radiometer was used (Fritchen, 1965). The net radiometer simply replaced the visible radiation sensor in a plexiglass holder and was pulled back and forth through the crop along nine meters of outrigging cables by a reversible motor and pulley system. Net radiation at five levels in each stand of corn was measured. A net radiometer was also mounted above each stand of corn.

Air temperature, and CO_2 and water vapor concentrations were measured using a complex air sampling system. This system was designed, constructed and operated by M. Johnson, G. Drake and Dr. E. R. Lemon. It will be described here only in very general terms. Details of the system can be found in Lemon et al. (1970). The central component of this sampling system was a double shielded air intake nozzle. It served the dual role of being an inlet to the air sampling system as well as providing an aspirated, radiation shielded mount for thermocouples. Ten nozzles were connected in parallel at a particular level above the ground. Air drawn in at each nozzle was sucked into a manifold which was in turn connected to a heated copper alloy conduit pipe. This pipe transported the air from a given level to laminated polyethylene - aluminum mylar bags which were situated in an air conditioned trailer at the edge of the experimental field.

Each nozzle consisted of a glass tube mounted concentrically inside a larger acrylic tube. The thermocouples were concentrically mounted inside the glass tube. For radiation shielding, the glass tube was covered with aluminized mylar. Also the acrylic tube was covered with a 1.25 cm layer of styrofoam which was in turn covered with aluminized mylar. The nozzle had an outside diameter and a length of approximately 5 and 25 cm respectively. One thermocouple in a nozzle represented one junction of a ten junction thermopile. Each thermopile was referenced to the level immediately below it. Thus there were two sets of junctions at each level. The lowest level was referenced to an ice bath.

A carbon-vane, oil-less rotary pump drew the air from the nozzles at a given level in the field to a set of storage bags in the air conditioned trailer. Air was sampled simultaneously at all levels for one-half hour periods. At the end of a 1/2 hour period the air from all the tubes was redirected to another set of empty bags. Air from the filled set of bags was then sequentially directed through an infrared water vapor analyzer (Modern Controls) which measured the absolute water vapor concentration at each level. The air then passed through the sample cell of a differential infrared CO_2 analyzer. (Mine Safety Appliance Co., Model LIRA 100). Air from the highest level above the ground was directed through the reference cell. The CO_2 concentration at this reference height was also measured with an absolute CO_2 analyzer. (Mine Safety Appliance Co., Model LIRA 200.) The millivolt signals from the analyzers were recorded on strip-chart recorders. Converted water vapor and CO_2 concentrations were subsequently plotted versus height above the ground surface. Gradients were estimated from smoothed curves drawn through these plotted points.

Wind measurements were made by L. H. Allen, Jr. in connection with the study of momentum exchange. Wind velocity was measured with cup annemometers above the vegetation(Cardion West, C. W. Thornthwaite Associates). The pulses from the cup annemometers were registered on printing counters. (Machine Electrification, Model MEK ZDG V). These counters printed accumulated counts for 5 min. intervals. Within the vegetation, heated thermocouple annemometers were used to obtain 5 and 30 minute mean values (Hastings - Roydist Inc., Air Meter Model Rm-IX, Probe Model N-7B).

Incoming total and diffuse solar radiation and total and diffuse visible radiation were measured as a part of the study. Solar radiation was measured with two Epply pyranometers. Visible radiation was measured with two custom mounted selenium cells. (The design of this sensor is described in Chapter I). Shade rings were placed over one of each of the above types of instruments to record the incoming diffuse solar and visible radiation.

Finally, soil heat flux plates (National Instrument Laboratories, Inc.) were used to measure the heat flux into the soil. A set of plates were placed just below the soil surface in each of the two portions of the field.

Millivolt signals from the heat flux plates, all of the radiometers, all of the thermocouples and all of the heated thermocouple annemometers were fed into a 100 channel data logger (A. D. Data Systems Incorporated). They were recorded sequentially on a 7-track magnetic tape. (Digital Tape Recorder: Digi-Data Corp.) The 100 channels could be sampled as often as once every two seconds. The 7-track tape was read and analyzed by an IBM 360/65 computer. Average half hour values were punched out

on cards. Values from the smoothed CO_2 and water vapor profiles at small height intervals were also punched out on cards. A computer program written by M. Groom read the values of air temperature, CO_2 and water vapor concentration, net radiation and the soil heat flux from cards and used these data for the energy balance calculations. The program fit the air temperature and net radiation data to polynomial functions of height. The temperature polynomial, when differentiated, supplied the necessary temperature gradients. Water vapor and CO_2 gradients were supplied by finite differences between the small height increments. Thus the program was able to calculate the eddy diffusivity as a function of height for a particular set of data along with the vertical fluxes of CO_2, sensible and latent heat.

A study of plant water relations was made simultaneously with the above measurements by R. W. Shawcroft. Leaves near the top of the crop and near the bottom were sampled periodically. The leaf stomatal resistance using a Van Bavel porometer (Van Bavel et al. 1965) and leaf relative water content were measured. The soil moisture tension using tensiometers was also measured in connection with this water relations study.

The above measurements represented a set of parameters which provided information needed in the model as well as numbers with which to verify the model. At this point a summary of information required by the model is in order.

First of all the values of air temperature, CO_2 and water vapor concentration, and wind velocity are needed at some reference height above the crop. Also values of net radiation, direct and diffuse solar radiation

and direct and diffuse visible radiation are needed above the crop. Finally the soil heat flux and soil moisture tension at the soil surface as well as the soil albedo are needed.

However, the above mentioned boundary conditions are only part of the input. The model itself is a complex function of plant characteristics which have to be known as well before any solution can be obtained. These plant parameters are of two types.

The displacement plane D, the roughness length z_o and the adjusted crop height (CAHT) which have been discussed earlier in this chapter are properties of the plant community as a whole.

On the other hand, individual leaf characteristics such as leaf transmittance and reflectance as described in Chapter I as well as mesophyll and carboxylation resistance and stomatal resistance as a function of light intensity are also needed.

Finally the leaf area density, the cumulative leaf area index and the leaf angle distributions as described in Chapter I represent a most important input to the model because we are particularly interested in studying the effects of crop architecture on the various exchange processes already mentioned. Only by incorporating a detailed description of the plant community in the mathematical model, can one do this.

Results and Discussions

At this time, the crop simulation model has not been extensively tested against the measurements. Three test periods on the 1968 unthinned corn (1145-1215, Aug. 15; 0845-0915, Aug. 18 and 1145-1215, Aug. 18) are reported here as examples. The test periods were relatively cloud free so that incoming solar radiation was almost constant over each half-hour interval. However, the test periods differed in that August 15 was much drier than August 18. The drier conditions were clearly reflected in the leaf resistance and water content. The effect of water stress will be considered in detail below.

First of all it is important that wind velocity can be predicted in the vegetation from measurements at the reference height. The wind velocity is used in equation (124) to calculate boundary layer resistances. Figure (30) represents a typical wind profile with D = 140 cm, z_o = 17 cm and CAHT = 180 cm. This profile was measured in the period 1145-1215, August 15. In general, for the purposes of the model, the theory predicted the wind velocity with height in the crop quite adequately. There is some discrepency at the bottom of the crop. Here the measured values remain constant while the theoretical values continue to decrease. This discrepancy is not serious to the model output but is interesting nonetheless. The measurements indicate an entrainment of air underneath the vegetation.

The eddy diffusivities for heat, calculated by the model show a number of differences from the values calculated from energy balance measurements as illustrated in Figure (31). First, the model consistently

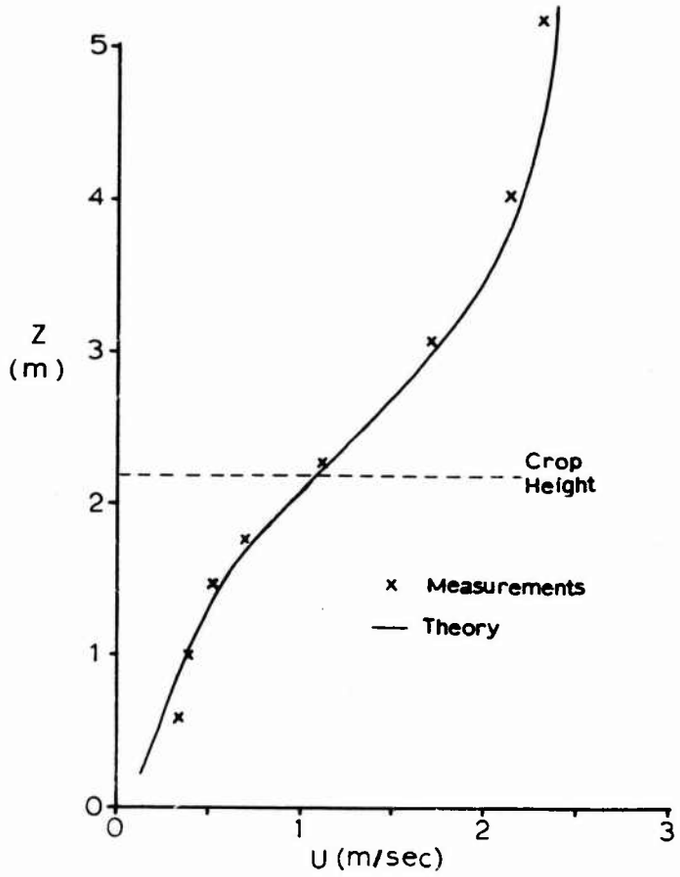

Figure 30. Wind velocity (u) as a function of height (z).

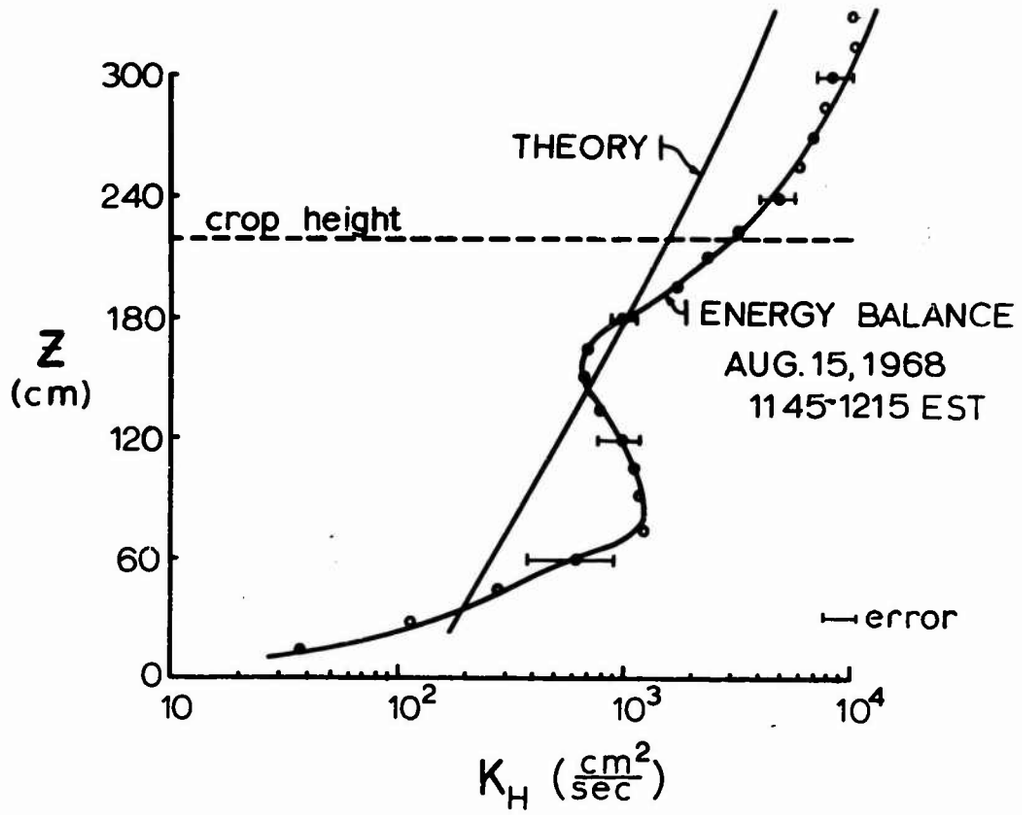

Figure 31(a). Eddy diffusivity for sensible heat (K_H) as a function of height (z) (Aug. 15, 1200).

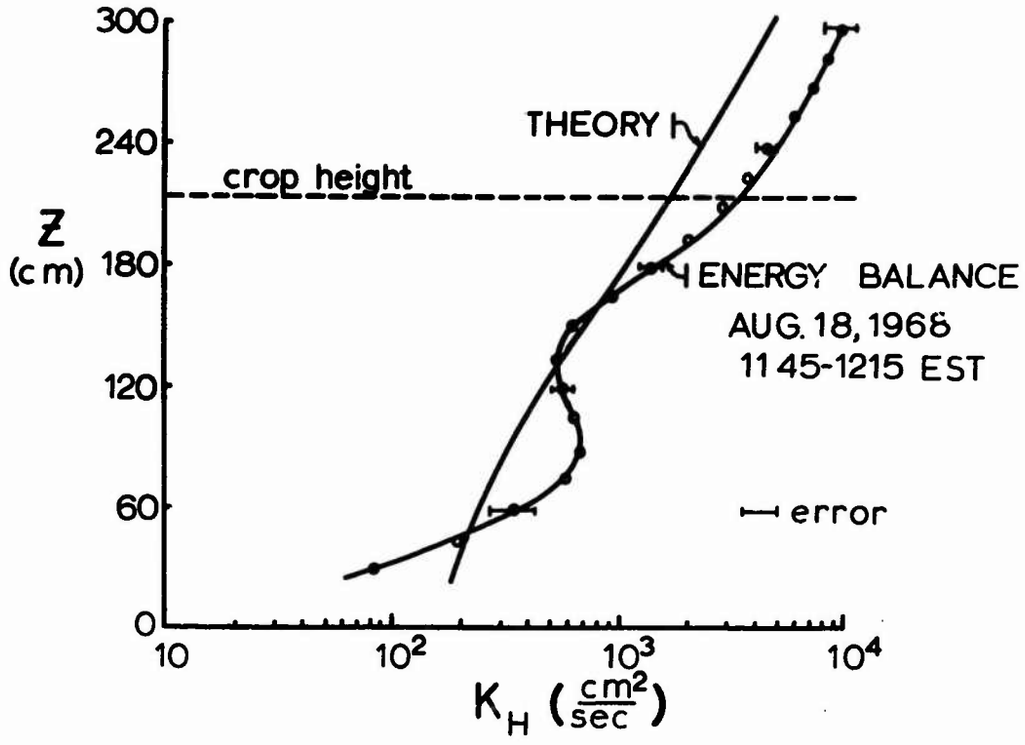

Figure 31(b). Eddy diffusivity for sensible heat (K_H) as a function of height (z) (Aug. 18, 1200).

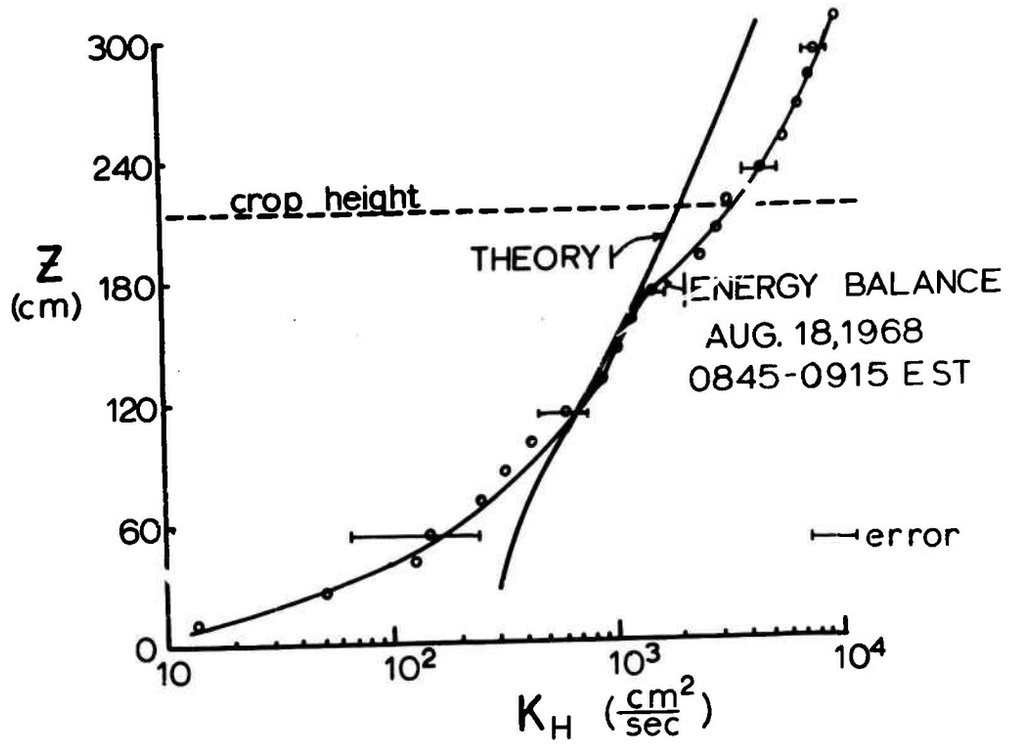

Figure 31(c). Eddy diffusivity for sensible heat (K_H) as a function of height (z) (Aug. 18, 0900).

underestimated the eddy diffusivities above the crop. In the crop, the theoretical values of K_H decrease approximately in an exponential manner. However, the measured mid-day profiles of K_H in the crop show a curious "S" shape as one moves down into the crop. This 'dip' in the profile is not as apparent as the 0845-0915 test period. The dip remains a mystery at this time. Further examination of more data is in order before making any suggestions as to its cause.

Figures (32-34) shows theoretical and measured profiles of CO_2 and water vapor concentrations, air temperature and net radiation. The total vertical fluxes above the crop of CO_2 and sensible and latent heat are given in Table II. Although the agreement between theory and measurements if far from perfect there are consistent trends in the data. The most obvious difference is the smaller amount of sensible heat and the larger amount of latent heat generated by the model.

This larger amount of sensible heat could explain in part the larger eddy diffusivities above the crop. The larger sensible heat flux increases the z/L ratio which was described in the theory. This in turn increases the K_H/K_M ratio. However, even on August 15 when the theory and measurements came closest to agreeing, K_H measured by the energy balance method was approximately twice as large as the theory predicted. An unsteady state condition in the field could also lead to a larger exchange coefficient. This larger eddy diffusivity from the measurements made matching theoretical to measured profiles much more difficult. Thus, boundary values in the model were set at values which matched the theoretical values of air temperature, CO_2 and water vapor concentration to measured values at the top of the crop. This made comparison within the crop much easier in Figures (32-34).

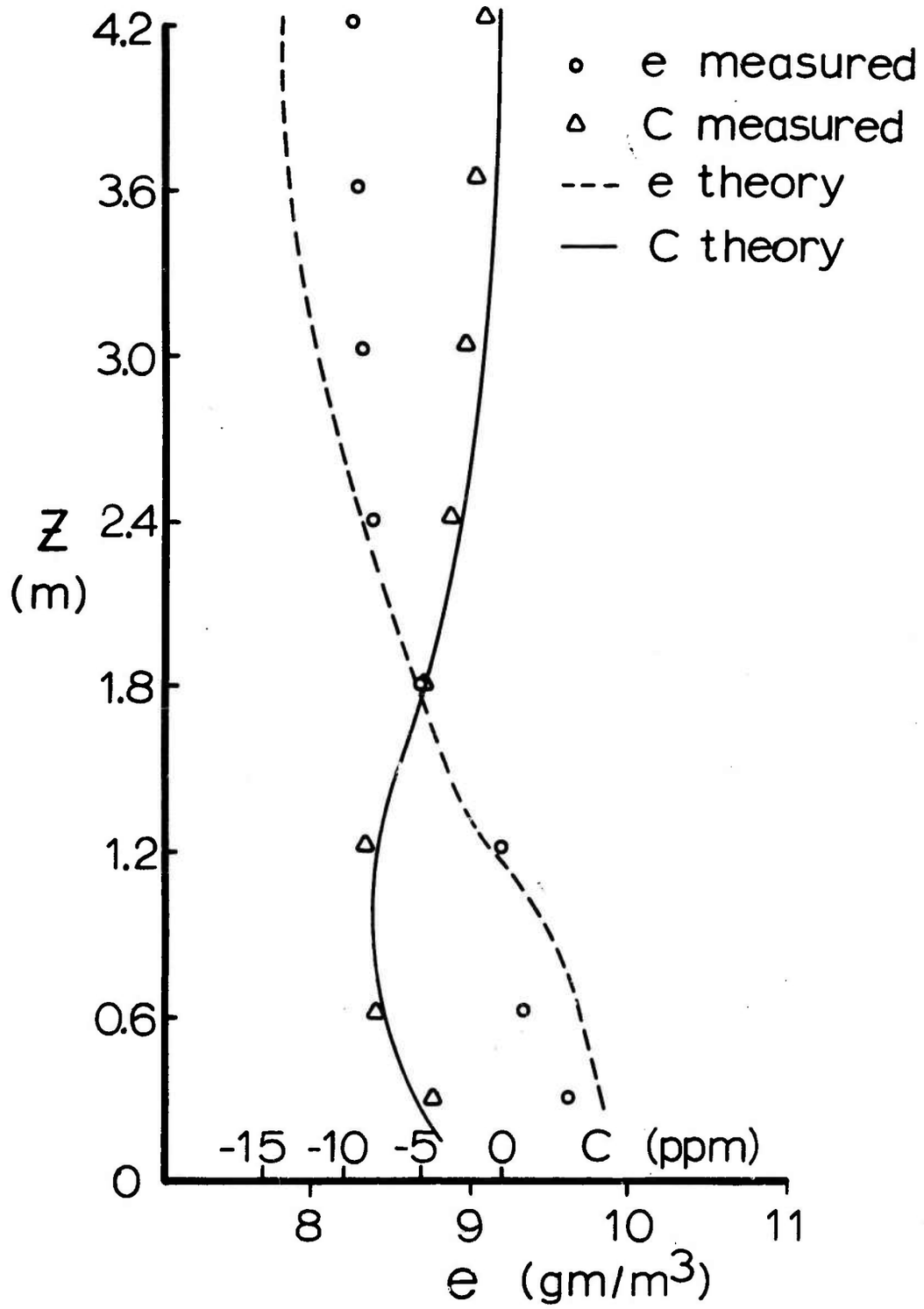

Figure 32(a). Theoretical profiles of CO_2 and water vapor concentration (e) with measurements (Aug. 15, 1200). The CO_2 concentrations as shown are subtracted from the concentration at the reference height.

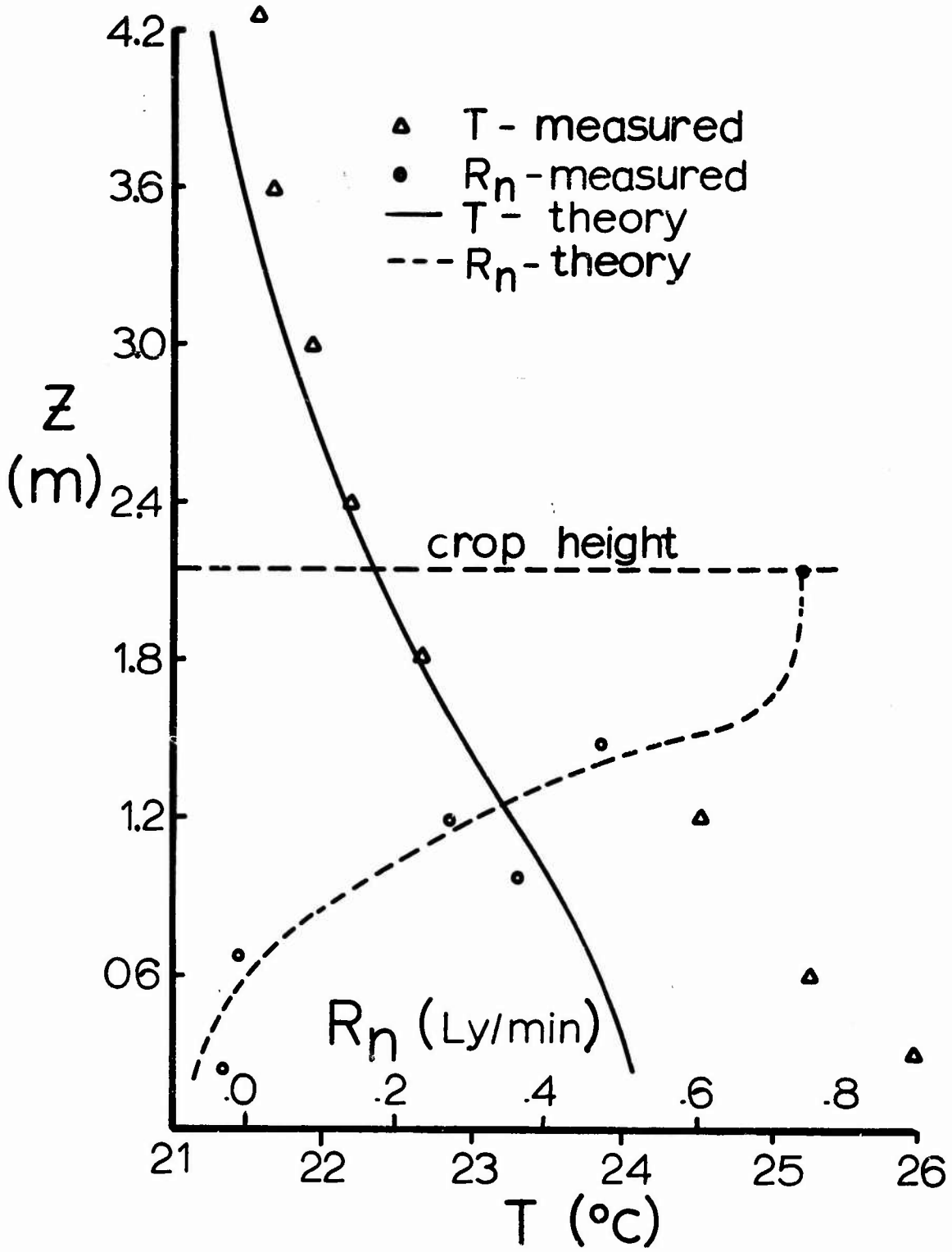

Figure 32(b). Theoretical profiles of air temperature and net radiation with measurements (Aug. 15, 1200).

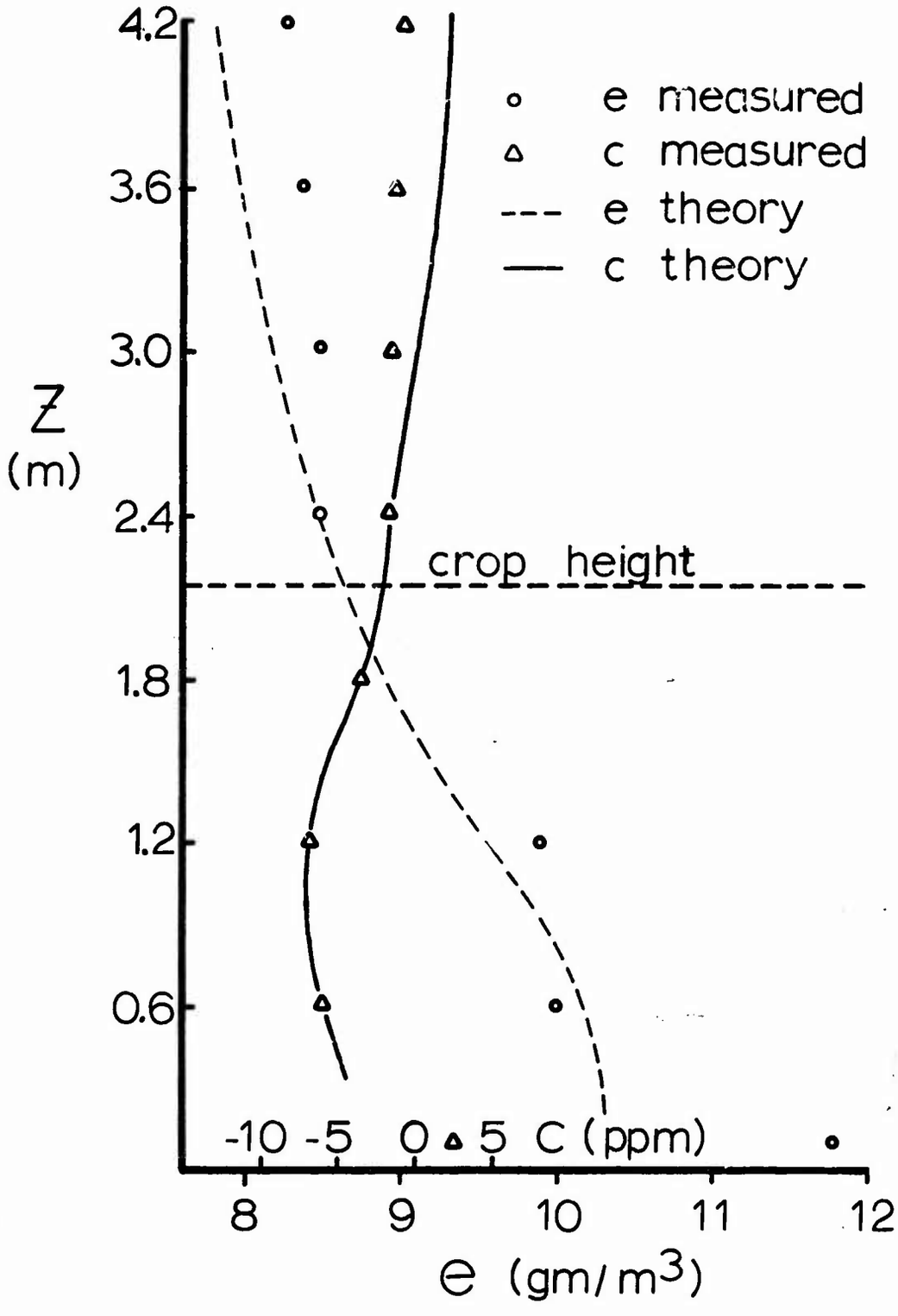

Figure 33(a). Theoretical profiles of CO_2 and water vapor concentration (e) with measurements (Aug. 18, 1200). The CO_2 concentrations as shown are subtracted from the reference height.

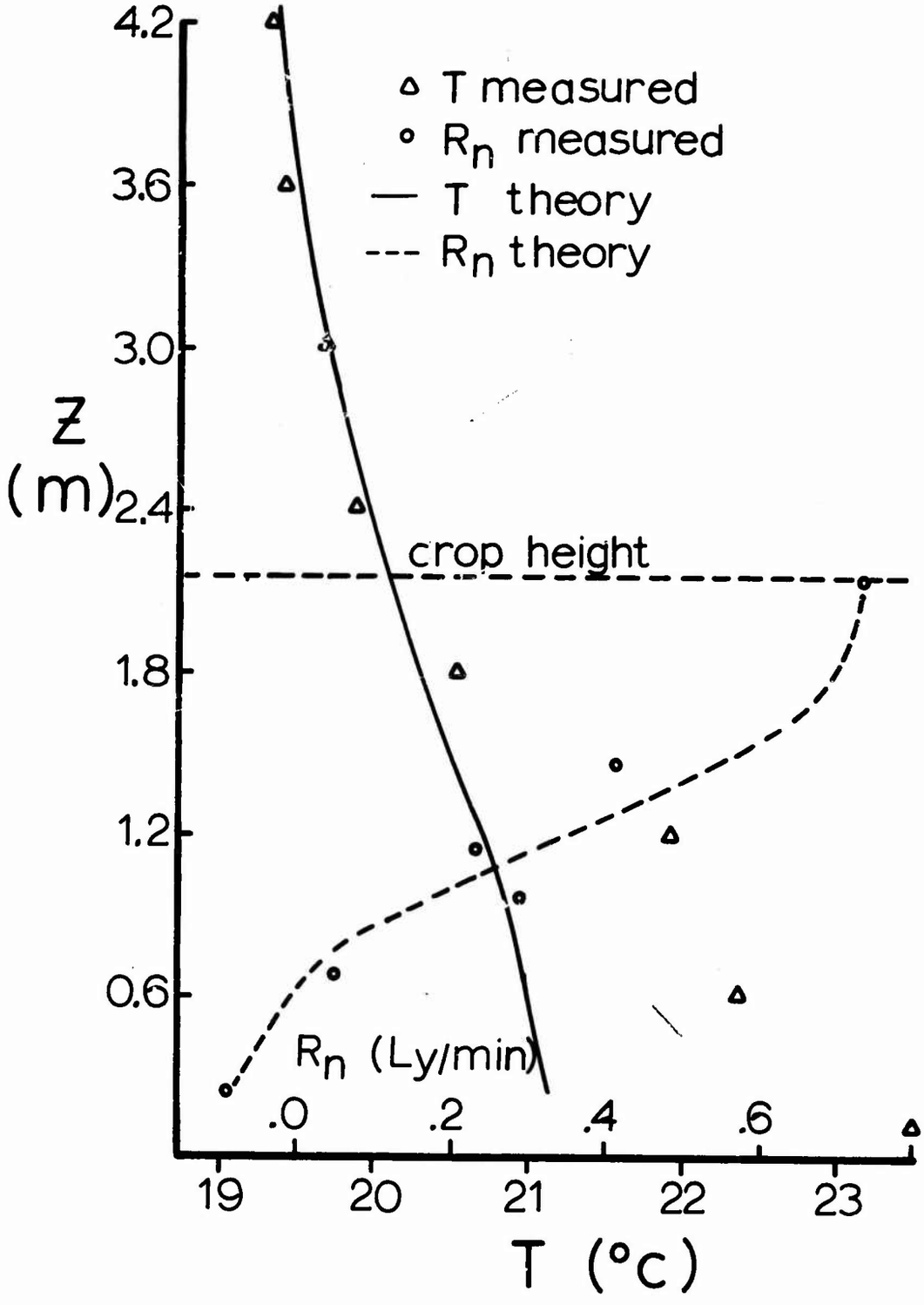

Figure 33(b). Theoretical profiles of air temperature and net radiation with measurements (Aug. 18, 1200).

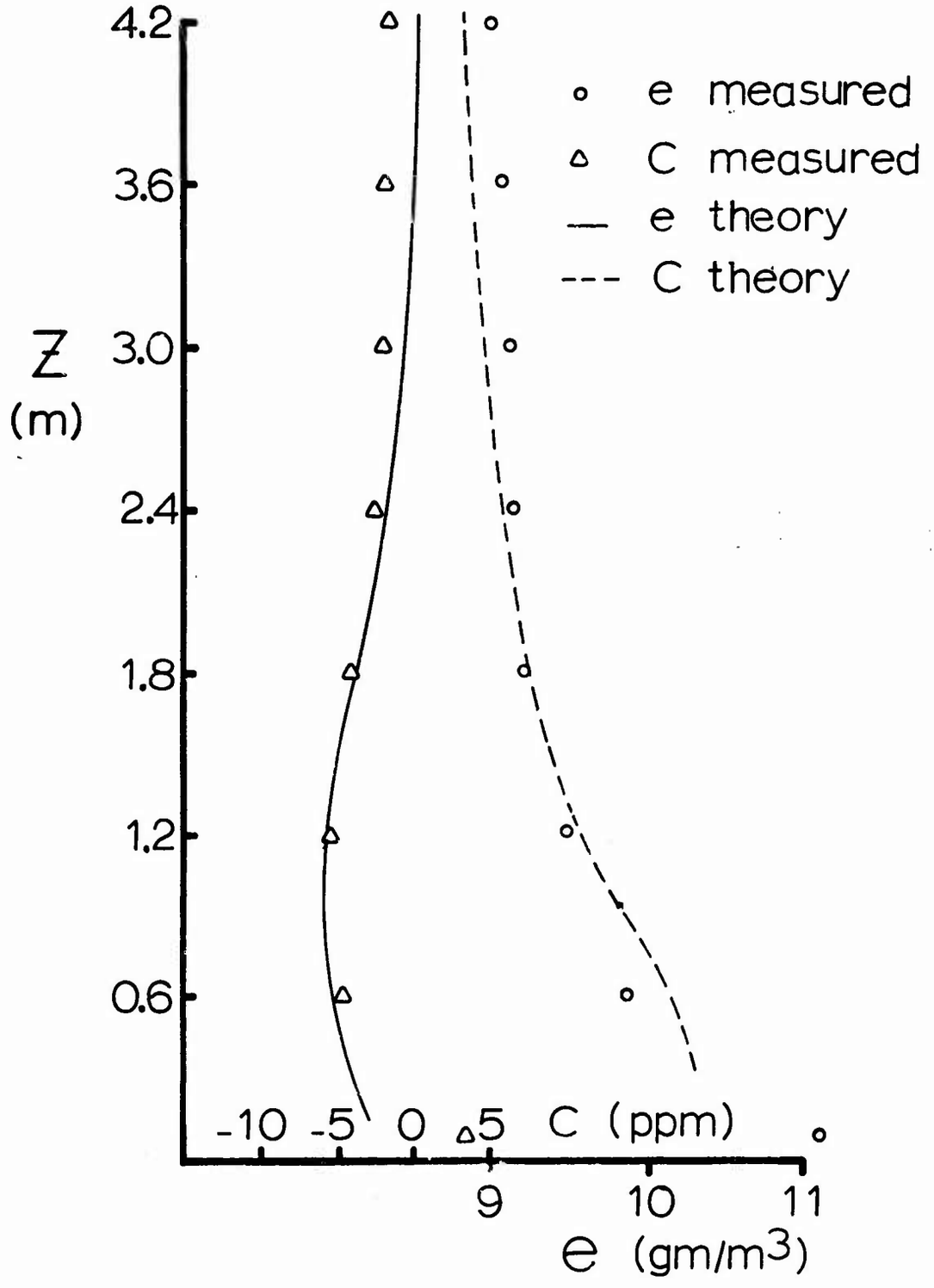

Figure 34(a). Theoretical profiles of CO_2 and water vapor concentration (e) with measurements (Aug. 18, 0900). The CO_2 concentrations as shown are subtracted from the concentration at the reference height.

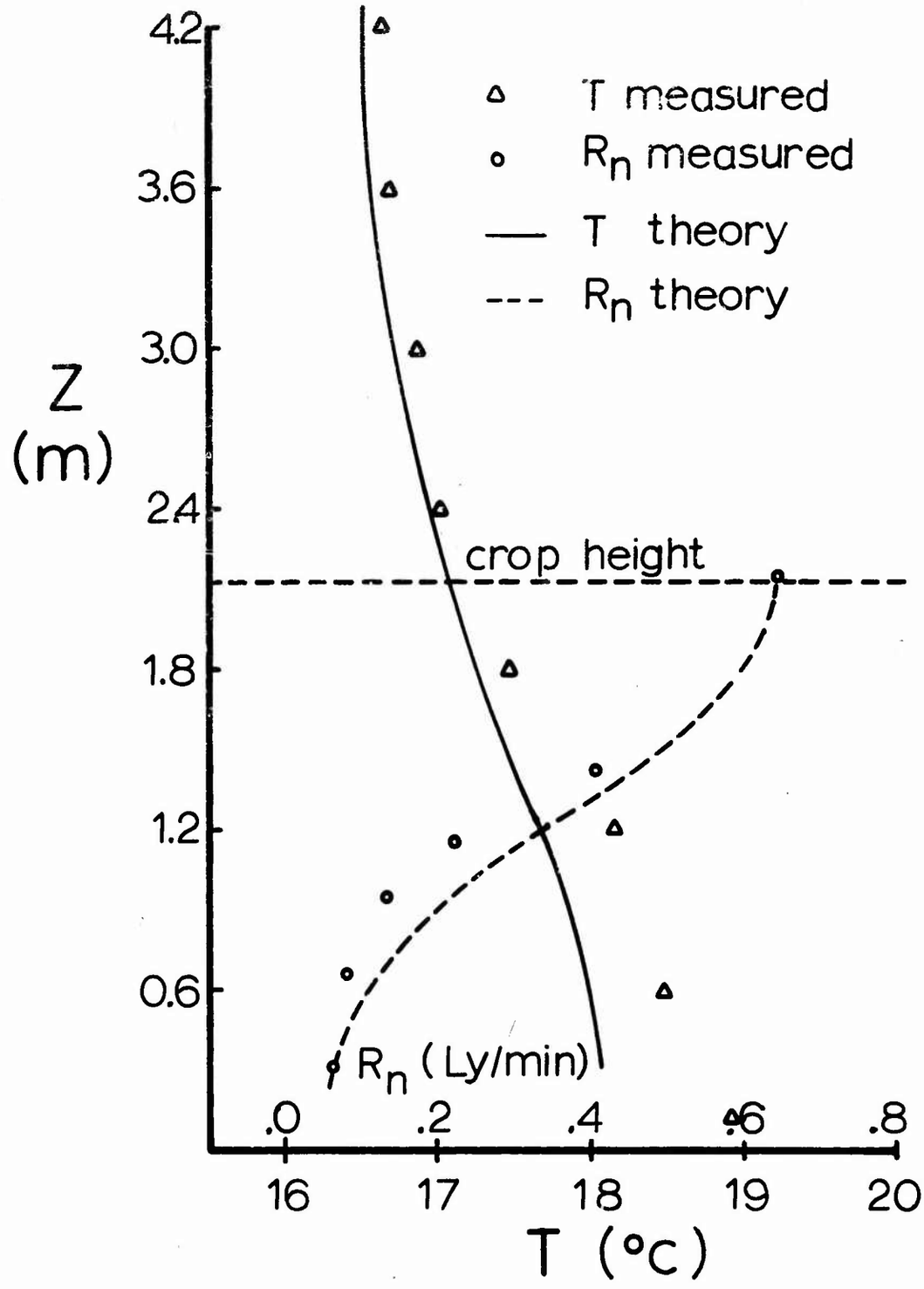

Figure 34(b). Theoretical profiles of air temperature and net radiation with measurements (Aug. 18, 0900).

TABLE II

Mean theoretical and energy balance values for the total flux of sensible and latent heat and of CO_2 from the unthinned corn crop.

1968	Sensible Heat	Latent Heat	Photosynthesis
	(cal/cm^2/min)		
Aug. 15: 1145-1215 EST			
Energy Balance	0.53	0.37	.020
Theory	0.39	0.53	.024
Aug. 18: 0845-0915 EST			
Energy Balance	0.42	0.18	.021
Theory	0.26	0.47	.025
Aug. 18: 1145-1215 EST			
Energy Balance	0.54	0.40	.025
Theory	0.24	0.71	.031

Immediately apparent in the within the crop comparison is the relatively large difference between the theoretical and measured air temperatures. Although the theoretical water vapor concentrations are in general higher than the measured in keeping with the higher theoretical amounts of latent heat, the discrepancy is not as apparent as in the temperature profile.

These temperature differences in the air stream could be caused by an inadequate theoretical treatment at the soil surface. There is a stronger source of sensible heat in the field than predicted by the model. This extra heat could come in part from the soil surface itself. The visible radiation study of Chapter I indicated that approximately 7-10% more radiation penetrates to the soil surface than is predicted by the model. The soil surface itself at the experimental site is to a large extent covered with stones which are dry and heat up readily since rock has a lower specific heat than moist soil. Also the latent heat flux at the soil surface is very difficult to calculate. This arises from the difficulty in predicting mean or effective soil moisture tension at the surface. In the model, a value is assumed which gives approximately equal sensible and latent heat fluxes from the soil surface. This combination of factors leads to an underestimation of the soil surface temperature. It is significant that the discrepancy between theory and measurements is less at 0900, Aug. 18 when the amounts of radiation reaching the soil surface is about one-half of the amount at 1200 hours.

The model does show good agreement between theory and measurements both in the profiles of CO_2 and in the estimations of net photosynthesis. There is a small consistant overestimation by the model. However,

considering the errors involved in the energy budget measurements and the uncertainties associated with stomatal resistance and leaf chamber measurements along with the various assumptions made in the model, the agreement between theory and measurement for net photosynthesis is quite adequate.

What is especially noteworthy in these test periods are the resulting effects of increasing stomatal resistance. The averaged measured leaf resistance in the uppermost leaves at 1200 on August 15 was 2.87 sec/cm. This average value was very close to 0.97 for the time periods of August 18. Thus for the dry day, γ_o, the minimum leaf resistance was changed from 0.97 to 2.87 sec/cm. This was reflected in the theoretical amounts of sensible and latent heats which were much closer to the measured values for this test period. Curiously, the energy balance measurements of latent heat and sensible heat do not reflect the effects of larger stomatal resistances on the drier day (Aug. 15).

The energy balance measurements do agree with the model when estimating net photosynthesis in that both theoretical and measured values of net photosynthesis are higher on the day of smaller leaf resistances for the same time periods (1200). At this time, both days had approximately equal amounts of solar radiation. Air temperature, and wind velocities were similar as well. While there are many other factors involved, there is evidence here to suggest that the leaf resistance had a significant effect on the photosynthesis rate. However, more extensive comparisons are needed to verify the effect.

Conclusions

The limited comparison of the model to field measurements made in this study is not meant to be a critical test of the model. Much more extensive work remains before the model can be truly evaluated. However, in this initial stage, the model does show signs of becoming a powerful tool to be used in the understanding of crop-environment interactions. Especially encouraging has been the manipulation of the stomatal resistance to give a decrease in photosynthesis. This provides a means to study parameter significance in the water use efficiency of plants.

Improvements over previous models are that no extinction coefficient had to be assumed for the penetration of visible or net radiation into the crop as long as the distribution of the leaf area is random. Also no extinction coefficient was used to describe the eddy diffusivity with height in the crop. The eddy diffusivity was coupled directly with the wind velocity which was in turn predicted in the crop. The treatment of visible radiation distribution on plant leaves was extended to include the distribution of near infrared radiation as well. This along with a treatment of thermal radiation allowed the net radiation to be calculated.

This model also represents an attempt to incorporate the effects of leaf area density on the mixing processes in the crop. However, in general the theory did not adequately reflect the energy balance measurements both above and within the crop. A much fuller treatment of turbulent exchange in vegetation still needs to be developed.

Similarly there is still much work to be done in effectively dealing with the soil surface. It is especially difficult to estimate the flux of

water from any soil surface because of the difficulty in estimating the soil moisture tension. More detailed models will include treatments of unsaturated water flow in soils to the soil surface and to roots. The model by Cowan (1965) is an example of this type of work.

In general, the use of mathematical models helps considerably in systematically attacking the problems of understanding the complex interactions between the plant community and the environment. This model attempted to sort out and evaluate factors which contribute to net photosynthesis over a short time period. While this in no way represents an understanding of all the growth processes, it does allow one aspect of growth to be singled out and studied intensively.

LITERATURE CITED

Allen, L. H. Jr. 1968. Turbulence and wind speed spectra within a Japanese larch plantation. J. of App. Met. 7:73-78.

Allen, L. H. Jr. and K. W. Brown. 1965. Shortwave radiation in a corn crop. Agron. J. 57:575-580.

Allen, W. A. and Richardson A. J. 1968. Interaction of light with a plant canopy. J. Opt. Soc. America 58:1023-1028.

Anderson, M. C. 1964. Light relations of terrestrial plant communities and their measurements. Biol. Reviews 39:425-486.

Anderson, M. C. 1966. Stand structure and light penetration II. A theoretical analysis. J. of App. Ecology. 3:41-54.

Black, J. N. 1955. The interaction of light and temperature in determining the growth rate of subterranean clover. Aust. J. of Biol. Sciences 8:330-344.

Brower, R. and C. T. de Wit. 1968. A simulation model of plant growth with special attention to root growth and its consequences. Proceedings of the Fifteenth Eastern School in Agricultural Science, University of Nottingham. Ed. by W. J. Whittington.

Bulley, N. R., C. D. Nelson and E. B. Tregunna. 1969. Photosynthesis: Action spectra for leaves in normal and low oxygen. Plant Physiology 44:678-684.

Chamberlain, A. C. 1968. Transport of gases to and from surfaces with bluff and wavelike roughness elements. Quart. J. Roy. Met. Soc. 94:318-332.

Chartier, P. 1966a. Étude du microclimat lumineux dans la végétation. Ann. Agronomiques 17:571-602.

Chartier, P. 1966b. Étude theorique de l'assimilation brute de la feuille. Annales de Physiol. végétale 8:167-196.

Chartier, P. 1969. A model of carbon dioxide assimilation in a leaf. In 'Productivity of Photosynthetic Systems, Models and Methods', IBP/PPP Technical Meeting, Sept. 1969, Trebon, Czeckoslovakia (In Press).

Cionco, R. M. 1965. A mathematical model for air flow in a vegetative canopy. J. of App. Mat. 4:517-522.

Conte, S. D. 1965. Elementary Numerical Analysis, McGraw Hill Book Company.

Cowan, I. R. 1965. Transport of water in the soil-plant-atmosphere system. J. App. Ecol. 2:221-239.

Cowan, I. R. 1968. Mass, heat and momentum exchange between stands of plants and their atmospheric environment. Quart. J. Roy. Met. Soc. 94:523-544.

Davidson, J. L. and J. R. Philip. 1958. Light and pasture growth. In: climatology and microclimatology. Proc. Canberra Sym. (1956), Arid Zone Research XI, UNESCO Paris.

Duncan, W. G., R. S. Loomis, W. A. Williams and R. Hanau. 1967. A model for simulating photosynthesis in plant communities. Hilgardia 38:181-205.

Ellison, T. H. 1957. Turbulent transport of heat and momentum from an infinite rough plane. J. of Fluid Mech. 9:456-467.

Federer, C. A. and C. B. Tanner, 1966a. Spectral distribution of light in the forest. Ecology 47:555-560.

Federer, C. A. and C. B. Tanner. 1966b. Sensors for measuring light available for photosynthesis. Ecology 47:654-657.

Fritschen, L. J. 1965. Miniature net radiometer improvements. J. of App. Met. 4:528-532.

Gaastra, P. 1959. Photosynthesis of crop plants as influenced by light, carbon dioxide, temperature and stomatal diffusion resistance. Meded. Landbouwhogeschool, Wageningen 59:1-68.

Gebhart, B. 1961. Heat Transfer. McGraw Hill Book Company.

Glenday, A. C. 1955. The mathematical separation of plant and weather effects in field growth studies. Aust. J. Agric. Res. 6:813-822.

Heichel, G. H. 1968. Intervarietal photosynthetic investigations on corn (Zea Mays L.) I. Varietal differences in net photosynthesis. II. Photosynthetic response to leaf water potential. Thesis (Ph.D.) Cornell University, Ithaca, New York.

Heichel, G. H. and R. B. Musgrave. 1969. Varietal differences in net photosynthesis of Zea Mays L. Crop Science 9:481-483.

Hesketh, J. D. and R. B. Musgrave. 1962. Photosynthesis under field conditions IV. Light studies with individual corn leaves. Crop Science 2:311-315.

Hunt, L. A., I. I. Impens and E. R. Lemon. 1967. Preliminary wind tunnel studies of the photosynthesis and evapotranspiration of forage stands. Crop Sci. 7:575-579.

Hunt, L. A., I. I. Impens and E. R. Lemon. 1968. Estimates of the diffusion resistance of some large sunflower leaves in the field. Plant Physiology 43:522-526.

Idso, S. B. 1968. A holocoenotic analysis of environment - plant relationships. Techn. Bull. 264, Ag. Exp. Station, U. of Minnesota.

Isobe, S. 1962. Preliminary studies on physical properties of plant communities. Bull. Natn. Inst. Agric. Sci. Tokyo, A. 9:29-67.

Kanemasu, E. T., G. W. Thurtell and C. B. Tanner. 1969. Design, calibration and field use of a stomatal diffusion porometer. Plant Physiol. 44:881-885.

Kasanago, H. and M. Monsi. 1954. On the light transmission of leaves and its meaning for the production of matter in plant communities. Jap. J. of Bot. 14:304-324.

Kerr, J. P., G. W. Thurtell and C. B. Tanner. 1968. An integrating pyranometer for climatological observer stations and mesoscale networks. J. of App. Met. 6:688-694.

Kestin, J. 1966. The effect of free stream turbulence on heat transfer rates. Advances in Heat Transfer 3:1-31.

Kuiper, P. J. C. 1961. The effects of environmental factors on the transpiration of leaves with special reference to stomatal light response. Meded. Landbouwhogeschool, Wageningen 6(17):1-49.

Lake, J. V. 1967. Respiration of leaves during photosynthesis. I. Estimates from an electrical analogue. Aust. J. of Biol. Sciences. 20:487-493.

Lemon, E. R. 1960. Photosynthesis under field conditions. II. An aerodynamic method for determining the turbulent carbon dioxide exchange between the atmosphere and a corn field. Agron. J. 52:697-703.

Lemon, E. R. 1962. Energy and water balance of plant communities. In Environmental Control of Plant Growth. Ed. by L. T. Evans. Academic Press.

Lemon, E. R. 1965. Micrometeorology and the physiology of plants in their natural environment. Plant Physiology, a Treatise. Vol 4: 203-227. Ed. by F. C. Steward. Academic Press.

Lemon, E. R., W. Covey, S. D. Ling, D. E. Ordway, A. Ritter, D. A. Spence, J. Stoller and H. S. Tan. 1963. The energy balance at the earth's surface. Part II. U.S.D.A. Production Research Report, No. 72. (DDC).

Lemon, E. R., Allen, L. H. Jr., M. Johnson, G. Drake, D. W. Stewart, J. L. Wright. 1970. Instrumentation for micrometeorological investigations. Interim Report 70-2, Microclimate Investigations, N.E.B., S.W.C.D., U.S.D.A. Bradfield Hall, Cornell University, Ithaca, New York (In press).

Loomis, R. S., W. A. Williams, W. G. Duncan, A. Dovrat and F. Nunez. 1969. Quantitative descriptions of foliage display and light absorption in field communities of corn plants. Crop Science 8:352-356.

Maisel, D. S. and T. K. Sherwood. 1950. Evaporation of liquids into turbulent gas streams. Chem. Eng. Progr. 46:131-138.

Monsi, M. and T. Saeki. 1953. Uber den Lichtfactor in den Pflanzengesehi-schaften und seine Bedeutung fur die Stoffproduktion. Jap. J. Bot. 14:22-52.

Monteith, J. L. 1965. Light distribution and photosynthesis in field crops. Ann. Bot., London. (N.S.) 29:17-37.

Monteith, J. L. and G. Szeicz. 1960. The carbon dioxide flux over a field of sugar beet. Quart. J. Roy. Met. Soc. 86:205-214.

Moss, D. N. 1966. Respiration of leaves in light and darkness. Crop Science 6:351-354.

Nichiporovich, A. A. 1961. Properties of plant crops as an optical system. Soviet Pl. Physiol. 8:428-435.

Niilisk, H., T. Nilson and J. Ross. 1969. Radiation in plant canopies and its measurement. In 'Productivity of Photosynthetic Systems, Models and Methods.' IBP/PP Technical Meeting, Trebon, Sept. 1969. Trebon, Czechoslovakia (In Press).

Owen, P. R. and W. R. Thompson. 1963. Heat transfer across rough surfaces. J. Fluid Mech. 15:321-334.

Panofsky, H. A. 1961. An alternative derivation of the diabotic wind profile. Quart. J. Roy. Met. Soc. 87:109-110.

Panofsky, H. A. 1965. Reanalysis of Swinbank's Kerang Observations. In 'Flux of Heat and Momentum in the Planetary Boundary Layer of the Atmosphere': Final Report AFCRL - 65-531, Penn. State University.

Parkhurst, D. F., P. R. Duncan, D. M. Gates and F. Kreith. 1968. Wind-tunnel modelling of convection of heat between air and broad leaves of plants. Agr. Met. 5:33-47.

Pearman, G. I. 1965. Preliminary studies of the loss of heat from leaves under conditions of free and forced convection. Aust. J. Bot. 13:153-160.

Perrier, A. and M. Hollaire. 1968. A theoretical approach of microturbulence and transfers in the plant community as a means of study of crop production. A paper presented at the 8th National Conference in Agricultural Meteorology, May, 1968. Ottawa, Canada.

Philip, J. R. 1964. Sources and transfer processes in the air layers occupied by vegetation. J. of App. Met. 3:380-395.

Rabinowitch, E. I. 1951. Photosynthesis and Related Processes. Kinetics of Photosynthesis. Interscience Publishers, New York.

Sellers, W. D. 1962. A simplified derivation of the diabotic wind profile. J. of Atm. Science 19:180-181.

Snedecor, G. W. 1956. Statistical Methods 5th ed., Iowa State Univ. P ess.

Sutton, O. G. 1955. Atmospheric Turbulence. London: Methuen and Co. Ltd., New York: John Wiley and Sons, Inc.

Swinbank, W. C. 1964. The exponential wind profile. Quart. J. Roy. Met. Soc. 90:119-135.

Swinbank, W. C. 1968. A comparison between predictions of dimensional analysis for the constant-flux layer and observations in unstable conditions. Quart. J. Roy. Met. Soc. 94:460-467.

Takeda, T. and A. Kumera. 1957. Analysis of grain production in rice plants. Proc. Crop. Sci. Soc. Japan 26:165-175.

Thom, A. S. 1968. The exchange of momentum, mass and heat between an artificial leaf and the airflow in a windtunnel. Quart. J. Roy. Met. Soc. 94:44-55.

Turner, N. C. 1969. Stomatal resistance to transpiration in three contrasting canopies. Crop Science 9:303-307.

Van Bavel, C. H. M., F. S. Nakayuma and W. L. Ehrler. 1966. Measuring transpiration resistance of leaves. Plant Physiology. 40:535-540.

Waggoner, P. E. 1969. Predicting the effect upon net photosynthesis of changes in leaf metabolism and physics. Crop Science 9:315-320.

Waggoner, P. E. and W. E. Reifsnider. 1968. Simulation of the temperature, humidity and evaporation profiles in a leaf canopy. J. of App. Met. 400-409.

Watson, D. J. 1947. Comparative physiological studies on the growth of field crops. I. Variation in net assimilation rate and leaf area between species and varieties, and within and between years. Ann. Bot. London. (NS) 11:41-76.

Watson, D. J. 1952. The physiological basis of variation in yield. Advances in Agronomy 4:101-145.

Williams, R. F. 1946. The physiology of plant growth with special reference to the concept of net assimilation rate. Ann. Bot., London (N.S.) 10:41-72.

Wilson, W. J. 1960. Inclined point quadrants. New Phytologist 59:1-8.

Wit, C. T. de. 1965. Photosynthesis of leaf canopies. Versl. Landbouwk. Onderz. 663, 57 p.

Wright, J. L. and K. W. Brown. 1967. Comparison of momentum and energy balance methods of computing vertical transfer within a crop. Agron. J. 59:427-432.

UNCLASSIFIED

Security Classification

DOCUMENT CONTROL DATA - R & D

(Security classification of title, body of abstract and indexing annotation must be entered when the overall report is classified)

1. ORIGINATING ACTIVITY (Corporate author)	2a. REPORT SECURITY CLASSIFICATION
Microclimate Investigations, SWC-ARS-USDA Bradfield Hall; Cornell University Ithaca, New York 14850	UNCLASSIFIED
	2b. GROUP

3. REPORT TITLE

SIMULATION OF NET PHOTOSYNTHESIS OF FIELD CORN

4. DESCRIPTIVE NOTES (Type of report and inclusive dates)

Interim Report

5. AUTHOR(S) (First name, middle initial, last name)

D. W. Stewart and E. R. Lemon

6. REPORT DATE	7a. TOTAL NO. OF PAGES	7b. NO. OF REFS
December 1969	133	63

8a. CONTRACT OR GRANT NO.	9a. ORIGINATOR'S REPORT NUMBER(S)
Cross Service Order 2-68	USDA-ARS-SWC No. 407
b. PROJECT NO.	C.U. Research Report No. 878
c. DA Task 1TO-61102-B53A-17	9b. OTHER REPORT NO(S) (Any other numbers that may be assigned this report)
d.	ECOM 2-68I-6

10. DISTRIBUTION STATEMENT

Distribution of this document is unlimited

11. SUPPLEMENTARY NOTES	12. SPONSORING MILITARY ACTIVITY
	U.S. Army Electronics Command Atmospheric Sciences Laboratory Fort Huachuca, Arizona

13. ABSTRACT

A crop of corn was treated as a random array of leaf elements. A mathematical model was developed which expressed the net photosynthesis rate of an individual leaf as a function of the light flux density and CO_2 concentration at the leaf surface and the leaf temperature. This model compared favourably with leaf chamber measurements made by Dr. R. B. Musgrave of Cornell University. The leaf model was used in a larger model which simulated the crop net photosynthesis rate. Methods were developed to estimate the light distribution, and leaf temperatures and CO_2 concentrations at leaf surfaces under field conditions. A computer routine similar to the Duncan model calculated light penetration and distribution in a crop. Good agreement was found between calculated values of light penetration and measurements at various levels in stands of corn. Measurements were made with custom mounted selenium cells. Calculations of leaf temperatures involved solving the energy balance equation at the leaf surfaces. This in turn involved solving for sensible and latent heat. Theory was developed to calculate eddy diffusivities in and above the crop which were used in one-dimensional continuity equations to describe turbulent transport between the atmosphere and sources and sinks in the crop. Total fluxes of CO_2, and sensible and latent heat were calculated along with profiles of air temperature, CO_2 and water vapour concentrations and net radiation. Profiles of these variables were measured as well. Reasonable agreement between energy balance calculations of CO_2 flux above the crop and the model were obtained. However, the model overestimated latent heat flux and underestimated sensible heat flux when compared to energy balance calculations.

DD FORM 1 NOV 68 1473 REPLACES DD FORM 1473, 1 JAN 64, WHICH IS OBSOLETE FOR ARMY USE.

UNCLASSIFIED

Security Classification

14. KEY WORDS	LINK A		LINK B		LINK C	
	ROLE	WT	ROLE	WT	ROLE	WT
Mathematical Model						
Vegetation						
Radiation regime						
Turbulent transport						
Sensible heat exchange						
Latent heat exchange						
Leaf temperatures						
CO_2 exchange						

ERRATA TO

Energy Budget at the Earth's Surface: A Simulation of Net Photosynthesis of Field Corn

D. W. Stewart, E. R. Lemon

R & D Technical Report ECOM 2-68 I-6
Interim Report 69-3
December 1969

Page	Line (L), Equation (Eq) or Figure (F)	Correction
13	L.2	. . . $\sin\theta_1 = z/r$, $\tan\phi = y/x$ and tan (IL) $= \frac{z}{y}$. ϕ is the angle . . .
13	Eq. 17	$\theta_1 = \arcsin \sqrt{\frac{\beta' \sin^2\phi}{1 + \beta' \sin^2\phi}}$
13	Eq. 20	$Sc\uparrow = \frac{\sin(LS) \cdot DI}{\sin(IS)} (\mu(1-E) + \lambda E)$
14	Eq. 21	$Sc\downarrow = \frac{\sin(LS) \cdot DI}{\sin(IS)} (\mu E + \lambda(1-E))$
14	L. 20	. . . radiation in the crop moving down and up . . .
18	Eq. 30	$Sc_i\downarrow = \bar{S}_i\downarrow (1 + \beta\downarrow + \beta^2\downarrow + \beta^3\downarrow + \ldots .)$
18	Eq. 31	$TH_i = (FOSR_i) \cdot SK + (1 - FOSR_i) \cdot \sigma \cdot \overline{TL}_i^4$
19	L. 10	. . . temperatures in increment i . . .
38, 40, 42	F. 14, 16, 17	ordinate is "percent transmission/10"
45	L. 3	"overestimate" should read "underestimate"

51	Eq. 58	$R = R_x \text{ EXP}[9000 \ln Q \ (\frac{1}{303} - \frac{1}{T})]$
55	L. 18	. . . combining (62) and (55), one obtains . . .
	L. 7	. . . μ einsteins/cm^3
75	L. 12 and 14	$(L'/u)^{\frac{1}{2}}$ instead of $(L/u)^{\frac{1}{2}}$
76	F. 27	should read "L' (cm) is the leaf width"
82	Eq. 84	$\frac{\partial u}{\partial z} = \frac{u^*}{kL} \ \{1 - \exp(- \frac{(z - D)}{L})\}^{-1}$
83	Eq. 88	$K_H = -H/(\rho C_p \frac{\partial T}{\partial z})$
84	Eq. 93	$\frac{\partial T}{\partial z} = \frac{H}{\rho C_p u^{*2}(-1.4 \exp(1.5(z/L)) + 3.0)} \frac{\partial u}{\partial z}$
84	Eq. 94 and 95	$T_{ch} = T_h - \frac{H}{\rho C_p u^* k}$ . . . . .
84	Eq. 96	$e_{ch} = e_h - \frac{\gamma' LE}{\rho C_p u^* k}$ (FY)
84	Eq. 97	$C_{ch} = C_h - \frac{N_t}{u^* k}$ (FY)
86	Eq. 102	$L = - \frac{u^{*3} T_h \rho C_p}{k g H}$
87	Eq. 107	$\tau = \rho \ell^2 (\frac{du}{dz})^2$
89	Eq. 119	$- \frac{\partial H}{\partial F} = \rho C_p (\frac{T_L - T}{r_a})$

ERRATA

90	Eq. 120	$-\frac{\partial H_i}{\partial F} = \rho C_p \frac{\sum_{j=1}^{20} (T_{L_{ij}} - T_i) \; FR_{ij}}{r_{ai}}$
90	Eq. 121	$H = f \; K \; \rho C_p \; \frac{\partial T}{\partial F}$
90	Eq. 122	$-\frac{\partial}{\partial F} (f \; K \; \frac{\partial T_i}{\partial F}) = \ldots .$
91	F. 29	In the figure, $f_1 \; K_1$ should be replaced by K_{ch}; $f_2 \; K_2$ by $f_1 \; K_1$; etc.
92	L. 17	. . . large values of Δz . . .
92	Eq. 127	$-f_n K_n \frac{(T_{n-1} - T_n)}{S} - \frac{FHS}{\rho C_p} = \frac{S}{r_{an}} \Sigma (T_{L_{nj}} - T_n) \; FR_{nj}$
93	L. 8	$-K_1 f_1$ should replace 0 in the second line, 1st column of the matrix AM.
93	L. 25	S^2/r_{a1} should replace S^2/r_{ai} in the first line, 2nd column of the matrix BM.
94	Matrix FH, L. 1	$\Sigma T_{L_{1j}} \cdot FR_{1j} \cdot S^2/r_{a1} + K_{ch} \cdot T_{ch} \cdot S/\Delta z$
	L. 6	$\Sigma T_{L_{nj}} \cdot FR_{nj} \cdot S^2/r_{an} + FHS \cdot S/\rho C_p$
94	L. 16	FR_{1j} should replace FR_{ij} in the term of the 1st line, 1st column of the matrix EM

95 Matrix FLE

$$\begin{pmatrix} S^2\,\Sigma e(T_{L_{1j}}) \cdot FR_{1j}/(r_{a1} + rs_{1j}) + K_{ch}\, e_{ch}\, S/\Delta z \\ S^2\,\Sigma e(T_{L_{2j}}) \cdot FR_{2j}/(r_{a_2} + rs_{2j}) \\ \vdots \\ S^2\,\Sigma e(T_{L_{nj}}) \cdot FR_{nj}/(r_{an} + rs_{nj}) + FLHS \cdot S/\rho C_p \end{pmatrix}$$

96 Matrix FC

$$\begin{pmatrix} S^2\,\Sigma fn(C_1 - ra_1 N_{1j}) FR_{1j} + K_{ch} C_{ch}\, S/\Delta z \\ \vdots \\ S^2\,\Sigma fn(C_n - r_{an} N_{nj}) FR_{nj} + FS \cdot S \end{pmatrix}$$

97 Eq. 135

$$R_{n_{ij}} = H_{ij} + LE_{ij}$$

and

$$R_{n_{ij}} = TH_{i+} + TH_{i+1}\uparrow - 2\sigma T_{L_{ij}}^{4} + A_j \cdot DS \cdot 0.7/\sin(IS)$$

99 Eq. 137

$$rzH = \rho C_p\, u^* \frac{(TS - T_{zh})}{H_s}$$

99 Eq. 138

$$rzE = \frac{\rho C_p}{\gamma'}\, u^* \frac{(e_s - e_{zh})}{LE_s}$$

99 L. 21 . . . equations, the friction velocity . . .

100 Eq. 140 $$rzH = \frac{u_{zh}}{u^*} + 0.52\left(\frac{u^* zh}{\nu}\right)^{0.45} (Pr)^{0.8}$$

100 L. 8 . . . numerical constants in equation (140) . . .

L. 9 . . . of Chamberlain (1968).

100 Eq. 141 $$R_{ns} = \frac{\rho C_p}{\gamma'} u^*\left(\frac{es - e_{zh}}{rzE}\right) + \rho C_p u^*\left(\frac{T_s - T_{zh}}{rzH}\right) + SHF$$

104 Eq. 148 $$K_H(z) = \frac{R_n(z) - SHF}{-\lambda \frac{\partial C(z)}{\partial z} - \rho C_p \frac{T(z)}{\partial z} - \frac{\rho C_p}{\gamma'} \frac{\partial e(z)}{\partial z}}$$

98 Eq. 136 $$LE_{ij} = \frac{\rho C_p}{\gamma'} \quad . \; . \; . \; .$$